Fakultät für Medizin

Institut für Neurowissenschaften

The role of Orai2 in mGluR1/5-mediated signaling and calcium homeostasis in CA1 pyramidal neurons

Hsing-Jung Chen

Vollständiger Abdruck der von der Fakultät für Medizin der Technischen Universität München zur Erlangung des akademischen Grades eines

Doctor of Philosophy (Ph.D.)

genehmigten Dissertation.

Vorsitzender: Univ.-Prof. Dr. Claus Zimmer

Betreuerin: Priv.-Doz. Dr. Jana Hartmann

Prüfer der Dissertation:

1. Univ.-Prof. Dr. Arthur Konnerth
2. Univ.-Prof. Dr. Thomas Misgeld

Die Dissertation wurde am 30.01.2018 bei der Fakultät für Medizin der Technischen Universität München eingereicht und durch die Fakultät für Medizin am 12.03.2018 angenommen.

Acknowledgements

This dissertation could not have been performed without the help and support of many people. I would like to thank my supervisors Dr. Jana Hartmann and Prof. Dr. Arthur Konnerth for their valuable contributions, patient guidance and encouragement during my graduate work. I would like to express my appreciation for Prof. Dr. Thomas Misgeld for being a member in my thesis committee and providing critical feedback. Similarly, I want to say thank you to Prof. Dr. Helmuth Adelsberger for his encouragement and advice. Furthermore, I would like to thank Prof. Dr. Feske for providing an Orai2$^{-/-}$ mouse. I want to specially thank Christine Karrer for preparing all reagents necessary for my experiments. In the same breadth, I would like to express my gratitude for technical support from Andi, Christian, Felix, Gabi, Karin, Petra, Rosi, and Tanja. Of course, I appreciated to work alongside my fantastic colleagues Antje, Arjan, Aylin, Benedikt, BJ, Carsten, Doug, Hongbo, Taka, Tatsuo, Yang, Yong-Hai and Zsuzsanna: It was a real pleasure to work with all of you. Finally, I also would like to extend my deepest gratitude to my family, my boyfriend Peter and my friends in Taiwan and in Germany for their constant support and understanding. Without the help from those people, I could have never completed this thesis.

Abstract

Calcium released from endoplasmic reticulum (ER) calcium stores into the cytosol is a universal second messenger that is crucial for the regulation of diverse biological functions in eukaryotic cells. In order to guarantee responsiveness of cells to external stimuli as well as to secure appropriate conditions for protein synthesis in the ER, homeostasis of the intraluminal calcium concentration must be maintained. The ubiquitously expressed Orai1 protein forms calcium release-activated calcium (CRAC) channels that are critical for the ER calcium store replenishment in many non-excitable cell types. Knowledge about calcium homeostasis in neurons is only beginning to emerge. In the brain, the homolog of Orai1, Orai2, is more abundant than Orai1 but its function in neurons is unknown. The focus of this project was the role of Orai2 in CA1 pyramidal neurons in the mouse hippocampus. Using a quantitative RT-PCR approach; I found that during early postnatal development (between P11 and P20) Orai2 expression is upregulated. Using a combination of confocal calcium imaging and the patch-clamp technique in acute hippocampal slices, I could investigate the contribution of Orai2 to calcium homeostasis in wild type (WT) and Orai2-deficient knockout ($Orai2^{-/-}$) mice. Inositoltrisphospate receptor (IP_3R)-dependent calcium release in somata of CA1 pyramidal neurons was evoked by local application of an agonist of group I metabotropic glutamate receptors mGluR1/5, dihydrophenylglycine (DHPG), by photolysis of caged IP_3 and by back-propagating action potentials (bAPs) in the presence of DHPG. Calcium release through ryanodine receptors (RyRs) was stimulated by local application of their agonist caffeine. In the absence of Orai2, the IP_3R-dependent calcium responses persist at P11-P16 but were largely abolished at P17-22 due to a deficit in ER calcium store homeostasis, consistent with an expression level-dependent function of Orai2. In

contrast to that, RyR-dependent calcium release remains unaltered in Orai2$^{-/-}$ mice at all postnatal ages tested, and was little affected by pharmacological blockade of Orai1/3. Moreover, experiments with alternating stimulation of IP_3Rs and RyRs in the same cells showed that there are two types of independent, largely non-overlapping ER calcium stores in CA1-pyramidal neurons, an IP_3-sensitive and a Ry-sensitive store. The possible role of calcium influx through voltage-gated calcium channels (VGCCs) for store refilling was tested by local application of ACSF supplemented with a high concentration of KCl, by depolarizing pulses in the voltage-clamp configuration and by pharmacological block of VGGCs with their antagonist D600. It was found that empty IP_3-sensitive stores cannot be refilled by activation of VGCCs and depend entirely on Orai2 for their calcium homeostasis. For Ry-sensitive stores the opposite is the case. In an analysis of different types of synaptic plasticity of Schaffer collateral (SC)-CA1 pyramidal neuron synapses, I found that the RyR-dependent long-term potentiation (LTP) and the mGluR1/5-dependent long-term depression (LTD) do not require Orai2 and thus are independent of the IP_3-sensitive calcium store. In contrast to that, suppression of LTP is impaired in the absence of Orai2. Taken together, my data suggest that the IP_3-sensitive ER calcium store in CA1 pyramidal neurons is (1) a novel type of calcium store that is largely independent from the well-characterized Ry-sensitive store, (2) uses a different mechanism for replenishment and (3) at synapses is complementary to the Ry-sensitive store on a functional level. Finally, I could also demonstrate (4) the importance of Orai2 for synaptic plasticity and homeostasis of this novel calcium store.

Glossary

ACSF	Artificial cerebrospinal fluid
AM	Acetoxymethyl ester
AMPARs	A-amino-3-hydroxy-5-methyl-4-Isoxazole propionate receptors
bAPs	Back-propagating action potentials
cAMP	Cyclic adenosine monophosphate
CA	Cornu ammonis
CICR	Calcium-induced calcium release
CNS	Central nervous system
Cp	Crossing point
CRAC	Calcium release-activated calcium entry
DAG	Diacylglycerol
DHPG	Dihydroxyphenylglycine
ER	Endoplasmic reticulum
fEPSP	Field excitatory postsynaptic potentials
G-proteins	GTP-binding proteins
HFS	High-frequency stimulation
iGluRs	Ionotropic glutamate receptors
IP_3	Inositoltrisphosphate
IP_3Rs	Inositol trisphosphate receptors

LSD	Least Significant Difference
LTD	Long-term depression
LTP	Long-term potentiation
mGluRs	Metabotropic glutamate receptors
NA	Numerical aperture
NMDARs	N-methyl-D-aspartate receptors
OGB-1	Oregon Green 488 BAPTA-1 hexapotassium salt
PIP_2	Phosphatidylinositol 4,5-bisphosphate
PKC	Protein kinase c
PLC	Phospholipase c
Ry	Ryanodine
RyRs	Ryanodine receptors
SERCA	Sarco/endoplasmic reticulum Ca^{2+}-ATPase
SLM	Stratum lacunosum moleculare
SO	Stratum oriens
SOCCs	Store-operated calcium channels
SOCE	Store-operated calcium entry
SP	Stratum pyramidale
SR	Stratum radiatum
VGCCs	Voltage-gated calcium channels
WT	Wild type

Table of contents

1. Introduction

The brain can store memory traces from millisecond to decades (Destexhe and Marder, 2004). In order to store memory across multiple time scales, two distinct memory storage systems are employed: (1) a short-term memory storage system and (2) a long-term memory storage system (Buzsaki and Moser, 2013). The hippocampus plays a central role in the consolidation of information from short-term memory to long-term memory, including various "qualities" of memory such as declarative memory, episodic memory and spatial memory (Bird and Burgess, 2008; Buzsaki and Moser, 2013).

1.1 Hippocampal connectivity and function

"After the operation, this young man could no longer recognize the hospital staff nor find his way to the bathroom. […], yet could recall some trivial events that had occurred just before his admission to the hospital. His early memories were apparently vivid and intact." That was how Scoville and Milner described H.M., a young man who had had an operation to remove two-thirds of his hippocampus in an attempt to cure his severe seizures (Scoville and Milner, 1957). H.M. was not able to memorize the spatial and temporal information connected to a specific event. But H.M. was not alone. Similar anomalies were reported for about ten more patients who all underwent surgeries in which part of their hippocampus was removed (Scoville and Milner, 1957). H.M.'s case report has enabled researchers with the possibility to study the general function of the hippocampus: spatial navigation, learning, and memory (Milner et al., 1968). Until today, the hippocampus has remained an important experimental system for investigating

synaptic plasticity related to contextual and spatial information-storage mechanisms in normal and disease states (Bird and Burgess, 2008; Kim and Diamond, 2002; Neves et al., 2008).

How does the hippocampus process the various inputs from different regions of the brain and how does the hippocampus affect our spatial learning and episodic memory? Anatomically, the hippocampus consists of the cornu ammonis (CA) field, subiculum and dentate gyrus (**Figure 1.1**). The principal cell type in the CA field is the pyramidal neuron, a type of excitatory neuron that uses glutamate as its major neurotransmitter. The CA field can be further divided into CA1 and CA3[1] which receive input from the entorhinal cortex, the dentate gyrus and other brain regions such as the thalamic midline nuclei and amygdala (Bird and Burgess, 2008; Cutsuridis et al., 2010b). There is a microcircuit within the hippocampus connecting the CA-subregions (CA1, CA3 and dentate gyrus) which is referred to as the trisynaptic loop (Carr and Frank, 2012; Cutsuridis et al., 2010b). The trisynaptic loop is constituted by the following three pathways (projections): the perforant pathway, the mossy fiber pathway and the Schaffer collateral pathway (**Figure 1.1**).

The dentate gyrus is the input region of the hippocampus. The principal cell type of the dentate gyrus is referred to as granule cell. The dentate gyrus receives input from the entorhinal cortex via the perforant pathway and projects to CA3 via the mossy fiber pathway. Next part of the hippocampal microcircuit is the Schaffer collateral pathway, in which pyramidal cells of CA3 provide synaptic input to pyramidal cells of CA1.

[1] some studies divide the CA subregions even more detailed into CA1, CA2, CA3 and CA4, see also Cutsuridis et al., 2010b

Eventually, the entorhinal cortex receives projections either directly from CA1 or indirectly from CA1 via the subiculum (Amaral and Witter, 1989; Andersen et al., 1969). Thus, CA1 serves as the major output area of the hippocampus.

Within the CA1 region, four layers have been described: Firstly, the stratum oriens (SO) in which the basal dendrites of pyramidal neurons are located; secondly, the stratum pyramidale (SP) which contains the somata of pyramidal neurons; thirdly the stratum radiatum (SR) which contains the proximal part of apical dendrites; fourthly, the stratum lacunosum moleculare (SLM) in which the distal dendritic tufts of pyramidal neurons are located (**Figure 1.1**). Many experiments and computational models suggest that synaptic input to CA1 and output from CA1 are involved in learning and memory (Carr and Frank, 2012; Cutsuridis et al., 2010a). These findings make CA1 a popular brain region for studying the mechanisms of learning and memory. Indeed, by now a lot is known about how the hippocampus' involvement in memory formation: First, the series of case studies on H.M. have contributed to the understanding of the role of the hippocampus in spatial learning and episodic memory. Second, the trisynaptic loop of the hippocampus offers a general view about how neural signals are transmitted and processed (see also **Figure 1.1**). Third, CA1 lesioned rodents exhibit difficulties in object recognition, spatial information processing, temporal pattern separation and contextual memory retrieval (Cutsuridis et al., 2010a; Hoge and Kesner, 2007; Lee and Kesner, 2004). Nevertheless, many details about signal integration and information processing in the hippocampal microcircuit are still unknown. This assessment is particularly true for molecular mechanisms involved in hippocampal memory formation.

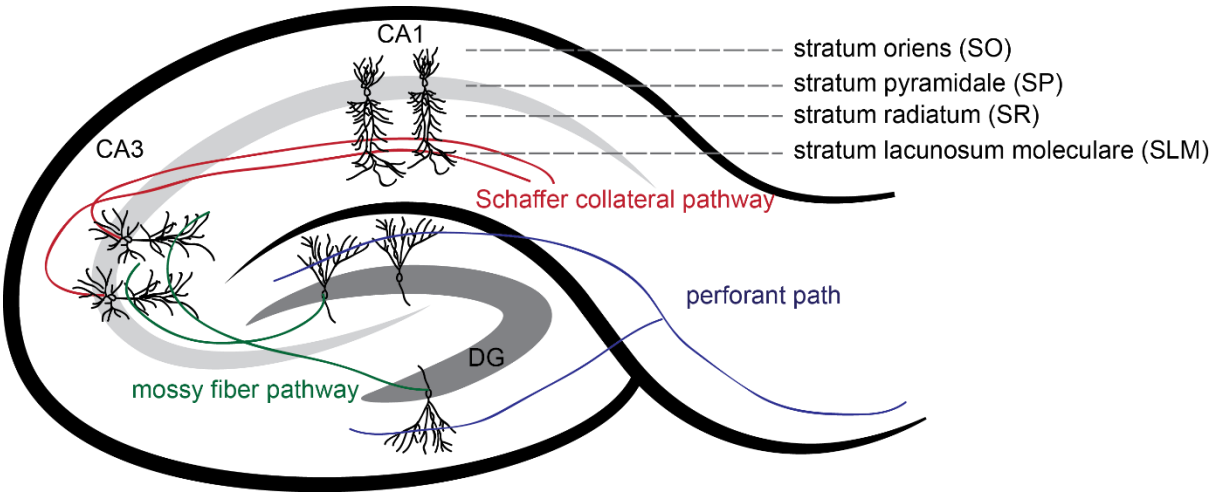

Figure 1.1 Structure and connectivity of hippocampus, the trisynaptic loop

There are three major pathways in the hippocampal microcircuit. The dentate gyrus and CA3 receive inputs from the entorhinal cortex via the perforant pathway. The dentate gyrus projects to CA3 via the mossy fiber pathway. The Schaffer collateral pathway connects CA3 to CA1. In stratum lacunosum moleculare (SLM) and stratum radiatum (SR) apical dendrites of pyramidal cells are located. Stratum oriens (SO) consists of basal dendrites. The stratum pyramidal (SP) is constituted by cell bodies of pyramidal neurons (Cutsuridis et al., 2010b). Modified from (Moser, 2011)

1.2 Synaptic plasticity and calcium

Synaptic plasticity

The brain undergoes activity-dependent changes or so-called synaptic plasticity in order to adapt to internal and/or external stimulation. In 1949, Donald Hebb proposed the hypothesis that learning and memory depends on synaptic plasticity. The term synaptic plasticity describes the ability of synapses to change their metabolism and/or the growth of neuronal processes in response to stimulation (Hebb, 1949). These activity-dependent changes could be observed from the protein level in single synapses up to the functional level of entire brain circuits (Destexhe and Marder, 2004).

Hebbian or associative learning occurs when simultaneous activation of neurons leads to significant changes in the efficiency of synapses that connect them. This synaptic plasticity can be roughly divided into structural and functional plasticity. Structural plasticity is defined as the change of morphology of synapses. Functional plasticity refers to the alteration of synaptic strength (Caroni et al., 2012; Zhang and Linden, 2003). Both types of plasticity play a critical role in shaping cell excitability (Kotaleski and Blackwell, 2010) and could be achieved by an alteration of the amount of presynaptic neurotransmitter release or by a change of activity of postsynaptic glutamate receptors which, in turn, leads to changes of intracellular calcium concentration through postsynaptic glutamate-induced depolarization (Balschun et al., 1999a; Bear and Abraham, 1996; Emptage et al., 2001; Hayashi et al., 2000; Lu et al., 1997; Mayford et al., 1996; McHugh et al., 1996; Raymond and Redman, 2006; Reyes and Stanton, 1996; Whitlock et al., 2006; Zucker, 1999; Zucker and Regehr, 2002). Moreover, special attention has been paid to the adjustment of long-term use-dependent decrease (long-term depression, LTD) and increase (long-term potentiation, LTP) of synaptic strength since they are related to learning and memory in CA1 (Bear and Abraham, 1996; Tang et al., 1999; Whitlock et al., 2006).

Calcium

Calcium is a universal intracellular messenger. A tight regulation of the calcium concentration in the cytosol and intracellular compartments is necessary for normal responsiveness of the neuron and in order to prevent cellular damage (Clapham, 1995). In neurons, the cytosolic calcium concentration at rest is around 100 nM, which is four

orders of magnitude lower than the extracellular calcium concentration. During neuronal activation, the cytosolic calcium concentration can reach 1 mM (Clapham, 1995). This dynamic change of cytosolic calcium concentration is involved in many biological pathways, including the regulation of neuronal function and synaptic plasticity (Berridge et al., 2003; Berridge et al., 2000; Ghosh and Greenberg, 1995; Luebke et al., 1993; Zamponi et al., 2005). Two major pathways increase the cytosolic calcium concentration: (1) calcium influx through calcium-permeable channels in the plasma membrane and (2) calcium release from endoplasmic reticulum (ER) stores. In neurons, calcium influx is mediated by voltage-gated calcium channels (VGCC) and receptor-operated calcium channels (such as ionotropic glutamate receptors, (see **section 1.3**). An example for a receptor-operated calcium channel is the N-methyl-D-aspartate receptors (NMDAR). Calcium influx through NMDARs has been shown as a critical process for short-term and long-term synaptic plasticity (Liu et al., 2004; McHugh et al., 1996; Tsien et al., 1996). Beside NMDA receptors, also other glutamate receptors are important for synaptic plasticity and hippocampal-dependent learning and memory (Luscher et al., 2000).

1.3 Glutamate receptors - ionotropic and metabotropic

Glutamate is the principal excitatory neurotransmitter in the central nervous system (CNS). It is released from terminals of the presynaptic region and binds to various kinds of glutamate receptors on the postsynaptic membrane for further signal transmission. Glutamate receptors can be divided into two major types: ionotropic glutamate receptors (iGluRs), which form glutamate-gated cation channels; and metabotropic glutamate receptors (mGluRs), which couple to GTP-binding proteins (G-proteins) in order to

activate downstream signaling cascades. Based on sequence homology, sensitivity to pharmacological agents and electrophysiological properties, iGluRs are further divided into three groups: NMDARs, a-amino-3-hydroxy-5-methyl-4-isoxazole propionate receptors (AMPARs) and kainate receptors. According to their sequence similarity and type of downstream effector, mGluRs are divided into three groups with a total of eight subtypes (Hollmann and Heinemann, 1994) (**Figure 1.2**).

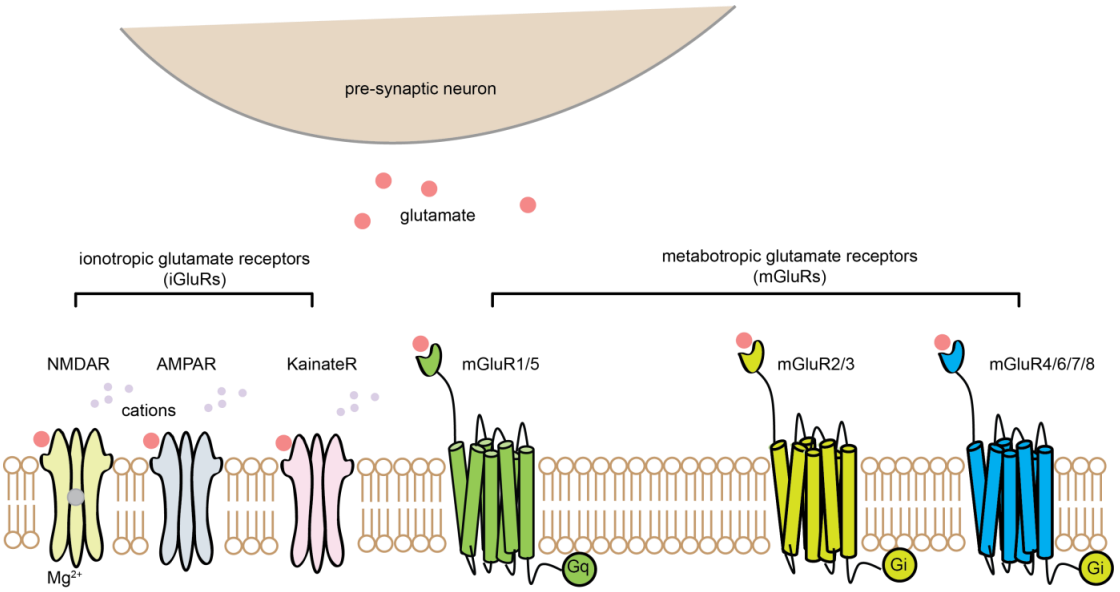

Figure 1.2 Classification of glutamate receptors

There are two major types of glutamate receptors, iGluRs and mGluRs. NMDAR, AMPAR and KainateRs belong to iGluRs, which can form cation-permeable channels to depolarize postsynaptic neurons upon glutamate binding. In contrast to other iGluRs, when NMDARs are at resting state, extracellular magnesium ions diffuse into the channel pore and thus largely decrease the permeability of NMDARs. A strong depolarization is needed to remove the magnesium block to enable cation ions to pass through the channel pore in order to activate downstream signaling pathways. There are eight types of metabotropic glutamate receptors, mGluR1-8 which can be classified into three groups based on amino acid similarity and type of coupled G-protein. While group I mGluRs (mGluR1/5) are coupled to a Gq protein, group II (mGluR2/3) and group III mGluRs (mGluR4/6/7/8) are coupled to a Gi protein.

1.4 mGluR-mediated signaling pathways

Based on amino acid identity and downstream signaling pathways, the eight subtypes of mGluRs can be classified into group I (mGluR1/5), group II (mGluR 2/3) and group III (mGluR 4/6/7/8) glutamate receptors (Conn and Pin, 1997). Group II and group III

mGluRs are coupled to a Gi protein to inhibit cyclic adenosine monophosphate (cAMP) formation. Group I mGluRs are coupled to a Gq protein, which, in turn, can stimulate phospholipase c (PLC) to hydrolyze phosphatidylinositol 4,5-bisphosphate (PIP_2) into Inositoltrisphosphate (IP_3) and diacylglycerol (DAG). IP_3 is one of the most important second messengers in cellular signaling: IP_3 leads to calcium release from the ER when it binds to IP_3 receptors (IP_3Rs) on the ER membrane. DAG can further activate protein kinase c (PKC) which is an important kinase for many cellular pathways (Niswender and Conn, 2010) (**Figure 1.3**).

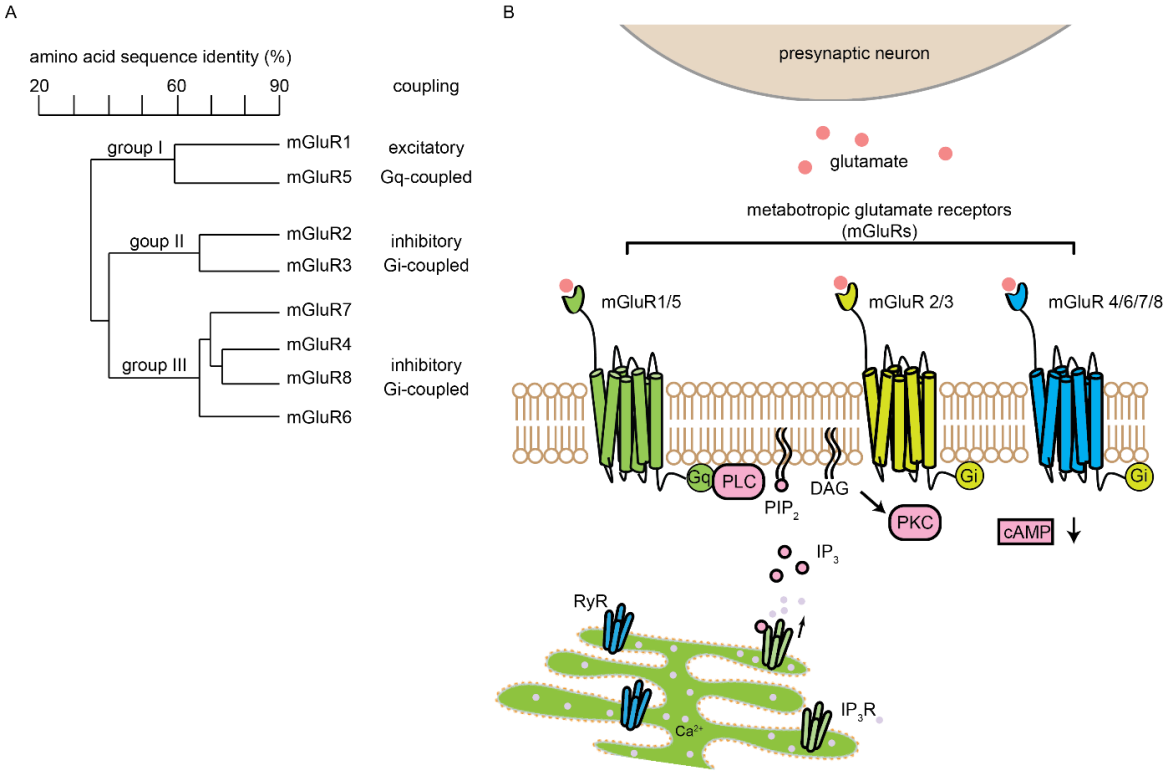

Figure 1.3 Amino acid sequence homology and downstream pathways of mGluRs

(A) Amino acid sequence identity between all known mGluR subtypes and their type of G-protein coupling. While mGluR1/5 are excitatory and coupled to a Gq protein, the rest of the mGluRs are inhibitory and coupled to a Gi protein (scheme is modified from (Pin and Duvoisin, 1995). **(B)** Schematic of mGluR-mediated pathways. Activation of mGluR1/5 triggers PLC to digest PIP_2 to IP_3 and DAG. IP_3 binds to IP_3 receptors (IP_3R), which are located on the ER membrane to release calcium from ER stores. Group II and III mGluRs inhibit the activity of adenylyl cyclase, leading to a decrease in cAMP accumulation.

1.5 Group1 mGluRs in hippocampal function

Potentially, the downstream signaling pathways of mGluR1/5 are therapeutic targets for diverse neurological disorders such as chronic pain, addictive disorders, depression (Niswender and Conn, 2010), Parkinson's disease (Ferreira et al., 2017), Alzheimer's disease (Um et al., 2013), Huntington's disease (Ribeiro et al., 2010) and Fragile X Syndrome (Yan et al., 2005). Additionally, previous studies indicate that mGluR1/5 play a pivotal role in synaptic plasticity and memory formation in the hippocampus (Mukherjee and Manahan-Vaughan, 2013; Niswender and Conn, 2010). Indeed, the Allen brain atlas (Lein et al., 2007) confirms mGluR1 and mGluR5 expression in the hippocampus of adult mice, with mGluR5 being expressed at higher levels (**Figure 1.4**).

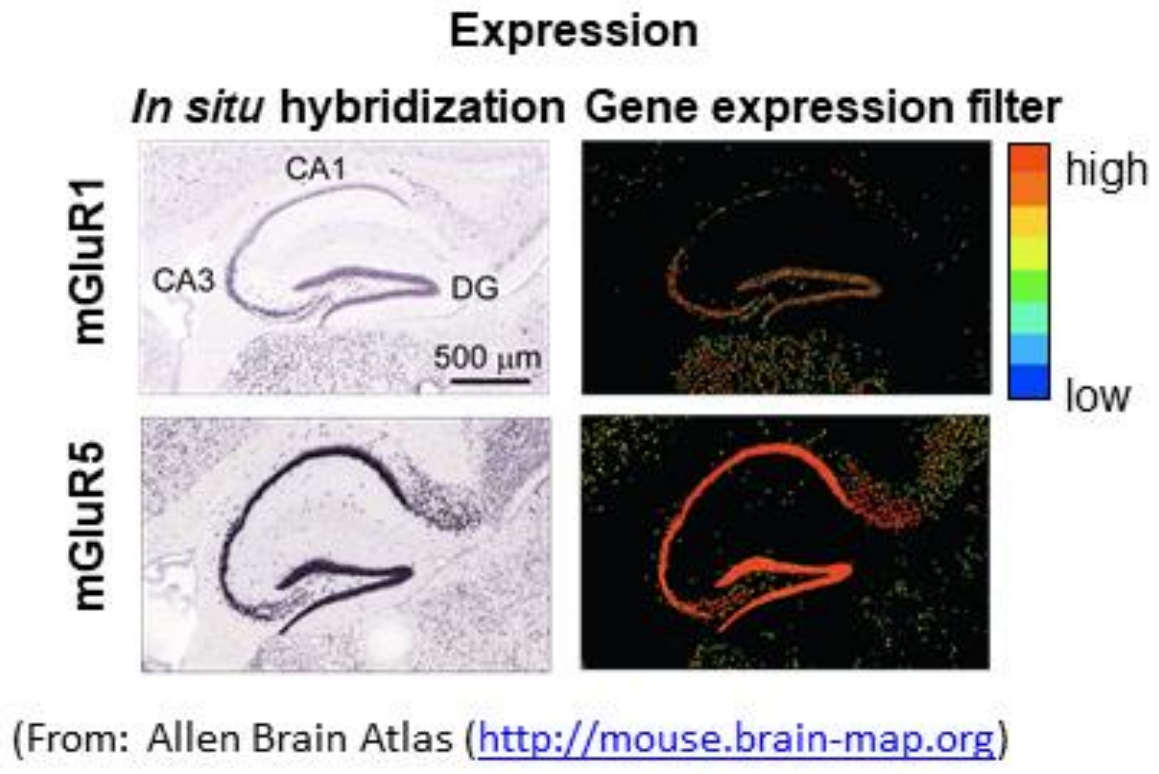

Figure 1.4 Expression of mGluR1 and mGluR5 in hippocampus

Left: In situ hybridization with mGluR1 and mGluR5 mRNA probes in a brain of an adult mouse (P56). *Right:* Expression intensity shown in pseudocolor. mGluR5 shows higher expression than mGluR1 in the CA1 region. (http://mouse.brain-map.org)

Both mGluR1/5 are involved in regulating hippocampal synaptic plasticity (Mannaioni et al., 2001). Activation of mGluR1/5 through synaptic stimulation or agonist application can trigger mGluR-dependent LTD and protein synthetization in CA1 (Huber et al., 2000; Oliet et al., 1997). Disrupted mGluR5-mediated synaptic transmission - due to knockout of the mGluR5 gene or pharmacological blockade of mGluR5 - results in impairments of spatial learning and LTD induction in rodents (Lu et al., 1997; Neyman and Manahan-Vaughan, 2008; Popkirov and Manahan-Vaughan, 2011; Purgert et al., 2014). However, the molecular details involved in mGluR5-mediated LTD are unknown. The IP_3-dependent release of calcium ions from the ER is a possible candidate mechanism downstream of mGluR5: Schnabel and colleagues have shown that mGluR-mediated LTD induction is blocked after emptying the ER calcium store by a SERCA pump (sarco/endoplasmic reticulum Ca^{2+}-ATPase) antagonist (Schnabel et al., 1999). Furthermore, two-photon glutamate uncaging experiments revealed that IP_3-mediated calcium release from the ER calcium store in spines is required for mGluR5-mediated LTD induction in CA1 pyramidal neurons (Holbro et al., 2009; Reyes and Stanton, 1996). Thus, the proposed hypothesis that the IP_3-sensitive ER calcium store could be involved in hippocampal CA1 synaptic plasticity is supported by experimental evidence (Luscher and Huber, 2010)

1.6 Calcium release from the ER store and synaptic plasticity

The intraluminal calcium concentration in the ER reaches up to 400 μM, which is up to 1000 times higher than the cytosolic calcium concentration. This high concentration is established by SERCA activity, from which subtype 2 (SERCA2) is highly expressed in the CA1 region (Lein et al., 2007). When SERCA is inhibited in the presence of an

antagonist (thapsigargin or cyclopiazonic acid (CPA)), the calcium store is emptied through leak channels (Nelson et al., 2007; Tu et al., 2006), such as Presenilin 1 and Presenilin 2. It was reported that in some cases of familial Alzheimer's disease Presenilins are mutated (Borchelt et al., 1997; Cruts et al., 1998; Selkoe, 2001). This observation, in turn, reiterates the importance of the ER calcium store for physiological brain function. Moreover, LTP and LTD in CA1 are impaired when SERCA is blocked (Harvey and Collingridge, 1992; Reyes and Stanton, 1996). IP_3Rs are calcium channels in the ER membrane. The calcium release kinetics of IP_3Rs shows a bell-shaped dependency on the cytosolic calcium concentration (Bezprozvanny et al., 1991) while requiring the binding of IP_3 to IP_3Rs to open their pore (Mattson et al., 2000). Nevertheless, the refilling mechanisms of the IP_3R-dependent calcium pool and the role of IP_3R-mediated calcium release in synaptic plasticity still needs to be studied further.

In addition to IP_3 receptors, there is a second type of calcium channel in the ER membrane, namely ryanodine receptors (RyRs). RyRs are calcium-sensitive themselves and are responsible for the so-called calcium-induced calcium release (CICR). The properties of the ryanodine-sensitive calcium pool and potential refilling mechanisms in CA1 have been studied (Garaschuk et al., 1997). Moreover, the role of RyRs for different forms of synaptic plasticity in CA1 pyramidal neurons is rather well established (Balschun et al., 1999b; Johenning et al., 2015; Reyes-Harde et al., 1999).

1.7 Expression pattern and function of IP_3Rs and RyRs

There are three types of IP_3Rs (IP_3R_1, IP_3R_2 and IP_3R_3) and three types of RyRs (RyR_1, RyR_2 and RyR_3). IP_3R_1 is expressed widely throughout the rodent brain, especially in

cerebellar Purkinje cells and pyramidal cells of CA1. IP_3R_2 is highly expressed in the spinal cord and glial cells. IP_3R_3 can be found in many different brain regions and neuronal cell-types, such as cerebellar granule cells and the stratum oriens of CA1 (Furuichi et al., 1994; Vermassen et al., 2004). RyR_1 is primarily expressed in skeletal muscle cells, but it can also be found in several neuronal cell-types, including cerebellar Purkinje cells. RyR_2 can be detected in cerebellar Purkinje cells and in the cerebral cortex. RyR_3 is expressed in hippocampal neurons, thalamus and in cerebellar Purkinje cells (Furuichi et al., 1994; Lanner et al., 2010).

1.8 IP_3- and Ry-sensitive calcium pools: identical or separate pools

The role of the ER calcium store in neuronal function has been studied best in cerebellar Purkinje cells (Finch and Augustine, 1998; Hartmann et al., 2014; Miyata et al., 2000; Takechi et al., 1998). In Purkinje cells, IP_3Rs and RyRs potentially share the same calcium pool (Khodakhah and Armstrong, 1997). However, findings from PC12 cell cultures of hippocampal primary neurons suggest that IP_3- and Ry-sensitive stores are not identical: When IP_3R- and RyR-mediated calcium signals were functionally mapped, it was found that IP_3R- and RyR- mediated calcium signals were not completely co-localized (Koizumi et al., 1999). Furthermore, in primary hippocampal cultures IP_3-mediated calcium release from the ER could be successfully induced in sustained presence of RyR-specific agonist caffeine, i.e. under conditions in which Ry-sensitive calcium stores are depleted (Murphy and Miller, 1989). Moreover, in primary hippocampal glia cell cultures it has been reported that the calcium distribution in the ER is not homogenous and that two calcium pools exist. One is sensitive to caffeine, the other one is sensitive to thapsigargin (Golovina and Blaustein, 1997). While these

findings suggest that the ER calcium store in the hippocampus consists of more than one (spatial and/or functional) pool, culture systems contain all cell types present in the hippocampus with CA1 pyramidal cells being a minority.

The subcellular localization pattern of IP_3Rs and RyRs could potentially help to resolve the degree of overlap between ER calcium stores. Immunostainings against IP_3Rs and RyRs in hippocampus show that IP_3Rs are mainly located in CA1 and that RyRs are located mainly in CA3 as well as dentate gyrus. Consistent with imaging results (Koizumi et al., 1999), IP_3Rs are located at the cell body and dendritic shafts of CA1 pyramidal neurons, whereas RyRs are enriched in axons and dendritic spines in CA1 pyramidal neurons (Sharp et al., 1993).

1.9 Calcium release-activated calcium entry

An intact calcium homeostasis is critical for diverse processes of protein expression such as protein synthesis and protein folding. Accordingly, the depletion of calcium from the ER results in ER stress. The term ER stress describes a condition in which (1) misfolded proteins accumulate in the ER and (2) impaired ER calcium homeostasis can eventually trigger the cell death pathway (Lindholm et al., 2006).

In case of diminished intraluminal calcium concentration, store-operated calcium channels (SOCCs) are activated to allow for calcium influx and refill ER calcium stores by SERCA activity. This process is also called store-operated calcium entry (SOCE) or capacitive calcium entry, with the concept dating back to the 1980s (Putney, 1986;

Takemura et al., 1989). During these early days, the properties of SOCC-mediated calcium release-activated calcium entry (CRAC) were characterized in immune cells without knowing the molecular identity of SOCCs. It was found that SOCCs are activated in case the ER is calcium depleted, that SOCCs are regulated by intracellular calcium and that SOCCs are sensitive to Ni^{2+} and Cd^{2+} (Lewis and Cahalan, 1989). The difference between SOCCs and VGCCs is that SOCCs exhibit no voltage-dependent gating (Hoth and Penner, 1992; Lewis and Cahalan, 1989). In a RNA interference (RNAi)-based screen for genes involved in CRAC in a Drosophila cell line, researchers found two proteins crucial for ER refilling: *stromal interaction molecule* 1 (STIM1) and Orai1. STIM1 was later identified as the calcium sensor in the membrane of the ER, whereas Orai1 is the actual pore-forming subunit of the CRAC channel (Feske et al., 2006; Prakriya et al., 2006; Roos et al., 2005; Vig et al., 2006; Yeromin et al., 2006) (**Figure 1.5**). STIM1 oligomerizes when the ER calcium pool is emptied, moves to the plasma membrane to interact with Orai1 protein and eventually forms STIM1-Orai1 clusters. The STIM1-Orai1 clusters, in turn, allow for calcium influx through Orai1 channels to refill the ER calcium pool via SERCA pumps (Luik et al., 2008; McNally et al., 2012; Park et al., 2009; Peinelt et al., 2006; Penna et al., 2008; Soboloff et al., 2012; Zhang et al., 2005). Although most of the studies about store-operated calcium entry were performed on non-excitable cells, an increasing body of evidence indicates that SOCE is also important for maintaining calcium homeostasis and synaptic plasticity in neurons of the CNS (Majewski and Kuznicki, 2015). In cerebellar Purkinje cells, STIM1 is important for mGluR1-mediated synaptic transmission and calcium homeostasis. The calcium release through both IP_3Rs and RyRs is largely reduced or absent due to a lack of proper store filling at resting membrane potential. The cerebellar function reflected in

motor behavior is severely impaired in Purkinje cell-type-specific STIM1 knockout (STIM1^{pko}) mice (Hartmann et al., 2014). In primary hippocampal neuronal cultures, it was shown earlier that activation of mGluR1/5 signaling with bath applied DHPG increased the cytosolic calcium concentration in dendrites and activates STIM1 (Ng et al., 2011). Moreover, STIM1 and Orai1 are involved in synaptic plasticity, synaptogenesis, chemical LTP-induction and transcriptional regulation of hippocampal neurons (Dittmer et al., 2017a; Korkotian et al., 2017).

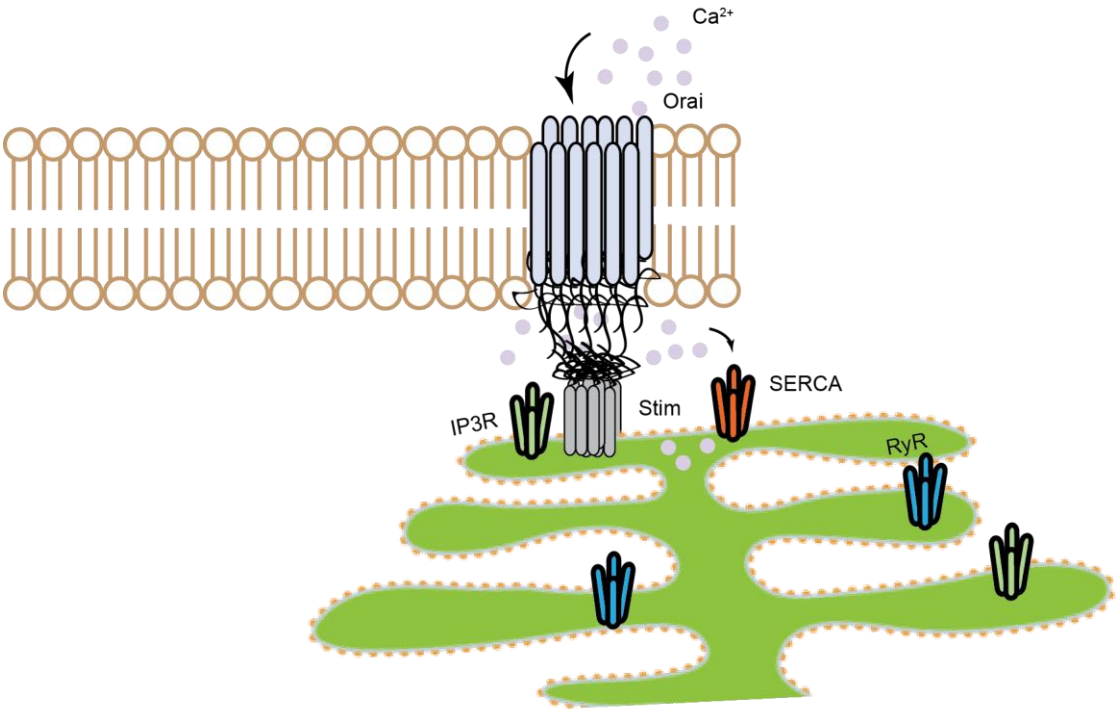

Figure 1.5 STIM-Orai forms a complex to refill ER calcium store.

Orais are located on the plasma membrane, while STIM is located on the ER membrane. In case the calcium concentration in the ER decreases, STIM1 accumulates and moves in direction of the plasma membrane to bind to Orai. Once the STIM1-Orai complex is formed, calcium enters into the cell through the Orai channel and is pumped into the ER via SERCA.

Most SOCCs studies have been focusing on STIM1-Orai1 complex-mediated store refilling. There is little known about STIM2 and the two other members of the Orai family

(Orai2 and Orai3) regarding ER store refilling in the CNS. So far, it has been revealed that Orai2 and Orai3 also possess SOCCs characteristics (DeHaven et al., 2007; Hoth and Niemeyer, 2013; Mercer et al., 2006). STIM1 is highly expressed in the cerebellum, while STIM2 is mainly expressed in the hippocampus. In cerebellum and hippocampus, Orai2 is the most abundant Orai protein (**Figure 1.6**). So far, there is limited knowledge about whether Orai2 is critical for store refilling and synaptic plasticity in the hippocampus. It has been shown that Orai2 forms a complex with STIM2/TRPC6 in order to maintain mushroom spines and ER calcium homeostasis in CA1 pyramidal neurons (Zhang et al., 2016). In a familial Alzheimer's disease (FAD) mouse model, the Presenilin-1 M146V knockin (KI) showed down-regulation of STIM2 protein, reduced SOCE in dendritic spines and a loss of mushroom spines. The resulting phenotype could be rescued by application of a TRPC6 agonist (hyperforin), by a SOCE modulator (NSN21778) or by transfecting TRPC6 and Orai2 (Sun et al., 2014; Zhang et al., 2016). Nevertheless, the function of Orai2 in in the CA1 region of the hippocampus is still unclear. Interestingly, our group recently found that ER-refilling and mGluR-mediated synaptic transmission in cerebellar Purkinje cells is impaired in the absence of Orai2 (Dijke, unpublished). Together with the importance of STIM1 in cerebellar Purkinje cells, this finding implies that the interaction between STIM1 and Orai2 could be important for the maintenance of calcium homeostasis.

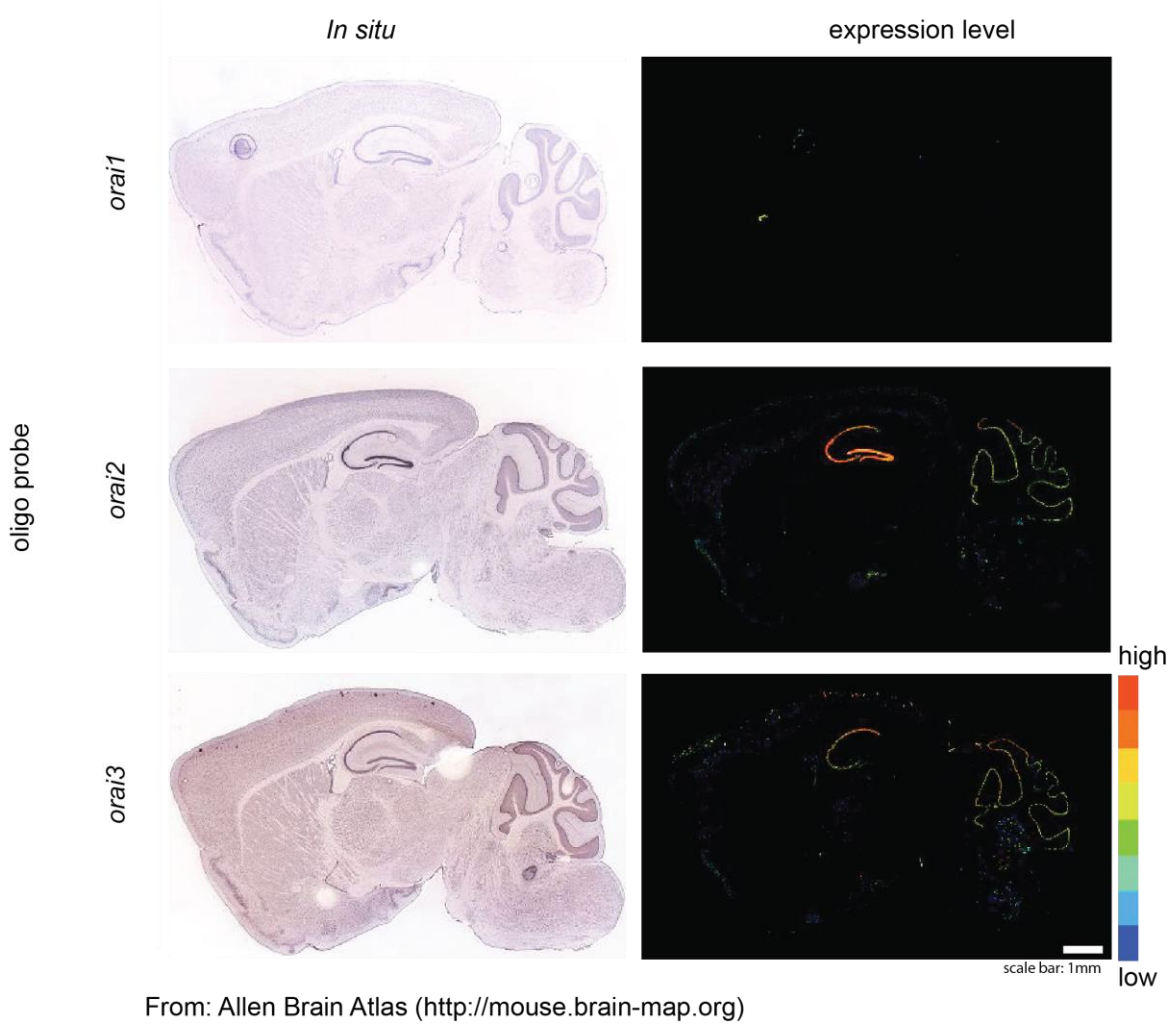

Figure 1.6 mRNA in situ hybridization with *Orai1-3* oligo probes.

Left: Image of *in situ* hybridization results from *Orai1-3* probes on adult mouse brain. Right: The transcript level in pseudocolor. The transcript level of Orai1 mRNA is relatively low compared to Orai2 and 3. Orai2 and 3 are mainly located in the hippocampal pyramidal cell layer and in the Purkinje cell layer of the cerebellum. The sample was derived from sagittal sections of P56 C57BL/6 animals.

In my graduate work, I aimed to study the role of Orai2 in group 1 mGluR-mediated synaptic transmission and calcium homeostasis in CA1 during mouse development. Moreover, I characterized the properties of the IP_3-sensitive ER calcium store. Here, I found evidence that the IP_3- and Ry-sensitive calcium stores are separable in CA1. Finally, my results also suggest different roles of IP_3- and ryanodine-sensitive calcium stores in the regulation of mGluR1/5-mediated synaptic transmission and plasticity.

2. Materials and methods

2.1 Animals

Mice were kept in an animal facility under a 12-hour light/dark cycle at temperature 22°C. Food and water was provided *ad libitum*. All animal experiments were performed in accordance with the policies established by the institutional animal welfare guidelines of the government of Bavaria, Germany. The Orai2 deficient mouse line was kindly provided by Prof. Dr. Feske. More details about ES cells and the targeting vector for generation of Orai2 deficient mice can be found at http://www.velocigene.com/komp/detail/14962 (**Figure 2.1)**. The genotype of Orai2-deficient (Orai2$^{-/-}$) mice was determined by PCR of tail tissue. The following primer pair was used: (forward: 5'- TGC TGA GAT GTC CCA GGA G-3' and reverse: 5'-GTC TGT CCT AGC TTC CTC ACT G-3'; product size: WT 207 bp, KO 611 bp).

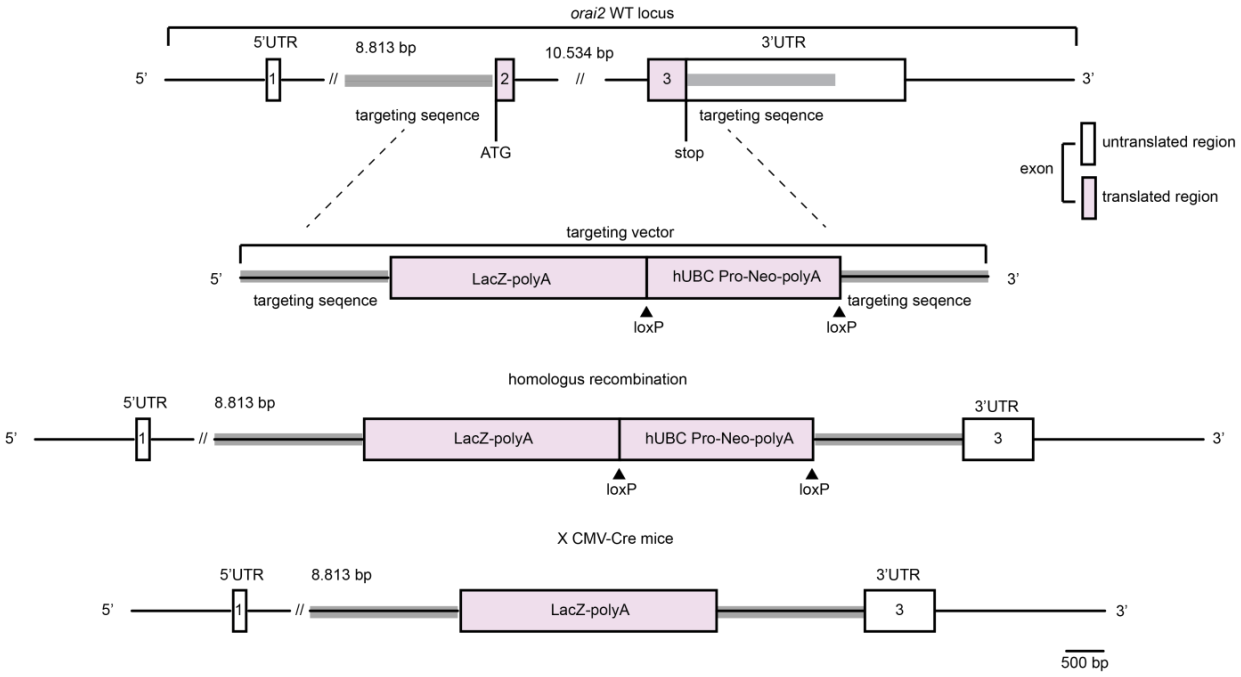

Figure 2.1. Generation of Orai2 $^{-/-}$ mice

Scheme showing the Orai2 gene locus in WT mice (top), the design of the targeting vector (second from top), the targeted Orai2 gene locus after homologous recombination (third from top) and after cre recombination (bottom). The solid boxes in the figure represent exons and the stripes represent introns. The white solid boxes indicate the untranslated region, and the pink boxes indicate the translated region. Thick stripes represent 5' or 3' targeting sequences. loxP sites are shown as triangle. Following homologous recombination, the whole protein-coding regions of the orai2 locus were replaced by LacZ and neo cassettes. The neo cassette can be removed by cre-mediated recombination. (modified from http://www.velocigene.com/komp/detail/14962)

2.2 Preparation of acute hippocampal slices

Acute horizontal hippocampal slices (300 μm) were prepared from C57BL/6 wild type (WT) and Orai2$^{-/-}$ mice between P11 and P30. Mice were anesthetized with CO_2 and decapitated. The brain was immediately removed and submerged in ice-cold slicing solution which contained 24.7 mM glucose, 2.48 mM KCl, 65.47 mM NaCl, 25.98 mM $NaHCO_3$, 105 mM sucrose, 0.5 mM $CaCl_2$, 7 mM $MgCl_2$, 1.25 mM NaH_2PO_4, and 1.7 mM ascorbic acid (Fluka, Switzerland). The osmolality was 290-300 mOsm. The pH value was adjusted to 7.4 and stabilized by bubbling with carbogen-containing solution (95% O_2 and 5% CO_2). Brain slices were cut with the use of a vibratome (VT1200S; Leica, Germany) and then transferred into recovering solution at room temperature for at least one hour before the experiment. The recovering solution contained 2 mM $CaCl_2$, 12.5 mM glucose, 2.5 mM KCl, 2 mM $MgCl_2$, 119 mM NaCl, 26 mM $NaHCO_3$, 1.25 mM NaH_2PO_4, 2 mM thiourea (Sigma, Germany), 5 mM Na-ascorbate (Sigma), 3 mM Na-pyruvate (Sigma), and 1 mM glutathion monoethyl ester (Santa Cruz Biotechnology, U.S.A). The pH-value was adjusted to 7.4 with HCl, the osmolality was adjusted to 290 mOsm.

2.3 Electrophysiological recordings

Individual hippocampal slices were transferred to the recording chamber, which was constantly perfused (2 ml/min) with artificial cerebrospinal fluid (ACSF) containing 2 mM $CaCl_2$, 20 mM glucose, 4.5 mM KCl, 1 mM MgCl2, 125 mM NaCl, 26 mM $NaHCO_3$, and 1.25 mM NaH_2PO4 and gassed with 95% O_2 and 5% CO_2 to ensure oxygen saturation and to maintain a pH value of 7.4. 10 μm bicuculline (Enzo, U.S.A) was added to the ACSF to block $GABA_A$ receptor-mediated synaptic transmission. The ACSF was used for bath application of different drugs as indicated in the respective results section (see **results**). Details about applied drugs are summarized in **Table 1**. The mGluR1/5 agonist DHPG (3,5-Dihydroxyphenylglycine, 0.5 mM; Abcam, U.S.A) and the ryanodine receptor agonist caffeine (40 mM; Sigma, U.S.A) were applied locally by a Picospritzer II (Parker instrumentation, General Valve, U.S.A) connected to a glass-pipette with around 8 MΩ resistance. DHPG was dissolved in ACSF; caffeine was diluted in caffeine ringer which contained 2 mM $CaCl_2$, 10 mM HEPES, 2.5 KCl, 1 mM $MgCl_2$ X $6H_2O$, 120 mM NaCl, 1.25 mM NaH_2PO_4. The pipette tip was placed 15-20 μm from the cell soma. Recordings were generally performed at room temperature; only LTD and LTP experiments were performed at 32°C.

Somatic whole-cell recordings from CA1 pyramidal neurons were performed using patch pipettes with a resistance of about 7 MΩ. Patch pipettes were filled with an internal solution containing 110 mM K-gluconate, 10 mM KCl, 10 mM HEPES, 4 mM Mg-ATP, 0.24 mM Na-GTP, 20 mM Na-Phosphocreatine (Sigma) and 100 μM of the fluorescent calcium indicator Oregon Green 488 BAPTA-1 hexapotassium salt (OGB-1; K_d 200 nM)

(Molecular Probes, U.S.A). The pH was adjusted to 7.3 with KOH. An EPC9/2 patch-clamp amplifier (HEKA, Germany) was used for voltage- and current-clamp measurements. The membrane potential was held at -70 mV without correcting for liquid junction potentials. PULSE software (HEKA) was used for data acquisition and the generation of stimulation protocols. Data were collected at 10 kHz and Bessel-filtered at 2.9 kHz. Igor 5 software (WaveMetrics, U.S.A) was used for the analysis of original current and voltage traces, as well as for statistical analysis.

2.4 Calcium imaging

Whole-cell patch-clamped CA1 pyramidal neurons were dialyzed with internal solution containing 100 μM of the calcium indicator OGB-1 for 10-15 minutes to equilibrate the dye in the cell before recording. Alternatively, cells were stained by multicell bolus loading (Stosiek et al., 2003) of the CA1 pyramidal neuron layer with 1 mM acetoxymethyl ester of the calcium-sensitive fluorescent dye Cal-520 (Cal-520 AM; K_d: 320 nM; AAT-Bioquest, U.S.A) and the help of a Picospritzer II (Parker instrumentation, General Valve, U.S.A). The preparation of staining solution was done according to a standard protocol (Stosiek et al., 2003). Cal-520 AM was dissolved in DMSO supplemented with 20% Pluronic F-127 (Life technology, U.S.A) to a concentration of 10 mM and subsequently diluted to 1 mM in 150 mM NaCl, 2.5 mM KCl, and 10 mM HEPES, pH 7.4. Fluorescence images were acquired by an upright multi-point confocal microscope (E600FN; Nikon, Japan) with a dual spinning disk (QLC 100; VTi, UK). A 40x water-immersion objective with numerical aperture (NA) 0.8 (Nikon) or a 60x water-immersion objective with NA 1.0 (Nikon) were used for image acquisition. The calcium

indicator was excited in a single-photon process with a 488 nm single wavelength Sapphire laser (Coherence, U.S.A). The laser power under the objective was set to < 0.15 mW. Images were acquired at 40Hz with a resolution of 80 X 80 pixels on a CCD camera (NeuroCCD; RedShirt imaging, U.S.A). A function generator (TG1010A; TTi, UK) was used to synchronize the spinning disk and CCD camera during imaging. When cells were whole-cell patch-clamped, imaging was performed simultaneously with electrophysiological recordings.

Image sequences were acquired using Neuroplex software (RedShirt imaging, U.S.A) and analyzed with the ImageJ plug-in "Time Series Analyzer" (https://imagej.nih.gov/ij/plugins/time-series.html; NIH, U.S.A). Fluorescence intensity was corrected by background subtraction. For background subtraction, fluorescence intensity was measured on a ROI that contained tissue without calcium dye staining. Temporal changes in fluorescence intensity of ROIs (region of interest) were expressed as relative percentage changes in fluorescence intensity: $\Delta F/F$ (%) = $((F-F_0)/F_0)$. F_0 is defined as baseline fluorescence, i.e. the fluorescence intensity before a given stimulus, and F is the fluorescence change over time. $\Delta F/F$ (%) values were calculated and plotted using Igor Pro 5 (Wavemetrics, USA).

2.5 IP_3 uncaging

For photolytic uncaging experiments, the internal saline was supplemented with NPE-IP_3 (400 mM; Invitrogen). A tapered lense optical fiber (working distance 6 ± 1 mm, spot diameter 6 ± 1 mm; Nanonics, Israel) was connected to a diode laser (Coherent Cube;

375 nm, 15 mW at the laser head) and directed onto the surface of the slice. IP_3 uncaging was achieved by 50 ms single light pulses through this fiber.

2.6 Extracellular field EPSP recordings

For extracellular recordings of field excitatory postsynaptic potentials (fEPSP), a glass electrode (2-5 MΩ) filled with ACSF was placed in the SR of CA1 **(Figure 2.1 A)**. Baseline synaptic responses were elicited by stimulating the Schaffer collateral pathway at a frequency of 0.033 Hz and the duration of 100 μs through a second glass electrode (2-5 MΩ) filled with 2 M NaCl. Stimulation trains were generated and programmed with a pulse stimulator (Model 2100; A-M systems, U.S.A). The stimulation strength was determined by the very stimulation intensity that evoked 50% of the maximal fEPSP amplitude and a typical fEPSP slope of 0.7-1 mV/ms. For LTP induction, after a stable baseline was established for at least 15 mins, LTP was induced by 4 bursts of high frequency stimulation (100 pulses at 100 Hz high-frequency stimulation (HFS) with 20 sec inter-burst interval (Oliet et al., 1997)). After HFS, the stimulation frequency was decreased to 0.033 Hz for another 40 mins. For LTD induction, after a stable baseline was established, LTD was induced chemically via bath-application of 100 μM DHPG for ten minutes under simultaneous synaptic stimulation. After ten minutes, DHPG was washed out and the stimulation frequency was maintained at 0.033 Hz for another 40 mins (Fitzjohn et al., 1999).

The slope of fEPSPs was measured in the first third of the rising phase (see also **Figure 2.2 B**). This value served as a measure of synaptic efficiency. The responses were

recorded at about 30 kHz sampling rate and analyzed with Igor Pro 5 (Wavemetrics, USA) using a customized macro.

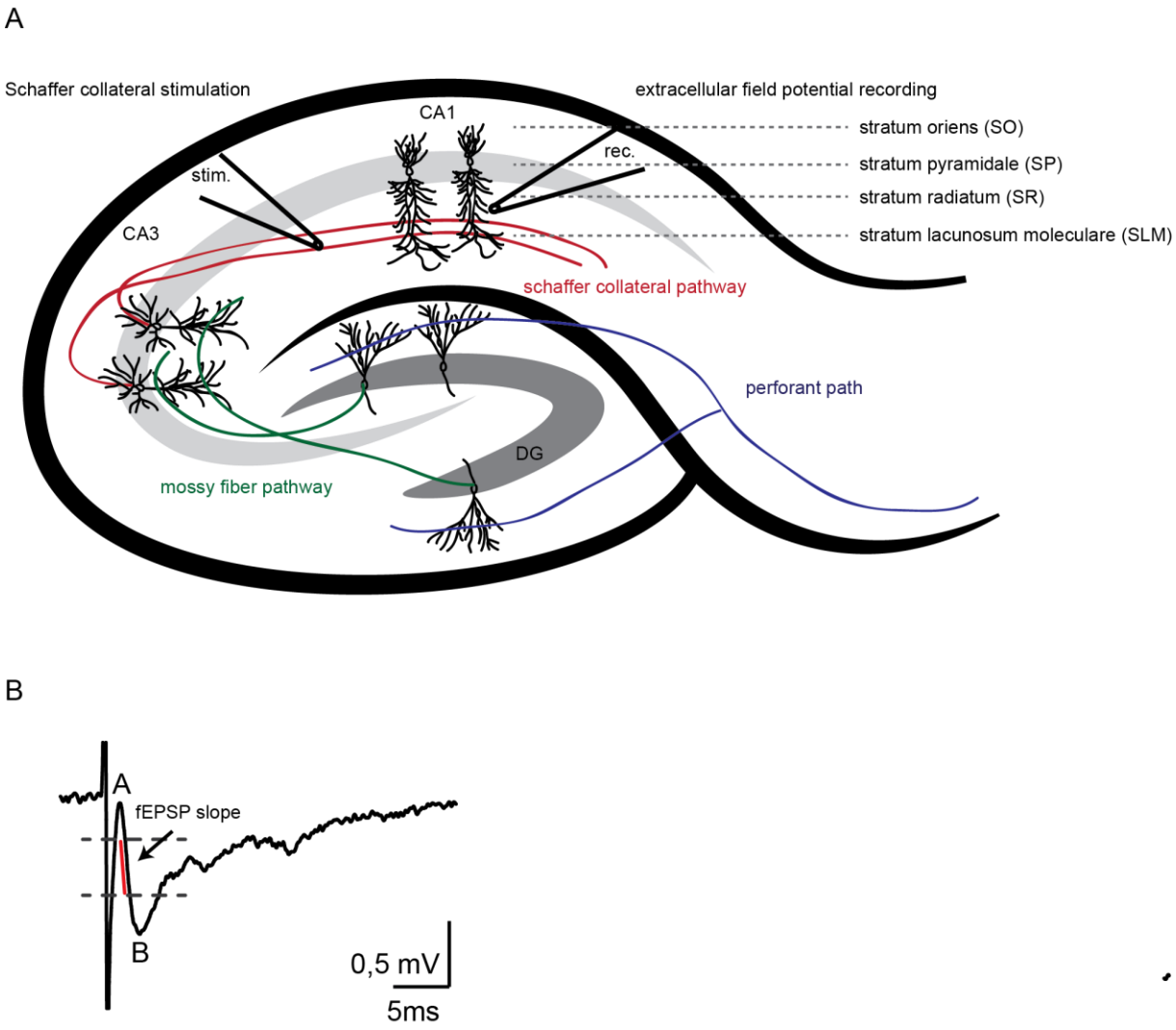

Figure 2.2 - Measurement of the slope of fEPSP in CA1

(A) The scheme depicts the hippocampal anatomy and experimental setting. The stimulation pipette (stim.) was placed close to the CA3 region in order to stimulate CA3 axon terminals on the Schaffer collateral pathway. The recording pipette was placed in stratum radiatum. (B) Representative trace of fEPSP for slope measurements. Point A represents the onset of the response (minimal amplitude) and B is the maximal amplitude of the response. The fEPSP slope is defined as the time and voltage difference between A and B (red line).

2.7 mRNA extraction and reverse transcription from CA1 tissue

CA1 tissue from different ages and genotypes was collected. Subsequently, mRNA was extracted using the NucleoSpin RNA Plus kit (Macheerey-Nagel, Germany). To eliminate genomic DNA, purified RNA was incubated in gDNA Wipeout Buffer (QuantiTect; Quiagen) for two minutes at 42°C prior to the reverse transcription step. Reverse transcription was performed by using the QuantiTect® Reverse Transcription kit (Quagen, Germany). After reverse transcription, 5 ng cDNA of each sample was used for further quantitative PCR analysis (see **section 2.9**).

2.8 mRNA extraction and reverse transcription from single cells

CA1 pyramidal neurons were harvested under visual control using a glass pipette (1-3 MΩ) filled with 50 mM Tris-HCl (pH8.3), 75 mM KCl, 3 mM $MgCl_2$ and 10 mM DTT (Promega, U.S.A) (Durand et al., 2006). After the pipette tip had reached the membrane of an individual CA1 pyramidal neuron, negative pressure was applied to suck the cell to into the tip of the pipette. The content of the pipette was then released into an RNAse-free Eppendorf-tube. The Eppendorf-tube was immediately transferred to liquid nitrogen and then placed at -80°C for long-term storage.

For reverse transcription reaction, cells were defrozen at 0°C and mixed with reverse transcription cell lysis buffer containing 2 mM dNTPs (Promega), 0.2% Igepal (Sigma), 40 U RNasin® Plus Rnase Inhibitor (Promega), 10 μM N6 random primers (Roche, Germany) at 70°C for five minutes. Subsequently, 200 U of MMLV reverse transcriptase (Promega) were added and the reverse transcription reaction was run at 37°C for two

hours. After reverse transcription, the QIAEX II gel extraction Kit (Qiagen, Germany) was used for cDNA clean-up.

2.9 Quantitative PCR with SYBR green

5 ng of tissue cDNA (see **section 2.7**) or 80% of the total extracted cDNA per cell (see **section 2.8**) were mixed with the qPCR reaction solution "LightCycler Faststart DNA Master SYBR Green I" (Roche) and 100 μM of primer sets (**Table 2**). 10% of the harvested material per cell or 5 ng of tissue cDNA was used for measuring the expression level of the house-keeping gene Glyceraldehyde dehydrogenase (*Gapdh*) as internal control for normalization. The primer sets and qPCR conditions are summarized in **Table 2 and 3**. The amplification of the product is reported by the increase in fluorescence of SYBR Green I. From the resulting fluorescence rising curves, the expression level of each gene was calculated by their so-called crossing point (Cp), at which the fluorescence rises above the noise level. For quantitative analysis, the expression level was calculated through the formula: expression level= 2^{-Cp}. The relative expression level of individual genes was normalized to *Gapdh*.

Since the majority of primers were not intron-spanning, original cell material was used as control for genomic DNA contamination in each reaction. Samples that showed positive signals without prior reverse transcription were discarded from further analysis.

2.10 Statistical analysis

Unless noted otherwise, data are presented as mean ± SEM and plotted with Sigmaplot 10 (Systat software, U.S.A). Statistical analysis was performed using SPSS 17 (IBM, USA). For two independent experimental groups, the independent Student's t-test was used for normally distributed data, and the Mann–Whitney U test was used for non-normally distributed data. For two related experimental groups, the paired Student's t-test was used for normally distributed data, and the Wilcoxon matched-pairs signed rank test was used for non-normally distributed data. Differences amongst more than two experimental groups were examined by a one-way ANOVA test (*post hoc* Least Significant Difference (LSD)). All images and figures were arranged by Adobe Illustrator (Adobe, U.S.A).

Table 1. list of drugs and reagents used in this study

Name	Aim	Concentration	Source	Note
Bicuculline	GABA-$_A$ receptor blocker	10 μM	Enzo	BML-EA1090050
Caffeine	Induce calcium release from RyR	40 mM	Sigma	C0750
Cyclopiazonic acid (CPA)	SERCA pump blocker	30 μM	Abcam	C1530
D600	VGCCs blocker	0.5 mM	Sigma	M5644
D-AP5	NMDA receptor blocker	30 μM	Abcam Tocris	Ab120003 0106
DHPG	Group1 mGluR agonist	0.5 mM	Abcam	Ab120007
Glutathione monoethyl ester	Slice preservation	1 mM	Santa cruz biotechnology	SC-203974
GYKI53655	AMPA receptor blocker	10 μM	Tocris	2555
Nickel	Calcium channel blocker	2 mM	Sigma	339350
Nifedipine	L-type calcium channel blocker	50 μM	Sigma	N7634
Nimodipin	L-type calcium channel blocker	50 μM	Sigma	N149
Omega-agatoxin IVA	P/Q type calcium channel blocker	200 nM	Peptide	4256
Ryanodine	Ryanodine receptor blocker	10 μM	Tocris	1329
Tetrodotoxin citrate (TTX)	Voltage gated sodium channel blocker	500 nM	Abcam	Ab120055
Reagents for single cell qPCR				
dNTPs		2 mM	Promega	U120-122D
Igepal C 630		0.2%	Sigma	I8896
LightCycler Faststart DNA Master SYBR Green I		20%	Roche	03003230001
MMLV		200U	Promega	M1701
N6 random primer		10 microM	Roche	11034731001
QXII-extraction kit			Qiagen	20021
RNasin Plus		40U	Promega	N2611

Table 2. List of primer pairs for single cell qPCR analysis

Gene (RefSeq)	Forward primer	Reverse primer	Size (bp)	Annealing temperature
Orai1 (NM 175423)	5'-CCT GTG GCC TGG TTT TTA TC-3'	5'-GTG CCC GGT GTT AGA GAA TG-3'	160	57°C
Orai2 (AM 712356)	5'-ACC ATG AGT GCA GAG CTC AA-3'	5'-GAG CTT CCT CCA GGA CAG TG-3'	162	57°C
Orai3 (NM 198424)	5'-GGG TAA ACC AGC TCC TGT TG-3'	5'-GCC TGG TCC ATG AGC ACT AT-3'	166	57°C
Stim1 (NM 009287)	5'-GGC CAG AGT CTC AGC CAT AG-3'	5'-TCC ACA TCC ACA TCA CCA TT-3'	200	57°C
Stim2 (NM 001081103)	5'-ATG TCG CTG AGT CCA CCT TG-3'	5'-TGC AGG TGA CTA TGT TTA TTC G-3'	179	57°C
Gapdh (BC 095932)	5'-AGG TCG GTG TGA ACG GAT TT-3'	5´-TGT AGA CCA TGT AGT TGA GGT CA-3	141	65°C

Table 3. qPCR experimental condition setting

	Orai1-3 and Stim1 and 2	Gapdh
MgCl2	2 mM	3 mM
Primer	0.5 μM	1.5 μM
Pre-incubation	95°C for 10 mins	95°C for 10 mins
Amplification (45 cycles)	95°C for 10 sec 57°C for 5 sec 72°C for 8 sec	95°C for 10 sec 59°C for 5 sec 72°C for 6 sec
Melting	65°C for 15 sec	65°C for 15 sec

3. Results

3.1 The role of Orai1-3 in mGluR1/5-mediated signaling in postnatal development

3.1.1 Postnatal developmental change of mGluR1/5-mediated calcium signaling in the absence of Orai2

In order to characterize group I mGluR-dependent signaling during development, the specific agonist DHPG (0.5 mM) was locally applied to the somata of whole-cell patch-clamped pyramidal neurons at postnatal periods P10-12, P13-16 and P17-22. Cells were dialyzed with OGB-1 through the patch pipette, and calcium imaging was performed concomitantly with the electrophysiological recording. At P10-12 and P13-16, DHPG-evoked calcium transients were observed in 80% of the cells (**Figure 3.1 A and B**). In electrophysiological recordings, a clearly discernable DHPG-mediated inward current (I_{DHPG}) was absent (**Figure 3.1 A**). This finding indicates that the DHPG-elicited calcium response does not result from calcium influx through the plasma membrane but from calcium release from internal stores.

In Purkinje cells, it was shown that mGluR1/5-mediated calcium release strongly depends on the replenishment of the intraluminal ER calcium concentration by the STIM/Orai complex (Hartmann et al., 2014; Hartmann and Konnerth, 2015). Orai2 is the most abundant Orai in CA1 (Lein et al., 2007). In order to study the role of Orai2 in the mGluR1/5 signaling pathway, a transgenic mouse line with the deletion of *Orai2* was used. I tested DHPG-responses in a global Orai2 knockout mouse line. At P10-12 and P13-16, mGluR1/5-mediated calcium signals in Orai2 knockout mice did not differ from

those recorded in wild type (WT; **Figure 3 A**, right and middle panel). At P10-12, 81% of the cells in WT and Orai2$^{-/-}$ responded to DHPG stimulation (**Figure 3.1 B**, left panel) with a median ΔF/F amplitude of 106% in WT and of 126.5% in Orai2$^{-/-}$ (**Figure 3.1 C**, left panel; not significant (n.s.): p=0.285). At P13-16, 86% of the cells in WT and 78% of the cells in Orai2$^{-/-}$ responded to DHPG stimulation (**Figure 3.1 B**, middle panel) with a median ΔF/F amplitude of 112% in both WT and Orai2$^{-/-}$, respectively (**Figure 3.1 C**, middle panel; n.s.: p=0.859). After P17, however, calcium transients mediated by activation of the mGluR1/5 signaling pathway could rarely be observed in Orai2$^{-/-}$ (**Figure 3.1 A,** right panel). At this developmental stage, 87% of the cells in WT but only 12.5% in Orai2$^{-/-}$ mice responded to DHPG stimulation (**Figure 3.1 B**, right panel) with a median ΔF/F amplitude of 67% in the WT and 0% in Orai2$^{-/-}$ (p<0.001) (**Figure 3.1 C**, right panel).

Changes in the fluorescence signal with regards to mean, delay, duration, and rise time of DHPG-evoked calcium transients in WT and Orai2$^{-/-}$ mice at the different postnatal developmental stages were analyzed. When only responsive cells were considered for calculation of the average, there was no significant difference in the calcium amplitudes of WT and Orai2$^{-/-}$ mice at P10-P12 (ΔF/F; WT: 112 ± 11.78%, Orai2$^{-/-}$: 137 ± 10.35%; p=0.126), P13-P16 (ΔF/F; WT: 133.83 ± 11.46%, Orai2$^{-/-}$: 148.71 ± 23.84%; p=0.495) and P17-P22 (ΔF/F; WT: 83.24 ± 8.88%, Orai2$^{-/-}$: 118.25 ± 36.83%; p=0.407) (**Figure 3.1 D**). Similarly, there was no significant difference in the delay time between both genotypes, although a slightly longer delay time was observed for P13-P16 in Orai2$^{-/-}$ mice (ΔF/F; WT: 0.93 ± 0.09%, Orai2$^{-/-}$: 1.47 ± 0.36%; p=0.237) (**Figure 3.1 E**). However, the duration of calcium signals was shorter in Orai2$^{-/-}$ mice at P10-P13 (WT:

16.44 ± 0.39 s, Orai2$^{-/-}$: 13.7 ± 0.85 s; p=0.03) (**Figure 3.1 F**). There was no significant difference in the rise time between genotypes at P10-P12 (WT: 1.69 ± 0.22 s, Orai2$^{-/-}$: 1.296 ± 0.2 s; p=0.112) and P13-P16 (WT: 1.7 ±0.21 s, Orai2-/-: 1.82 ± 0.2 s; p=0.455) (**Figure 3.1 G**). Taken together, these data indicate that Orai2 is important for mGluR1/5-mediated calcium signaling only later than P16.

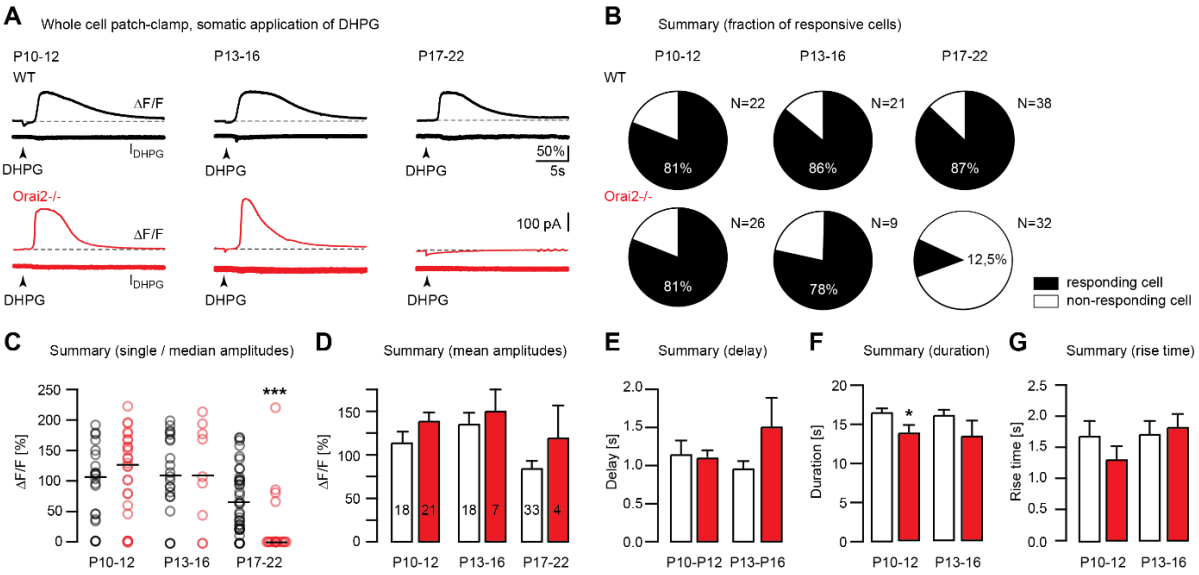

Figure 3.1- mGluR1/5-mediated calcium signals in the absence of Orai2 at different developmental stages

(A) Whole-cell patch-clamp recordings in combination with calcium imaging in CA1 pyramidal neurons of wild-type (WT) and Orai2$^{-/-}$ mice at different postnatal developmental stages. Cells were loaded with calcium indicator Oregon green BAPTA 1 (OGB-1, 0.1 mM). mGluR1/5 agonist, DHPG (0.5 mM; 10 psi for 200ms) was locally pressure-applied to the soma of pyramidal neurons in WT (upper, black) and Orai2$^{-/-}$ (bottom, red) mice. Relative fluorescence changes (ΔF/F) and the electrophysiological recording of DHPG-evoked current (I_{DHPG}) were measured at the soma. *Top traces:* Relative fluorescence changes (ΔF/F) in the soma. *Bottom traces:* the accompanying electrophysiological recording. **(B)** Fraction of DHPG-responding (black) and non-responding (white) cells in CA1 pyramidal neuron in WT (top) and Orai2 $^{-/-}$ mice (bottom) at P10-P12 (WT n=22; Orai2$^{-/-}$ n=28), P13-P16 (WT n=21; Orai2$^{-/-}$ n=9) and P17-P22 (WT n=38; Orai2$^{-/-}$ n=32). **(C)** Amplitude of DHPG-evoked calcium signals at the soma in WT and Orai2$^{-/-}$ during development. Each data point represents an individual measurement and lines represent the median of all measurements in each genotype and age group (same cell numbers in as in (B)). (n.s. p>0,05; *** p<0,001, Mann-Whitney-U-Test) **(D)** Mean amplitude ± standard error of the mean (SEM) of calcium transients at soma, quantified only in DHPG-responding cells at P10-P12 (WT n=18; Orai2$^{-/-}$ n=21), P13-P16 (WT n=18; Orai2$^{-/-}$ n=7) and P17-P22 (WT n=33; Orai2$^{-/-}$ n=4). (n.s. p>0,05, Mann-Whitney-U-Test) (E-G). Quantification of delay **(E)**, duration **(F)** and rising time **(G)** of DHPG evoked calcium transients in WT (black) and Orai2$^{-/-}$ mice (red) at P10-P12 and P13-P16. (n.s. p>0.05, Mann-Whitney-U-Test)

3.1.2 Expression of *Orai1-3* and *STIM1-2* during postnatal development

To characterize the regulation of *Orai2* during development, a quantitative RT-PCR analysis was performed on isolated hippocampal CA1 tissue from WT mice at P11, P18 and P60. The relative expression levels of five genes critically involved in calcium homeostasis (*Orai1-3* and *STIM1-2*) (Rosado et al., 2015; Varnai et al., 2009) were analyzed in relation to the housekeeping gene *Gapdh* (Huggett et al., 2005; Kozera and Rapacz, 2013).

I found that the amount of *Orai1* mRNA was highest at P11 and decreased during development (*Orai1/Gapdh*; P11: 2.45 ± 0.446% , P18: 1.2 ± 0.21586%, P60: 0.877 ± 0.106%) (**Figure 3.2 A**, left). Remarkably, during development *Orai2* showed a complementary pattern of expression to *Orai1*: The *Orai2* mRNA level at P11 was the lowest of the three measured time points and increased during development. At P60, the relative expression level of *Orai2* mRNA was the highest (*Orai2/Gapdh*; P11: 1 ± 0.253%, P18: 1 ± 0.272%, P60: 2 ± 0.411%) (**Figure 3.2 A**, middle). The expression of *Orai3* was low and did not change during development (*Orai3/Gapdh*; P11: 0.703 ± 0.131%, P18: 0.734 ± 0.146%, P60: 0.685 ± 0.0751%) (**Figure 3.2 A**, right). Akin to *Orai1,* the expression of *Stim1* decreased during development, (*Stim1/Gapdh*; P11: 3 ± 0.406%, P18: 2 ± 0.716%, P60: 2 ± 0.578%) (**Figure 3.2 A**, left). The expression of *Stim2* was low at P11 and increased from P11 to P18, similarly to *Orai2*, but there was only little change from P18 to P60 (*Stim2/Gapdh*; P11: 2 ± 0.863%, P18: 4 ± 0.645%, P60: 3 ± 1%) (**Figure 3.2 A**, right). The expression of *Orai1-3* was also measured in the absence of *Orai2* in the Orai2$^{-/-}$ mice. As expected, *Orai2* mRNA was not detectable in Orai2$^{-/-}$ mice, validating that there is indeed no gene transcription of *Orai2* in the

knockout. *Orai1* mRNA levels decreased during development in Orai2$^{-/-}$ mice. Similar to WT mice, the expression level of *Orai3* did not change during postnatal development in Orai2$^{-/-}$ mice (**Figure 3.2 A**, red bar). Taken together, these results show a developmental regulation of *Orai1/2* and *Stim1/2* expression.

Since in the hippocampal CA1 region many different cell types are present (such as glial cells and interneurons), the reported expression changes do not allow for direct conclusion about gene expression in CA1 pyramidal neurons. In order to address the question about the developmental profile of *Orai1/2* expression in these CA1 pyramidal neurons, I performed RT-qPCR on single CA1 pyramidal neurons at the three different postnatal stages.

Strikingly, the results of this analysis confirm the principal observations made on CA1 tissue: *Orai1* expression decreased during postnatal development (*Orai1/Gapdh*; P13: 8 ± 2.8%, P18: 2 ± 0.505%, P60: 0.914 ± 0.168%) (**Figure 3.2 C**, left); in contrast, the expression *Orai2* increased during postnatal development (*Orai2/Gapdh*; P13: 3 ± 0.699%, P18: 6 ± 3%, P60: 16 ± 3%) (**Figure 3.2 C**, right).

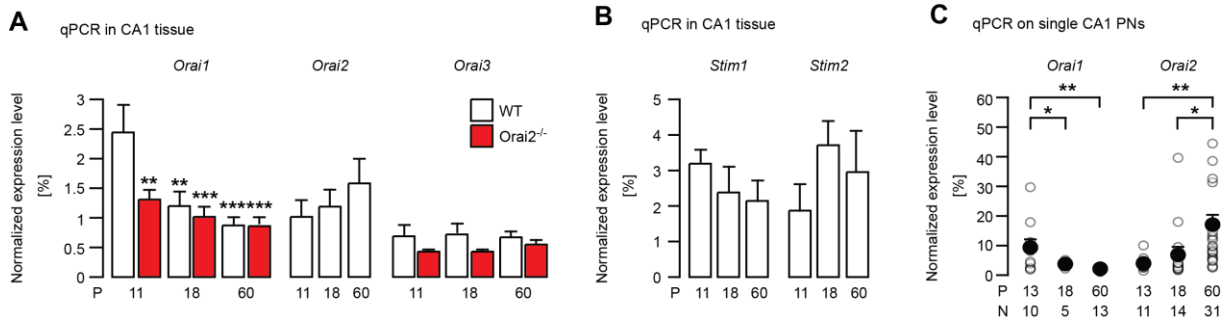

Figure 3.2- mRNA expression levels of *Orai1-3* and *Stim1-2* in CA1 tissue and *Orai1-2* in single CA1 pyramidal neurons during postnatal development.

(A-B) qPCR analysis from CA1 tissue showing the relative mRNA expression levels of *Orai1-3* (**A**, left to right) and **(B)** *STIM1-2* at P11, P18 and P60 in WT (white) and Orai2$^{-/-}$ mice (red) (** p<0,01, *** p<0,001, one-way ANOVA, post hoc: LSD; n=3, mean ± SEM). **(C)** Single-cell qPCR analysis of *Orai1* (left) and *Orai2* (right) mRNA expression from CA1 pyramidal neurons at different developmental stages: P13 (*Orai1* n=10; *Orai2* n=11), P18 (*Orai1* n=5; *Orai2* n=14) and P60 (*Orai1* n=13; *Orai2* n=31). Each unfilled circle represents an individual measurement, a solid black circle (and the accompanying line) indicates the mean ± SEM for each age group. (* p<0.05, ** p<0.01, one-way ANOVA, post hoc: LSD). All mRNA expression data were normalized to *Gapdh.*

3.1.3 Role of Orai1 and 3 are crucial for mGluR1-5 signaling in CA1 pyramidal neurons in early postnatal development

The developmental profile of DHPG-responsiveness in CA1 pyramidal neurons could be a result of changes in gene expression during postnatal development. To address this hypothesis, I applied DHPG to the somata of whole-cell patch-clamped CA1 pyramidal neurons and tested the sensitivity of the resulting calcium responses after bath application of GSK7975, an Orai1/3-specific antagonist, for 30 min prior to DHPG stimulation. Application of GSK7975 largely reduced DHPG-mediated calcium responses in WT and Orai2$^{-/-}$ at P10-12 (**Figure 3.3 A**). The amplitude of calcium transients evoked by DHPG stimulation were dramatically reduced in the presence of GSK7975, both in WT (∆F/F; before: 147.4 ± 21%, after: 5.63 ± 1.69%, p<0.001) and Orai2$^{-/-}$ (∆F/F; before: 130.5 ±16.3%, after: 11.25 ± 1.4%, p<0.001) mice (**Figure 3.3 B**). This finding supports the hypothesis that Orai1 and Orai3 are important for mGluR1/5-signaling during early postnatal development.

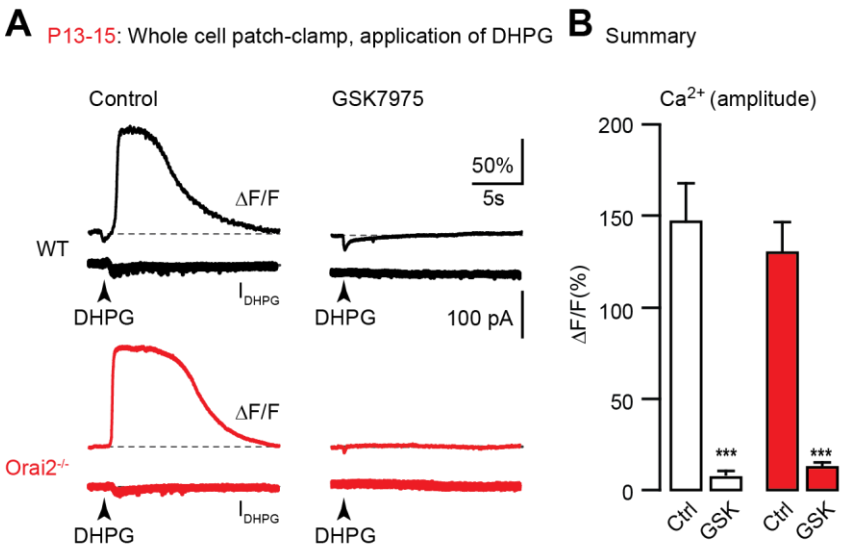

Figure 3.3- Calcium signals induced by local DHPG application in CA1 pyramidal neuron before P17 is sensitive to Orai1 and 3 antagonists, GSK7975.

(A) DHPG-elicited calcium transients and I_{DHPG} in WT (black) and Orai2$^{-/-}$ (red) in normal ACSF for control (left) and in 0.025 mM GSK7975 (right). **(B)** Mean relative calcium amplitude in Ctrl-ACSF (black) (WT n=5; Orai2$^{-/-}$ n=4) and in GSK7975 (white) (WT n=14; Orai2$^{-/-}$ n=12). (*** p<0.001, one-way ANOVA, post hoc: LSD)

3.1.4 Caffeine-mediated calcium signaling in the absence of Orai2

After having established the importance of Orai2 for IP_3R-dependent calcium signaling during late stages of postnatal development, I went on to address the question about its role for RyR-dependent calcium release. Similar to previous experiments, I locally pressure-applied caffeine (40 mM, 3 sec) to the somata of CA1 pyramidal neurons before P17 (P10-P16) and after P17 (P17-P22) in order to compare the resulting calcium responses in WT and Orai2$^{-/-}$ mice. Caffeine elicited robust calcium transients in WT and Orai2$^{-/-}$ mice at both developmental stages (before P17 and after P17) (**Figure 3.4 A**). There was no significant difference in the calcium transient amplitude at P10-P16 (Δ F/F; WT: 86 ± 12.30%, Orai2$^{-/-}$: 134 ± 26.36%, p=0.13) (**Figure 3.4 B**, left) and at P18-P22 (WT: 110 ± 21.68%, Orai2$^{-/-}$: 118 ± 10.71%, p=0.878) (**Figure 3.4 B**, right). In

summary, Orai2 has no role in the regulation of Ry-sensitive calcium in CA1 pyramidal neurons at any of the tested postnatal stages.

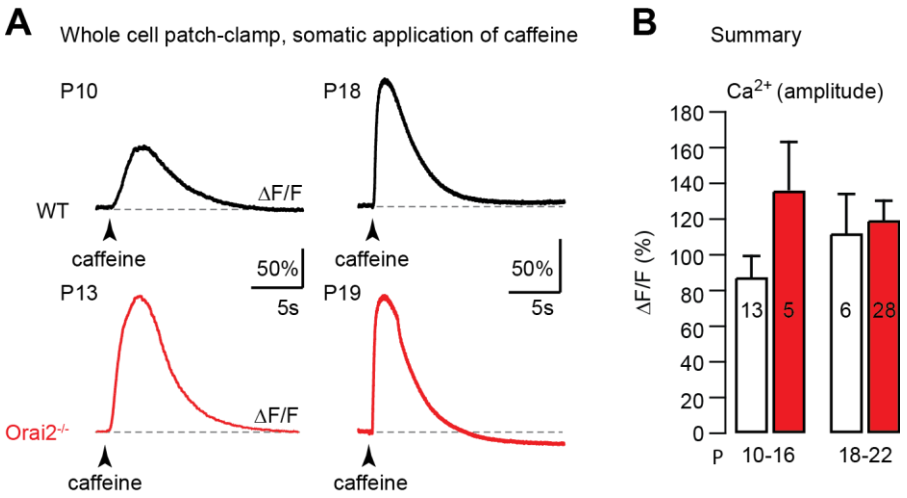

Figure 3.4- Caffeine-induced somatic calcium signals at different postnatal stages

(A) Local caffeine (40 mM; 10 p.s.i for 3 sec) application evoked calcium transients in the soma of CA1 pyramidal neurons in WT (*black*) and Orai2$^{-/-}$ (*red*) mice at P10-16 (*left*) and P17-22 (*right*). **(B)** Bar graph shows the mean ΔF/F amplitude ± SEM of caffeine-elicited calcium signals at the soma in WT (*black*) Orai2 $^{-/-}$ (*red*) and at P10-P16 (*left*, WT n=13; Orai2$^{-/-}$ n=5) and P17-P22 (*right*, WT N=6; Orai2$^{-/-}$ N=28). (n.s. p>0.05, Mann-Whitney-U-Test)

3.2 Properties of IP_3- and RyR-mediated calcium signaling in CA1 pyramidal neurons

3.2.1 Role of Orai2 for IP_3R-mediated calcium release

It is conceivable that in mature CA1 pyramidal neurons the group I mGluR-mediated calcium release signals in the absence of Orai2 could be impaired due to interruption of the signaling cascade downstream of the receptor. Alternatively, the IP_3-sensitive ER calcium stores could be depleted as a result of the absence of a replenishing mechanism as was shown for Orai1 in different cell types (Lewis, 2011; Prakriya and Lewis, 2015). To test these alternative hypotheses, I aimed to directly stimulate IP_3

receptors while bypassing the activation of mGluR1/5. To this end, I used the technique of IP_3 uncaging. Whole-cell patch-clamped CA1 pyramidal neurons at P18 were dialyzed with NPE-caged IP_3 (0.4 mM) together with the calcium indicator OGB-1. After five to ten minutes in the whole-cell configuration, DHPG was locally pressure-applied to the soma. Two minutes later, the cell was illuminated with a short UV pulse (375 nm, 50 ms, 15 mW) through a lensed fiber to induce the photolytic release of IP_3. The vast majority of cells showed DHPG- and IP_3-evoked calcium responses in WT mice at P17-P20 (**Figure 3.5 A**, left; 9/10 cells responsive). With the same stimulation protocols, neither DHPG- nor IP_3- mediated calcium responses were observed in the vast majority of cells in Orai2$^{-/-}$ mice (**Figure 3.5 A**, right; 1/8 cells responsive). The median $\Delta F/F$ amplitude in WT mice was 66% and 0% in Orai2$^{-/-}$ mice. The mean amplitude of the calcium transients was 63.2 ± 10.6 % in WT mice and 11.5 ± 11.5% in Orai2$^{-/-}$: mice ($p<0.01$) (**Figure 3.5 B**, upper). All of the tested cells (10 cells tested) in WT mice were responsive to IP_3-uncaging, but only 12.5% (1/8 cells tested) in Orai2$^{-/-}$ mice exhibited an IP_3-mediated calcium signal (median ($\Delta F/F$); WT: 84.5%, Orai2$^{-/-}$: zero mean: WT: 76.1 ± 9.04%, Orai2$^{-/-}$: 13.25 ± 13.25%, $p<0.01$) (**Figure 3.5 B**, bottom).

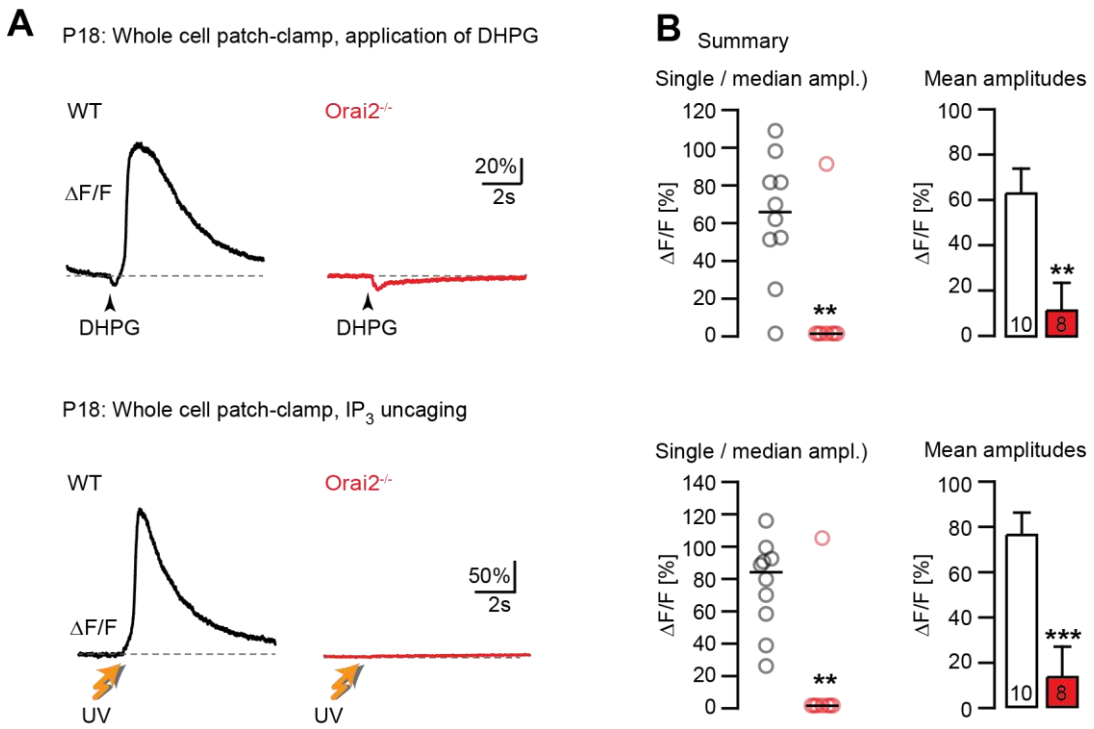

Figure 3.5- Impairment of IP_3-mediated calcium signals in the absence of Orai2

Cytosolic calcium transients were evoked by somatic DHPG pressure application (*top*) and photolytic release of IP_3 (*bottom*) in WT (*black*) and Orai2$^{-/-}$ (*red*) mice at P17-22. **(B)** Scatter plots (*left*) illustrate DHPG- (*top*) and of IP_3-elicited (bottom) ΔF/F amplitude. Each circle represents an individual recording in WT (black, n=10) and Orai2$^{-/-}$ mice (red, n=8), respectively. The line (black) indicates the median value of ΔF/F for each group. Bar graphs (right) indicate the mean amplitude of IP_3-mediated calcium signals by DHPG-application (*top*) and IP_3 uncaging (*bottom*) application. (** p<0.01; *** p<0.001; Mann-Whitney-U-Test)

3.2.2 Role of Orai2 for IP_3R-dependent calcium release evoked by back-propagating action potentials (bAPs)

It was previously shown that in CA1 pyramidal neurons IP_3R-dependent calcium release can be evoked by pairing bAPs with tonic stimulation of mGluR1/5 by bath application of DHPG (Nakamura et al., 2000). Both bAPs and IP_3R-dependent calcium release in spines play a crucial role for synaptic integration and certain types of synaptic plasticity (Sjostrom and Nelson, 2002; Zucker, 1999). In order to elucidate a possible involvement of Orai2 in these processes, I repeated the experimental design of Nakamura and

colleagues in WT and Orai2$^{-/-}$ mice (Nakamura et al., 2000). To this end, CA1 pyramidal neurons in acute hippocampal slices from P17-20 mice were dialyzed with the calcium indicator OGB-1 in the whole-cell current-clamp mode and four action potentials were induced by somatic current injection. The resulting calcium signals were recorded at the soma and the primary dendrite before and after DHPG bath application (**Figure 3.6 A**). In WT mice, bAPs induced a robust calcium signal under control conditions (**Figure 3.6 B**, left). The same current injection, however, in the presence of 0.01 mM DHPG was followed by a significantly larger and longer-lasting calcium transient (**Figure 3.6 B**, middle and right). In Orai2$^{-/-}$ experiments, the calcium signals that followed the four bAPs under control conditions were similar to those seen in WT mice (**Figure 3.6 C and D**, left; mean amplitude in the soma: ΔF/F; WT: 60.08 ± 5.66%, Orai2$^{-/-}$: 54.6 ± 4.84%, p=0.454; mean amplitude in the dendrite: ΔF/F; WT: 210 ± 33.12%, Orai2$^{-/-}$ 178 ± 14.53%, p=0.589). This indicates that the function of VGCCs is not affected by the absence of Orai2. However, in contrast to the wild type, in Orai2$^{-/-}$ mice DHPG failed to potentiate the bAPs induced calcium signal (**Figure 3.6 C,** middle and right). Bath-application of DHPG increased the amplitude of bAPs-induced calcium transients by ca. 150% both in the soma and the dendrite in WT mice. In Orai2$^{-/-}$ mice, in contrast, there was no difference between amplitudes of bAPs-induced calcium transient between both conditions. The ratio between both amplitudes is close to one and thus, highly significantly different between both genotypes. (**Figure 3.6 D**, right). Subtracting bAPs-evoked calcium transients recorded under control conditions from those measured in the presence of DHPG fully revealed the difference between both genotypes (median amplitude of the resulting transients ΔF/F: WT: 79.5%, Orai2$^{-/-}$: -2.5%; mean amplitude ΔF/F: WT: 75.2 ± 36.1%, Orai2$^{-/-}$: -3.3 ± 8.5%; p<0.01) (**Figure 3.6 E**, left and right).

These results again showed that Orai2 is required for IP_3-mediated calcium release in CA1 pyramidal neurons.

3.2.2 Independence of IP_3- and ryanodine (Ry)-sensitive ER calcium stores in CA1 pyramidal neurons

So far, my experiments have shown that IP_3R-mediated calcium stores appear to be devoid of releasable calcium ions in Orai2$^{-/-}$ mice. On the contrary, the filling state of Ry-sensitive stores appears to be unchanged in Orai2$^{-/-}$ mice. In order to study whether there is a crosstalk between IP_3- and Ry-sensitive calcium pools, I pressure-applied both agonists (DHPG and caffeine) alternately to the somata of the same CA1-pyramidal neurons in acute hippocampal slices from P17-19 mice. Cells were whole-cell patch-clamped and dialyzed with OGB-1 to measure the relative change of the cytosolic calcium concentration. Five to ten minutes into the whole-cell configuration, cells were consecutively stimulated with DHPG and caffeine with a 15-20 s long inter-stimulus interval (ISI). In WT mice, both local pressure application of DHPG and caffeine successfully evoked robust calcium transients during the first stimulation cycle. During the second and third cycle, the amplitude of DHPG-elicited calcium transient showed a gradual decrease (**Figure 3.7 A**, upper). The same stimulation protocol was performed in Orai2$^{-/-}$ mice. Here, the DHPG-mediated calcium signal was absent from the beginning but the caffeine-mediated calcium signal was intact in the first round of stimulation.

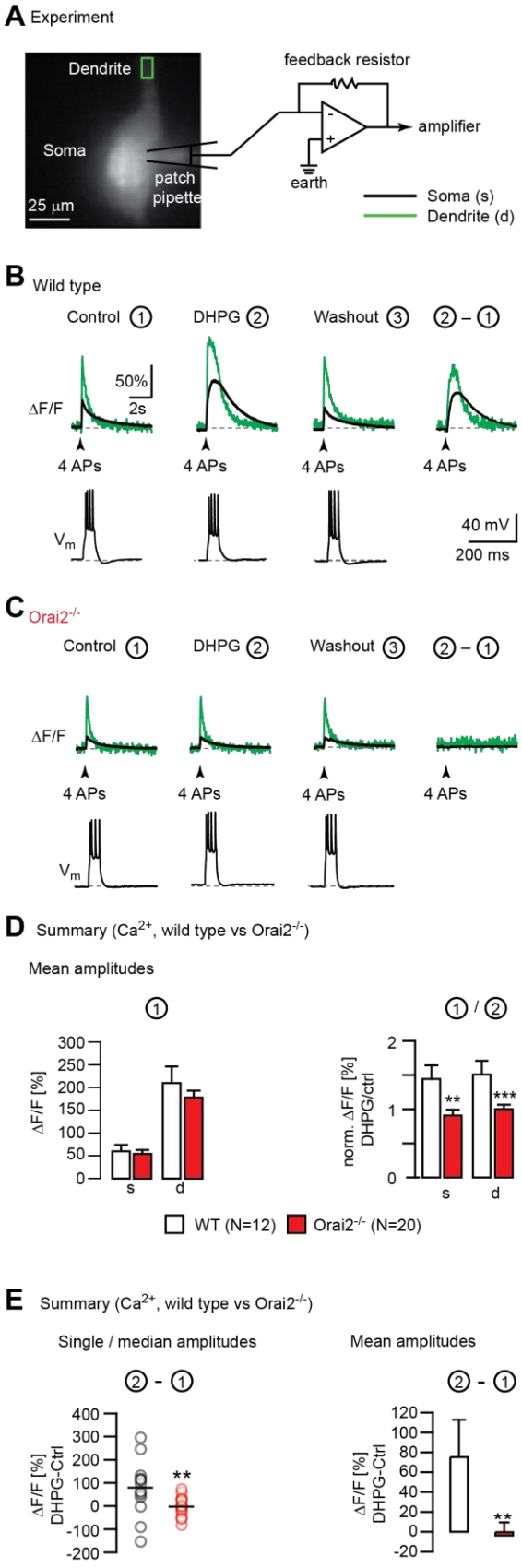

Figure 3.6- Absence of Orai2 abolishes the effect of DHPG on bAPs-evoked calcium signals.

(A) Confocal image of the soma and primary dendrite of a CA1 pyramidal neuron filled with OGB-1. Changes of OGB-1 fluorescence signals were measured in the soma (s) and primary dendrite (d). **(B-C)** Calcium transients were evoked by four actions potentials by somatic current injection to the soma under control ACSF and after bath-application of DHPG (0.01 mM) in **(B)** WT and **(C)** Orai2$^{-/-}$ mice. The upper traces show the relative changes of OGB-1 fluorescence at the soma (black) and dendrite (green). The bottom traces show the action potentials recorded at the soma. **(D)** Bar graph illustrates the mean ΔF/F amplitude evoked by bAPs in ACSF (left) and the ratio of the mean ΔF/F calcium amplitudes (DHPG vs. control) (right). **(E)** The Scatter plot (left) shows the difference between the ΔF/F amplitudes in control ACSF and in the presence of DHPG in individual cells. Bar graph (right) shows the mean difference between calcium signal amplitudes in the presence of DHPG and in control ACSF in the soma (s) and dendrites (d) in WT (*black*) and Orai2$^{-/-}$ (*red*) mice. Each bar indicates mean ± SEM. (** p<0.01, *** p<0.001; student t-test)

In summary, all eleven cells tested in WT mice were responsive to both DHPG and caffeine in the first round of stimulation. In contrast to WT cells, only 12.5% (2/16) of tested Orai2$^{-/-}$ cells showed a response to DHPG; however, all tested Orai2$^{-/-}$ cells responded to caffeine (**Figure 3.7 B**, left). Accordingly, the median (ΔF/F; WT: 52%, Orai2$^{-/-}$: zero) and mean (ΔF/F; WT: 96.7 ± 15.4%, Orai2$^{-/-}$: 111.9 ± 13.9%) amplitude of DHPG-evoked calcium transients is significantly different by a large margin, while caffeine-evoked calcium transients were not found to be significantly different (**Figure 3.7 B,** left and middle).

In WT mice, the DHPG-mediated calcium responses gradually decreased from the first stimulation to the third stimulation, while the caffeine response was sustained (**Figure 3.7 A**, top). In the Orai2$^{-/-}$ mice (see also **Figure 3.1**), DHPG failed to evoke calcium transients from the beginning while the calcium signals in response to caffeine gradually decreased in Orai2$^{-/-}$ mice similar to the WT (**Figure 3.7 A**, bottom).

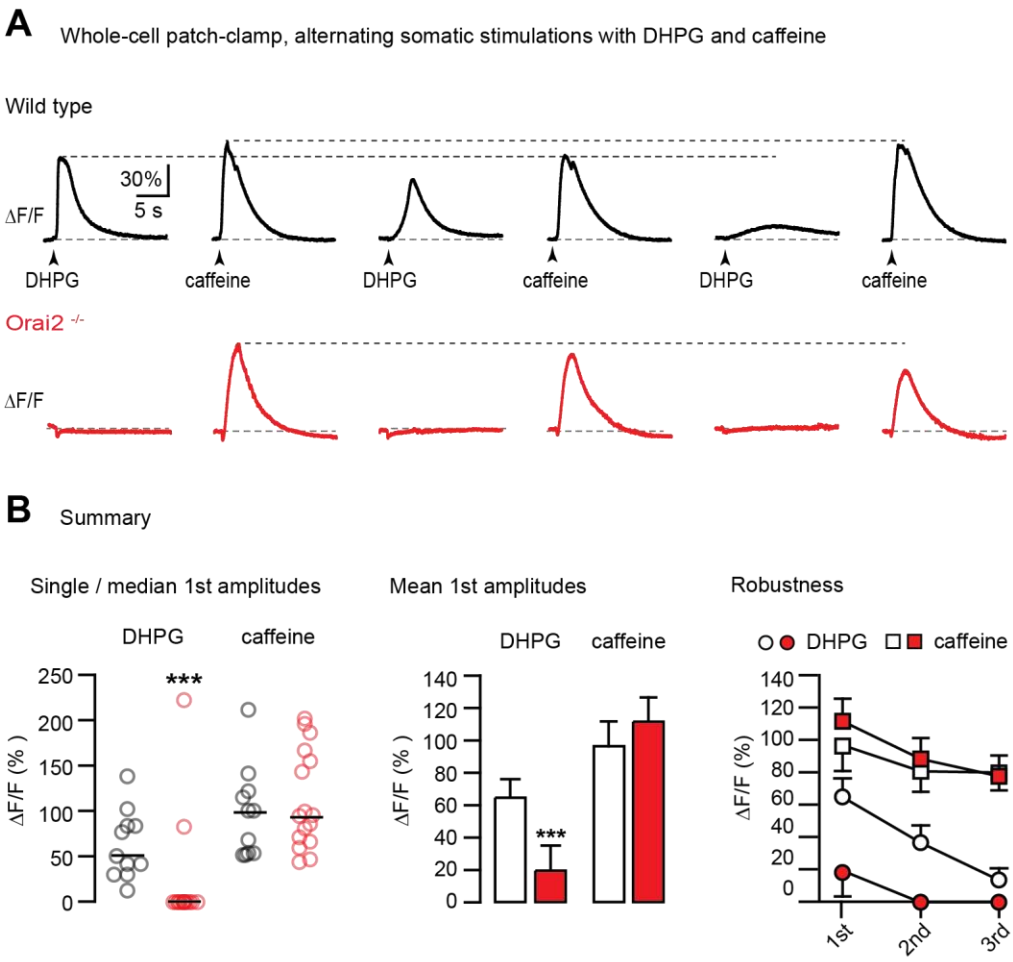

Figure 3.7- Alternating local DHPG- and caffeine applications to somata of CA1 pyramidal neurons

(A) Calcium transients elicited by local application of DHPG and caffeine to the soma of whole-cell patch-clamped CA1 pyramidal neurons in WT (*black*) and Orai2$^{-/-}$ (*red*) mice. **(B)** Scatter graph (*left*) shows the single ΔF/F values in individual cells in response to DHPG and caffeine. The line shows the median of each data pool. *Middle*: Mean amplitude of relative fluorescence changes (ΔF/F) (*** p<0.001, Mann-Whitney-U-Test). *Right*: Scatter line graph (right) illustrates the summary of cell responses to alternate DHPG (circle) and caffeine (square) stimulation for three cycles in WT (white, n=11) and Orai2$^{-/-}$ mice (red, n=16).

In another series of experiments, I replaced local DHPG-application with IP_3-uncaging performed (see above) to directly monitor IP_3-mediated calcium release. To this end, I consecutively stimulated the cell with local caffeine puff application and exposed the cell to UV light to release IP_3 from the NPE cage. This was done with an ISI of 15-20 s for

three to six cycles until the calcium response to IP_3 uncaging was depleted. In WT mice, photolytically-induced release of IP_3 and local caffeine application reliably evoked calcium transients in the first cycle (9/9 cells). During the next cycles, the IP_3-mediated calcium signal showed gradual decline while the caffeine-mediated calcium transients remained robust (**Figure 3.8 A**, upper). Moreover, the IP_3-mediated calcium pool was recharged after the cell was allowed to recover for five minutes at resting membrane potential (**Figure 3.8 A**, last panel) as indicated by the recovery of the IP_3 responsiveness of cells. Similar to previous experiments, in Orai2$^{-/-}$ cells the photolytic release of IP_3 largely failed to evoke calcium transients (**Figure 3.8 B and D**, left; only 1/15 cells responsive). Furthermore, the caffeine-elicited calcium signal was intact (**Figure 3.8 A**, bottom) in Orai2$^{-/-}$ cells as indicated by robust caffeine-mediated calcium signals and rapid recovery from partial reduction (**Figure 3.8 C**). The difference in the amplitude of the first IP_3-evoked calcium transient is highly significant for Orai2$^{-/-}$ cells (**Figure 3.8 D** left and middle; median of $\Delta F/F$; WT: 66.5%, Orai2$^{-/-}$: zero; mean: WT: 63.5 ± 8.5%, Orai2$^{-/-}$: 2.8 ± 2.8%). However, I did not find an obvious difference in the amplitude of caffeine-mediated calcium transients for both genotypes (**Figure 3.8 D,** left and middle; median of $\Delta F/F$; WT: 42.5%, Orai2$^{-/-}$: 60%; mean of $\Delta F/F$; WT: 56.0 ± 9.2%, Orai2$^{-/-}$: 52.2 ± 7.6%). Moreover, in both genotypes the amplitude of caffeine-mediated calcium release signals was unchanged by the decrease of the IP_3-mediated calcium signals during subsequent stimulations (**Figure 3.8 D,** right).

In summary, these results provide evidence that in pyramidal CA1 cells, IP_3Rs and RyRs release calcium ions from two largely non-overlapping calcium pools. Moreover, only one of the pools - the IP_3-sensitive calcium pool - is regulated by Orai2.

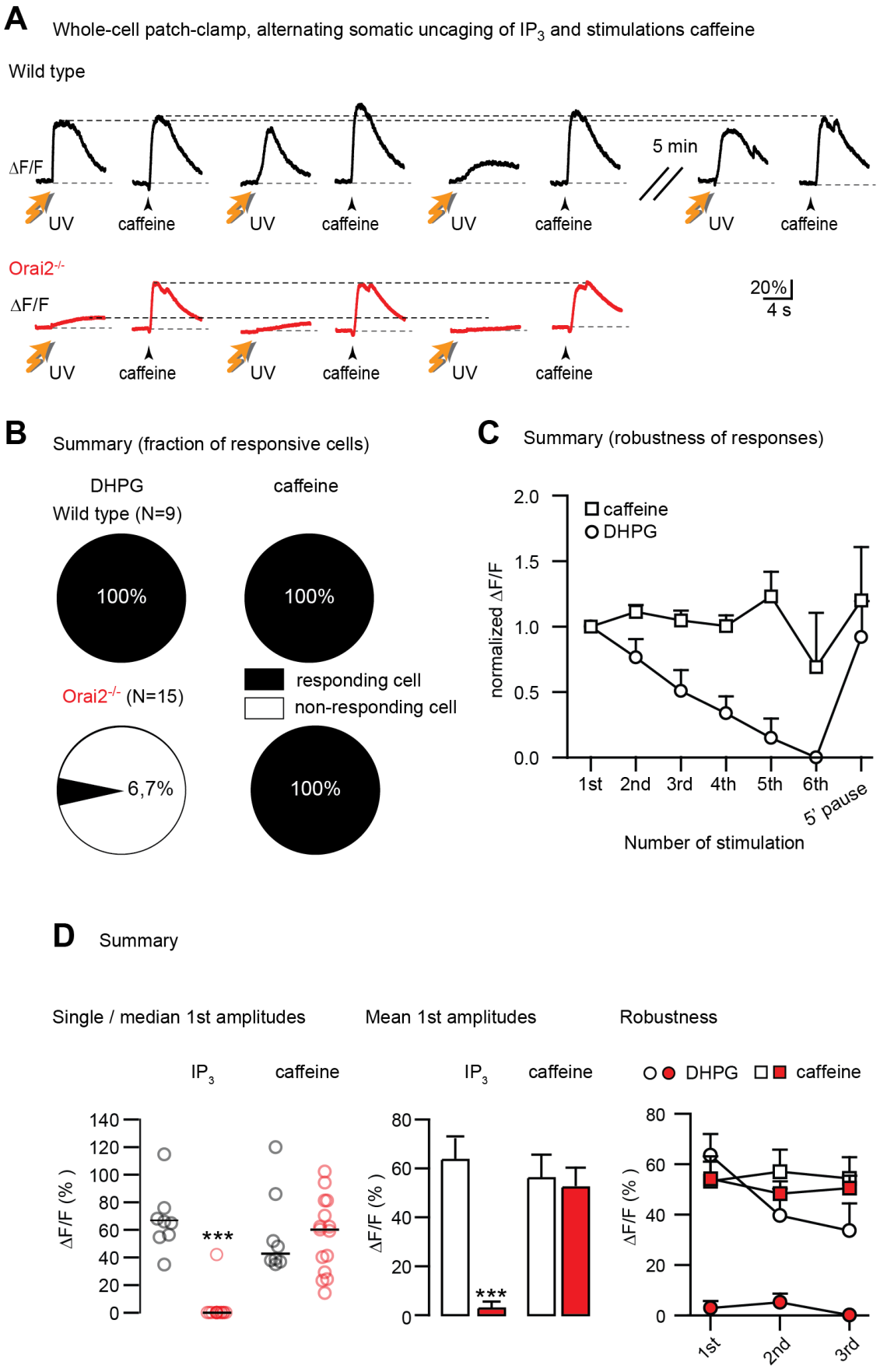
A
Whole-cell patch-clamp, alternating somatic uncaging of IP3 and stimulations caffeine
Wild type
ΔF/F
UV
caffeine
5 min
Orai2-/-
20%
4 s
B
Summary (fraction of responsive cells)
DHPG
caffeine
Wild type (N=9)
100%
Orai2-/- (N=15)
6,7%
responding cell
non-responding cell
C
Summary (robustness of responses)
caffeine
DHPG
normalized ΔF/F
2.0
1.5
1.0
0.5
0.0
1st
2nd
3rd
4th
5th
6th
5' pause
Number of stimulation
D
Summary
Single / median 1st amplitudes
Mean 1st amplitudes
Robustness
IP3
caffeine
DHPG
ΔF/F (%)
***
1st
2nd
3rd

Figure 3.8- Alternating uncaging of IP_3 and caffeine application to somata of CA1 pyramidal neurons

(A) Calcium transients evoked by IP_3 uncaging and local caffeine application in the somata of whole-cell patch-clamped CA1 pyramidal neurons in WT (*black*) and Orai2$^{-/-}$ (*red*) mice. Responses were evoked in an alternating manner with an interval of 15-20 s for at least three cycles until complete cessation of one of the responses. Cells were stimulated again after 5 min (*last panel*). **(B)** Pie charts represent the fraction of responding (black) and non-responding cells (white) to the given DHPG and caffeine stimulation in WT (*top*) and Orai2$^{-/-}$ (*bottom*) mice. **(C)** Scatter line graph of the mean $\Delta F/F$ amplitude of IP_3- (circle) and caffeine- (square) evoked calcium transients in WT mice. **(D)** Scatter graph (*left*) shows individual calcium signal amplitudes ($\Delta F/F$) of the first pair of responses evoked by IP_3 uncaging and caffeine application in WT (*black*, n=9) and Orai2$^{-/-}$ (*red*, n=15) mice. The black lines indicate the median values. *Middle*: Bar graph shows the mean amplitudes ($\Delta F/F$) of the first pair of IP_3- and caffeine-elicited calcium transients in WT and Orai2$^{-/-}$ mice. Right: Scatter line graph demonstrating the calcium signal amplitude changes in each stimulation cycle for IP_3 uncaging (*circle*) and caffeine application (*square*) in WT (*left*) and Orai2$^{-/-}$ (*red*). (n.s. $p>0.05$; *** $p<0.001$, Mann-Whitney-U-Test)

3.2.3 Partial overlap between caffeine- and IP_3-sensitive ER Ca^{2+} stores

The observation of **Figure 3.7 A** shows that in Orai2$^{-/-}$ mice repeated caffeine-responses result in a decrease of calcium, whereas in WT mice they are completely robust. This finding indicates that a fraction of the ER calcium content is shared between the Orai2-dependent IP_3-senstive and the Orai2-independent Ry-sensitive calcium pools. I performed additional experiments to elucidate to which degree there is crosstalk between IP_3- and Ry-sensitive ER Ca^{2+} stores. To this end, CA1 pyramidal neurons were whole-cell patch-clamped in acute hippocampal slices of P17-19 WT mice and filled with OGB-1. Shortly (15 s) after a first local puff application of DHPG the Ry-sensitive stores were emptied by six consecutive caffeine applications and the DHPG stimulation was repeated 15 s after the last caffeine pulse (**Figure 3.9 A**)

In order to completely and irreversibly empty Ry-sensitive calcium stores, 0.01 mM ryanodine was added to the bath solution, while caffeine and DHPG were locally pressure-applied. As expected, ryanodine eliminated the caffeine-mediated calcium

signal effectively. Moreover, six consecutive caffeine applications were not able to block the DHPG-induced calcium signal (**Figure 3.9 A** and **Figure 3.9 B**, left).

However, bath-application of ryanodine could not completely block DHPG-mediated calcium signals but showed a limited effect. The mean amplitude of DHPG-evoked calcium transients was 107.5 ± 7.4% ($\Delta F/F$) before perfusion with ryanodine and 91.1 ± 10.8% in the presence of ryanodine (**Figure 3.9 B**, right). This experiment was performed also in the reverse order, by stimulating RyRs with caffeine before and after emptying the stores with repeated consecutive DHPG-applications. Again, the caffeine-mediated calcium transients persisted after the complete rundown of DHPG responses (**Figure 3.9 C**). The amplitude of DHPG-evoked calcium signals was 15 % smaller after the Ry-sensitive stores were emptied with six consecutive caffeine puffs (**Fig. 3.9 A**) than at time point one (**Figure 3.9 D**, left). Analogously, emptying the IP_3-sensitive store lowers caffeine responses on average by 20% (**Figure 3.9 D**, right). Taken together, these data demonstrate that there are distinct ER calcium stores in CA1 pyramidal neurons, of which the first is sensitive to IP_3 and the second is sensitive to Ry. Nevertheless, the two mentioned pools do not seem to be mutually exclusive but share 15-20% of their respective calcium pool.

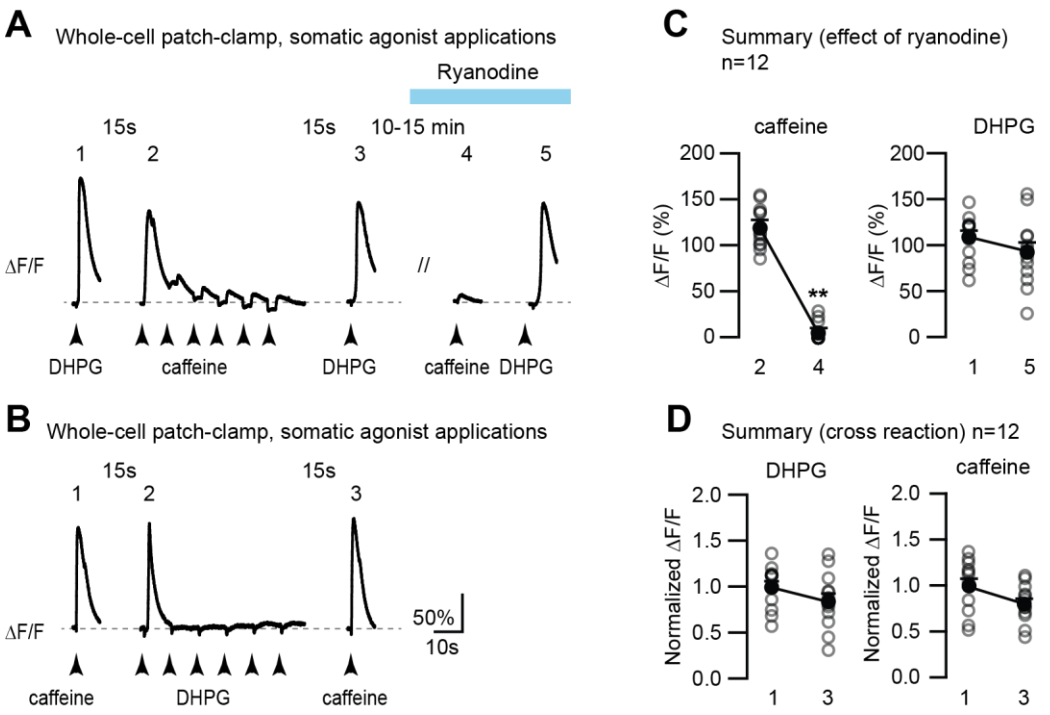

Figure 3.9- Independence of DHPG- and caffeine-evoked calcium transients in CA1 pyramidal neurons

(A) Traces showing fluorescence transients resulting from repeated alternating DHPG (#1 and #3) and caffeine (#2) applications (as indicated) to the soma of a whole-cell patch-clamped CA1 pyramidal neuron under control conditions and in the presence of ryanodine. Scaling is identical to (B). **(B)** Analogous experiment to A with a reversed order of caffeine and DHPG-applications. **(C)** Scatter graph shows the amplitude of caffeine evoked calcium transients before (#2) and after (#4) ryanodine bath-application (*left*), and DHPG mediated calcium signal before (#1) and after (#5) ryanodine application (*right*). Numbers under the graphs correspond to time points indicated in the example experiment shown in A. **(D)** Scatter graph illustrates the change in the amplitude of calcium transients evoked by DHPG stimulation before (#1) and after (#3) six consecutive caffeine pulses (*top*, n=12) and caffeine stimulation before (#1) and after (#3) six consecutive DHPG pulses (*bottom*, n=12). *White*: Individual calcium transient amplitudes (ΔF/F) normalized to the mean amplitude of DHPG or caffeine-evoked transients at time points 1 (#1) in A and B, respectively. *Black*: Mean ± SEM for each data pool. (*** p<0.001; n.s p>0.05, Wilcoxon signed rank test)

3.2.4 Time course of refilling of the IP_3-sensitive calcium store in CA1 pyramidal neurons

The properties of the Ry-sensitive calcium stores in CA1 pyramidal neurons have been extensively characterized (Garaschuk et al., 1997). The existence of a second type of

ER calcium store in CA1 pyramidal neurons is a novel discovery and thus the IP_3-sensitive, Ry-insensitive pool has not been studied in detail. Garaschuk and colleagues established a protocol to characterize the spontaneous refilling rate of the Ry-sensitive store via paired-pulse stimulation of caffeine with different inter-pulse intervals (Garaschuk et al., 1997). I adopted this stimulation protocol to study the spontaneous refilling rate of the IP_3- sensitive calcium store. The CA1 region in acute hippocampal slices was stained with the calcium indicator, Cal-520 AM to monitor change of the somatic calcium concentration of CA1 pyramidal neurons. IP_3R-dependent calcium release was activated by paired-pulse local DHPG application with 20, 30, 50, 80 and 110 s inter-pulse intervals. **Figure 3.10 A** shows a representative experiment with superimposed traces aligned to the time point of the first stimulation (102 paired-pulse DHPG applications were performed in 51 cells). The normalized mean amplitude of DHPG-evoked calcium transients is shown in **Figure 3.10 B**. The pooled data were fitted with a single exponential function that yielded a recovery constant of $\tau = 62.14$ s.

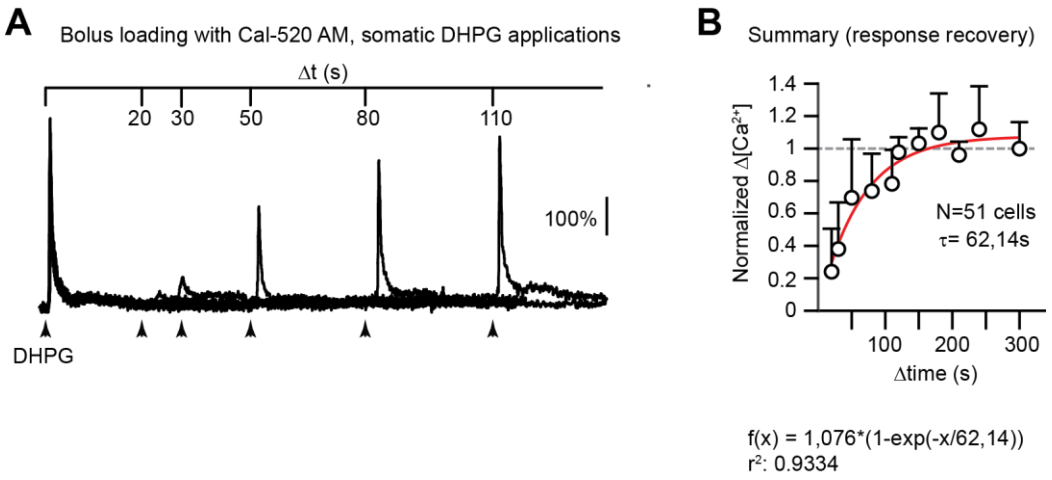

Figure 3.10- Spontaneous refilling of DHPG/IP_3-sensitive calcium stores

(A) Overlay of somatic fluorescence recordings from a CA1 pyramidal neuron loaded with the Cal-520 AM calcium indicator. Calcium transients were elicited by two paired DHPG pulses (0.5 s) at different time intervals as indicated on the top. For the figure, five traces were aligned to the time point of the first stimulation. **(B)** The amplitudes of the second responses in (A) and analogous experiments were normalized to the amplitude of the first responses and plotted against the lengths of time intervals between the respective stimulations. The increase of normalized second responses reflects spontaneous refilling of the DHPG/IP_3-sensitive calcium store. A single exponential fit to the data points yielded a time constant (τ) of 62 s for the spontaneous refilling. (Fitting curve: f(x) = 1.076(1-exp (-x/62.14)) with r^2=0.9334 (N=51)).

3.2.5 IP_3-sensitive calcium store is sensitive to nickel but not to D600

It was demonstrated that bath-applied nickel ions block the refilling of Ry-sensitive calcium stores in CA1 pyramidal neurons. Thus, ER stores can be refilled by VGCCs (Garaschuk et al., 1997). In order to test whether refilling of the IP_3-sensitive stores is also possible through the activity of VGCCs, I applied the same protocol as Garaschuk and colleagues (Garaschuk et al., 1997). Cells were stained with Cal-520 AM to monitor the changes of the calcium concentration in the soma. DHPG (0.5 mM) was locally applied for 0.5 s to monitor the filling state of the IP_3-sensitive calcium store. After a first control DHPG-pulse, a very high concentration of KCl (80 mM) was locally pressure ejected onto the cells for 3 s to achieve the depolarization that is required to activate

VGCCs. Subsequently, I applied six DHPG-pulses to empty the IP_3-sensitive calcium stores similar to previous experiments (**Figure 3.9 A,** #1). Again, DHPG-responses recovered to control levels after two minutes (**Figure 3.9 A**, #2). Both, (1) the spontaneous as well as (2) the high K^+-induced influx of calcium through VGCCs were abolished in the presence of nickel (2 mM in the external solution), an antagonist of calcium-permeable channels (**Figure 3.11 A**, #3 and #4). As expected from my previous experiments, DHPG failed to induce calcium transients in Orai2$^{-/-}$ mice. Remarkably, however, Orai2$^{-/-}$ cells remained unresponsive to DHPG even after calcium influx associated with the opening of VGCCs by local application of KCl (**Figure 3.11 B**). This observation indicates that in the absence of Orai2 CA1 pyramidal neurons cannot utilize the incoming calcium ions for refilling IP_3-sensitive stores.

The dependency of spontaneous refilling of IP_3-sensitive stores following six DHPG-pulses on calcium influx was tested also in the presence of 0.5 mM D600, an antagonist of VGCCs (**Figure 3.12**). It is important to point out that, compared to control conditions (time point one, **Figure 3.12 A**), the external presence of D600 reduced the amplitudes of DHPG-evoked calcium transients on average by 33% (time point three in **Figure 3.12 A, Figure 3.12 B**, left). However, under these conditions spontaneous refilling of the IP_3-sensitive store was not prevented by bath application of D600 (**Figure 3.12 A,** time point four). In addition, the efficiency of the refilling (i.e. refilling rate) was estimated by the ratio of the calcium amplitude at time point one (#1)/ time point two (#2) (Ctrl ratio) as well as by the ratio at time point three (#3) / time point four (#4) (D600 ratio). Practically, the IP_3-sensitive store was not altered by bath-application of D600 (Ctrl: 1.11± 0.04

(ratio of time point #1 and #2), D600: 0.99 ± 0.06 (ratio of time point #3 and #4) (**Figure 3.12 B**, right). These data suggest that the molecular mechanisms for spontaneous refilling of the ER calcium stores differs between IP_3- and Ry-sensitive stores: Both types of stores require calcium influx through the plasma membrane, however, in contrast to IP_3-sensitive stores, Ry-sensitive stores do not refill spontaneously when VGCCs are blocked.

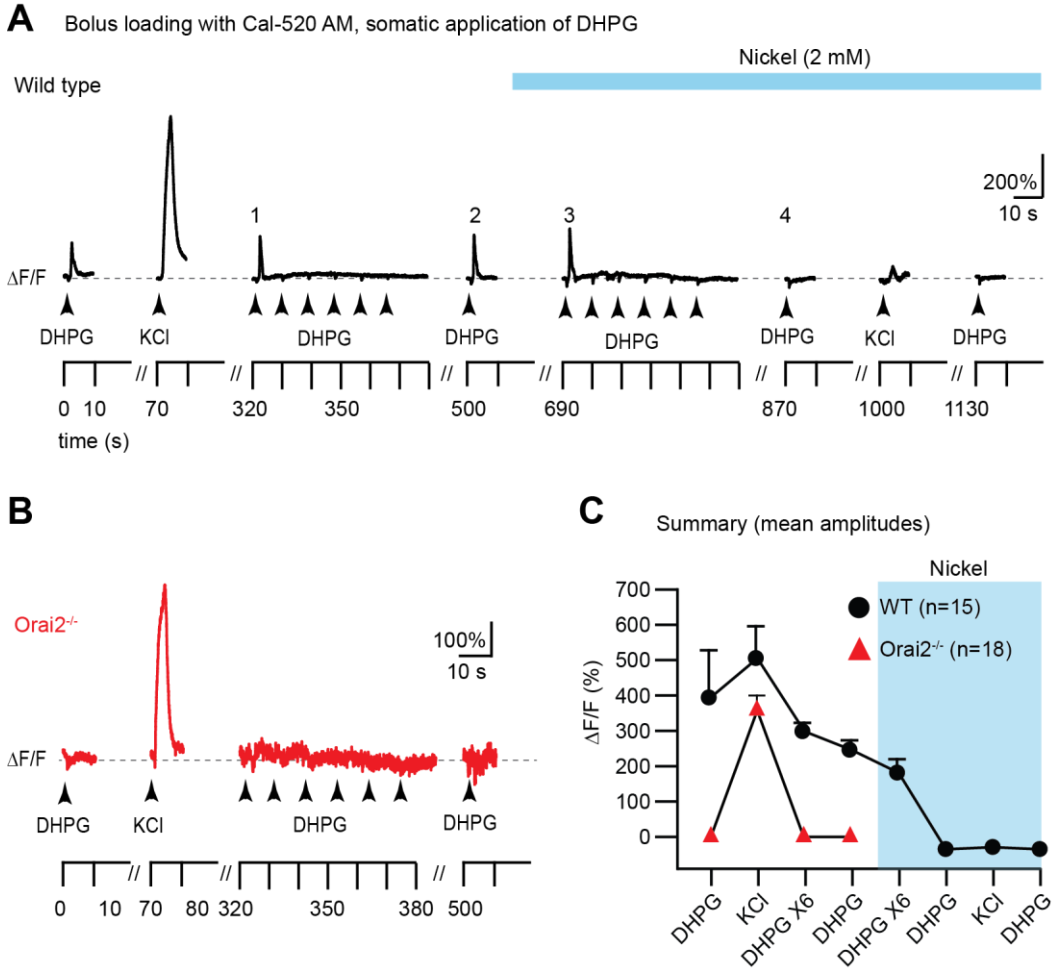

Figure 3.11- Blockade of calcium-permeable channels with nickel prevents the spontaneous refilling of the DHPG/IP_3-sensitive calcium store.

(A) DHPG/IP_3-sensitive store was emptied by six consecutive DHPG local applications (0.5 s, #1). The DHPG-evoked calcium transient recovered within 5 minutes (#2). The same stimulation protocol was applied in the presence of nickel (2 mM) in the bath (filled blue bar). The DHPG-evoked calcium transient does not recover after store emptying (#3 and 4). The KCl-evoked calcium transient through VGCCs was inhibited by nickel (arrowhead 15). **(B)** Analogous experiment in the Orai2$^{-/-}$ mouse. The DHPG-elicited calcium signal is absent in the absence of Orai2. **(C)** Summary

graph showing the mean (± SEM) amplitude of DHPG-evoked calcium transients at the respective time points indicated in (A) and (B). WT (*black*, n=15) and Orai2$^{-/-}$ (*red*, n=18) mice.

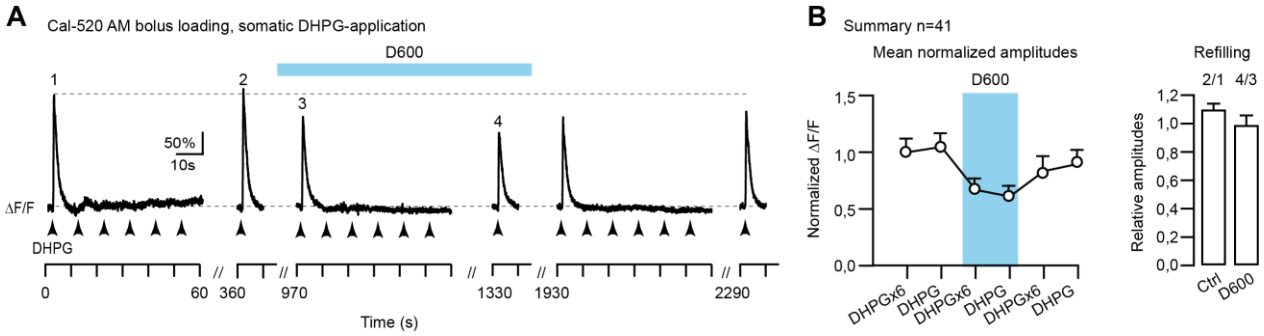

Figure 3.12- The spontaneous refilling of DHPG/IP$_3$-sensitive calcium stores is not affected by blockade of VGCCs with D600.

(A) Traces showing fluorescence transients resulting from repeated DHPG applications to the soma of a CA1 pyramidal neuron stained with Cal-520 AM under control conditions (ACSF) and in the presence of D600 (0.5 mM, filled blue bar). D600 does not prevent the recovery of the DHPG-evoked calcium transient (#4) after the store was emptied with six consecutive DHPG pulses applied with a time interval of 10 s **(B)** *Left:* Summary graph shows mean (±SEM) calcium response amplitude (ΔF/F) normalized to the first amplitude (y-axis) in response to different stimulation conditions (x-axis). *Right:* The bar graph showd the mean relative DHPG response amplitude before and after spontaneous refilling of the DHPG/IP$_3$-sensitive calcium stores. For both conditions (control and presence of D600) the DHPG response amplitude at the respective time point was divided as indicated. (n=41)

3.2.6 Spontaneous and depolarization-induced refilling of Ry-sensitive stores in Orai2$^{-/-}$ mice: Sensitivity to nickel and Orai1/3 blockade

Analogously to the experiment shown in **Figure 3.11 A**, I tested the spontaneous and KCl-induced refilling of the Ry-sensitive stores in Orai2$^{-/-}$ mice at P17-P20. Similar to the IP$_3$-sensitive stores in WT, nickel inhibited the spontaneous refilling of the Ry-sensitive store after it was emptied with six consecutive caffeine pulses (**Figure 3.13 A and B**).

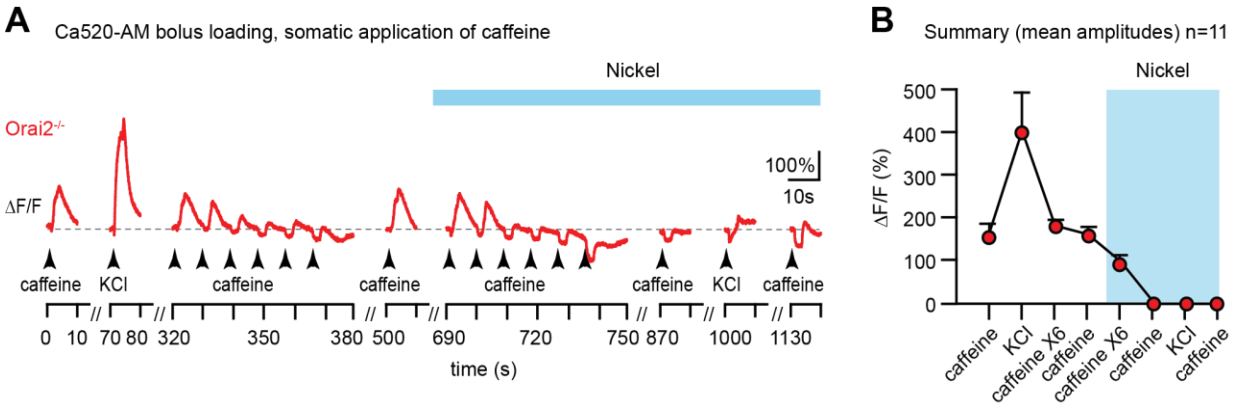

Figure 3.13- Nickel depletes the caffeine/Ry-sensitive calcium store in Orai2$^{-/-}$ mice.

(A) Traces showing fluorescence transients resulting from repeated alternating caffeine high KCl applications (as indicated) to the soma of a CA1 pyramidal neuron stained with Cal-520 AM under control conditions and in the presence of nickel. With the similar stimulation protocol as previously described, nickel blocks caffeine-evoked calcium responses in the absence of Orai2 (*filled blue bar*). **(B)** Scatter line graph shows the summary of the effect of nickel on spontaneous Ry-sensitive store refilling (n=11).

In their study, Garaschuk and colleagues suggested that the replenishment of the Ry-sensitive store at resting membrane potential occurs through capacitive calcium entry through calcium-permeable channels in the plasma membrane that are activated by depletion of the stores (Garaschuk et al., 1997). Nowadays, it is known that in many different cell types this function is fulfilled by Orai-channels (Kraft, 2015; Prakriya and Lewis, 2015; Soboloff et al., 2012). So far, I have shown that calcium release from the Ry-sensitive store is intact in Orai2$^{-/-}$ mice. However, besides Orai2, there are two other Orai homologs (Orai1 and Orai3) which could mediate capacitive calcium entry (Lewis, 2011). To test whether they are involved in spontaneous Ry-sensitive store refilling, caffeine was locally pressure-applied in the presence of the Orai1/3 antagonist GSK7975 (0.025 mM), and whole-cell patch-clamp recordings performed on CA1 pyramidal neurons in acute hippocampal slices from P18 Orai2$^{-/-}$ mice (**Figure 3.14 A**). Compared to control conditions, GSK7975 significantly reduced caffeine-evoked calcium transients but did not abolish them (mean amplitudes ΔF/F; Ctrl: 139.83 ± 17.995%,

GSK7975: 92 ± 19.74%) (**Figure 3.14 C**, upper). This finding suggests that the Ry-sensitive calcium stores in CA1 pyramidal neurons are largely independent of Orai channels and thus profoundly distinct from known ER calcium stores of other neuronal cell types.

To test whether caffeine-induced calcium transients are the result of calcium release from the ER, I applied caffeine to whole-cell patch-clamped CA1 pyramidal neurons in the presence of the SERCA inhibitor CPA (0.03 mM) (**Figure 3.14 B**). CPA largely reduced caffeine-evoked calcium signals both in WT (ΔF/F; control: 75.4 ± 7.7%; CPA: 13.1 ± 3.8%) and in Orai2$^{-/-}$ mice (ΔF/F; control: 98.4 ± 8.9%; CPA: 10 ± 5.4%) (**Figure 3.14 C**, bottom). Thus, the Ry-sensitive calcium store in CA1 pyramidal neurons is indeed a part of the ER.

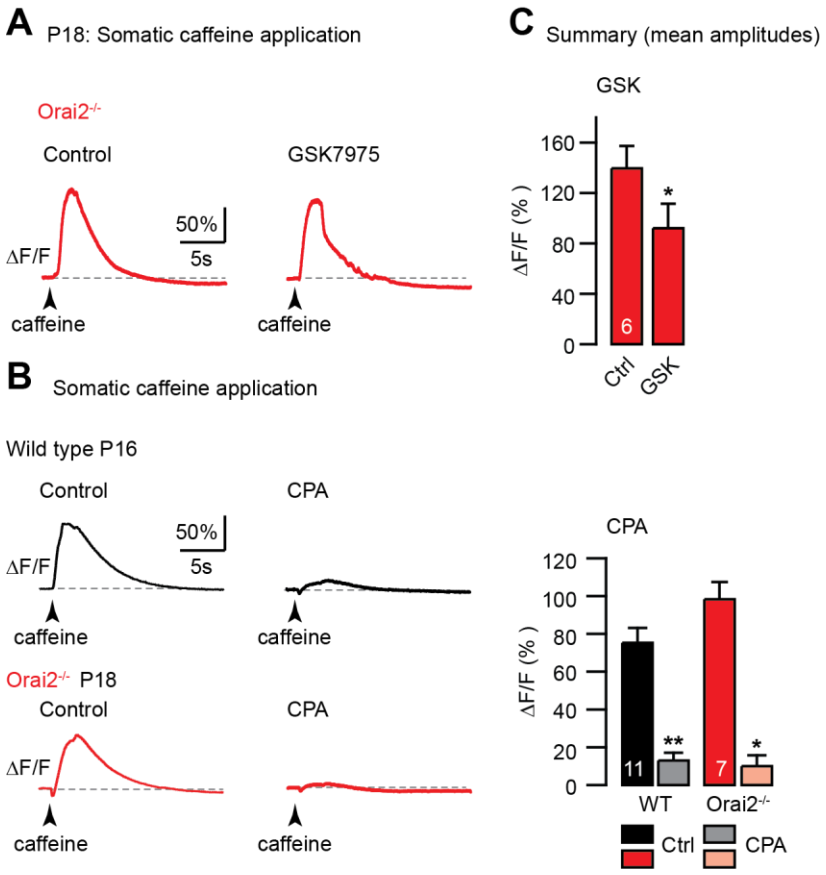

Figure 3.14- Effect of Orai1 and 3 antagonists, GSK7975 in caffeine mediated calcium release

(A) Calcium transients evoked by local pressure-application of caffeine (40 mM, 3 s) in normal ACSF (*left*) and in the presence of GSK7975 (right;0.025 mM, 30 min) in Orai2$^{-/-}$ mice (*red*). **(B)** Caffeine-evoked calcium transients in WT (*black,*) and in Orai2$^{-/-}$ (*red*,) mice in normal ACSF (*left*) and in the presence of CPA (*right*; 0.03 mM, 15 min). **(C)** *Top:* Bar graph representing the mean amplitude of caffeine-induced calcium transients (ΔF/F) in control ACSF and in the presence of GSK7975 (n=6). *Bottom*: Bar graph showing the mean (± S.E.M) amplitude of calcium transients in response to caffeine stimulation in control ACSF and in the presence of CPA in WT (n=11) and Orai2$^{-/-}$ (n=7) mice. (* p<0.05, ** p<0.01; Wilcoxon signed rank test) (*<0.05, Wilcoxon signed rank test)

3.2.7 Depolarization failed to rescue mGluR1/5-mediated calcium signals in Orai2$^{-/-}$ mice

Previously, it was demonstrated in cerebellar Purkinje neurons that empty ER calcium stores with disrupted calcium homeostasis can be filled by the activation of VGCCs through a short (one sec) depolarization to 0 mV (Garaschuk et al., 1997; Hartmann et al., 2014). In order to test whether this finding from Purkinje neurons can be reproduced for IP_3-sensitive stores in CA1 pyramidal neurons, I adopted the protocol from these studies: Whole-cell patch clamped CA1 pyramidal neurons in acute hippocampal slices from P17-22 mice were repeatedly stimulated with local DHPG application (0.5 mM, 0.2 s) with 20 s IPI until complete rundown of the DHPG-evoked calcium transients. Next, the holding potential was raised for one second from -70 mV to 0 mV to induce calcium influx through VGCCs. Four seconds after the depolarization pulse, DHPG again was pressure-ejected to the soma. Unlike in cerebellar Purkinje neurons, neither in WT nor in Orai2$^{-/-}$ mice the DHPG-evoked calcium transient was rescued by activation of VGCCs (**Figure 3.15 A-B and Figure 3.15 D**, left and middle). For Orai2$^{-/-}$ mice, I performed an additional experiment in which I stimulated CA1 pyramidal neurons first with DHPG and second with caffeine after the 1 s long depolarization. I found a depolarization increased caffeine response, indicating a supercharging of the Ry-sensitive store. Unlike in

cerebellar Purkinje neurons (Hartmann et al., 2014), however, the DHPG responses were not reconstituted in Orai2$^{-/-}$ mice, confirming the earlier finding with local high K^+ application (**Figure 3.15 C and D; see also Figure 3.11 B**). Taken together, these data demonstrate that IP_3- and Ry-sensitive stores in CA1 pyramidal neurons react differently to depolarization-evoked calcium influx. Ry-sensitive stores are refilled by calcium influx through VGCCs, while IP_3-sensitive calcium stores cannot be replenished by VGCCs.

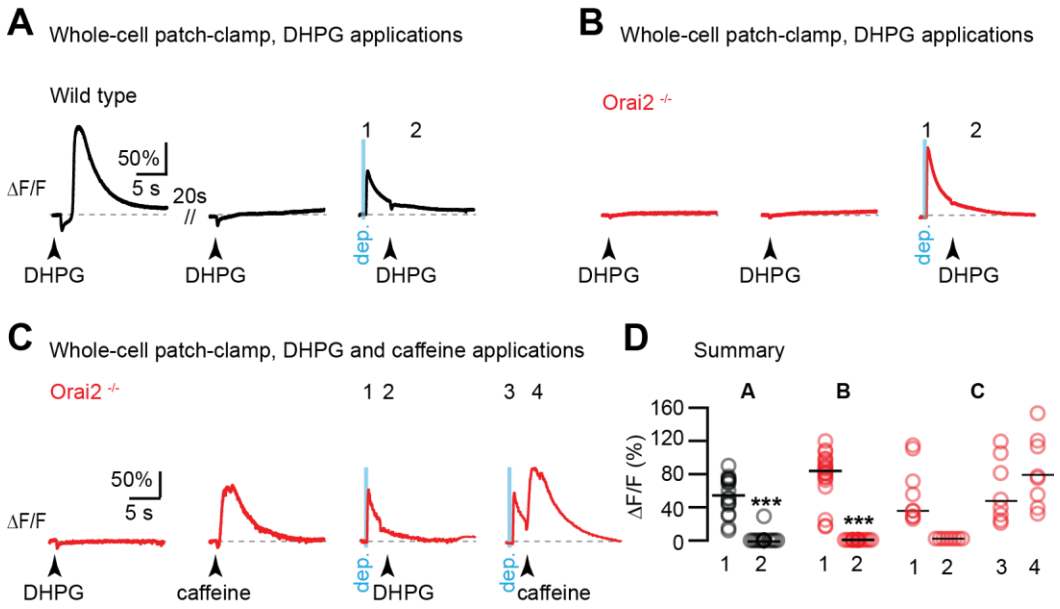

Figure 3.15- Caffeine/Ry-sensitive but not DHPG/IP3-sensitive stores are filled by depolarization-evoked calcium influx.

(A) Traces showing fluorescence recordings from the soma of a whole-cell voltage-clamped CA1 pyramidal neuron filled with OGB-1. *Left*: Calcium transient in response to the first DHPG-application. *Middle*: Calcium transient in response to the 4th DHPG-pulse applied with a 20s interval. *Right*: Calcium response to a change of the holding membrane potential from -70 mV to 0 mV for one second. DHPG was applied four seconds after the depolarization, and no calcium transient was evoked. **(B)** Analogous experiment in an Orai2$^{-/-}$ mouse. Same scaling as in (A). **(C)** Analogous experiment in an Orai2$^{-/-}$ mouse with the difference that DHPG and caffeine were subsequently applied to the same cell as indicated. **(D)** Scatter graph showing the individual amplitude (ΔF/F) of depolarization- (1) and DHPG- (2) or depolarization- (3) and caffeine- (4) evoked calcium transients in WT (A, *black*, n=18) and Orai2$^{-/-}$ (B, *red,* n=20; C, n=7) mice. Black lines indicate the median of each data group. (*** p<0.001, Mann-Whitney-U-Test**)** Orai2$^{-/-}$. (*** p<0.001; n.s p>0.05, Mann-Whitney-U-Test).

3.3 The roles of IP_3- and Ry-sensitive calcium stores for synaptic plasticity

A plethora of studies has shown that both pre- and postsynaptic calcium release from ER stores play a critical role in different forms of synaptic plasticity (Harvey and Collingridge, 1992; Raymond, 2007; Reyes and Stanton, 1996; Rose and Konnerth, 2001). However, many questions about the molecular mechanisms still remain open.

It has been shown that LTP at Schaffer collaterals (SC) synapses can be induced by 4 bursts consisting of 100 pulses given at 100 Hz high-frequency stimulation (HFS) with 20 s long inter-burst intervals (Oliet et al., 1997). Using the stimulation protocol of Oliet and colleagues (also see **section 2.6**), I aimed to address whether the IP_3-sensitive stores regulated by Orai2 are involved in LTP of SC synapses. In both genotypes, the slope of the fEPSPs was increased following the HFS stimulation and thus LTP could be successfully induced in the absence of Orai2 (**Figure 3.16 A,** left). This observation suggests that calcium release from IP_3-sensitive stores is not critically involved in the LTP induction in CA1. In the absence of Orai2, the average of the fEPSP slope after LTP induction was larger than in WT (WT: 141.43 ± 2.65%, $Orai2^{-/-}$: 162.20 ± 3.41%; $p<0.001$) (**Figure 3.16 A**, right). I repeated the same experiment in both genotypes in the presence of 0.01 mM ryanodine. This treatment strongly impaired the induction of LTP in both genotypes (**Figure 3.16 B**, left) These results suggest that ryanodine does not prevent LTP induction but LTP maintenance, which is consistent with findings about a critical role of RyR-dependent calcium release for LTP (Johenning et al., 2015; Lu and Hawkins, 2002). Moreover, the average fEPSP slope after LTP induction in WT is

smaller than in Orai2$^{-/-}$ (WT: 81.50 ± 2.91%, Orai2$^{-/-}$: 109.92 ± 4.26%) (**Figure 3.16 B**, right)

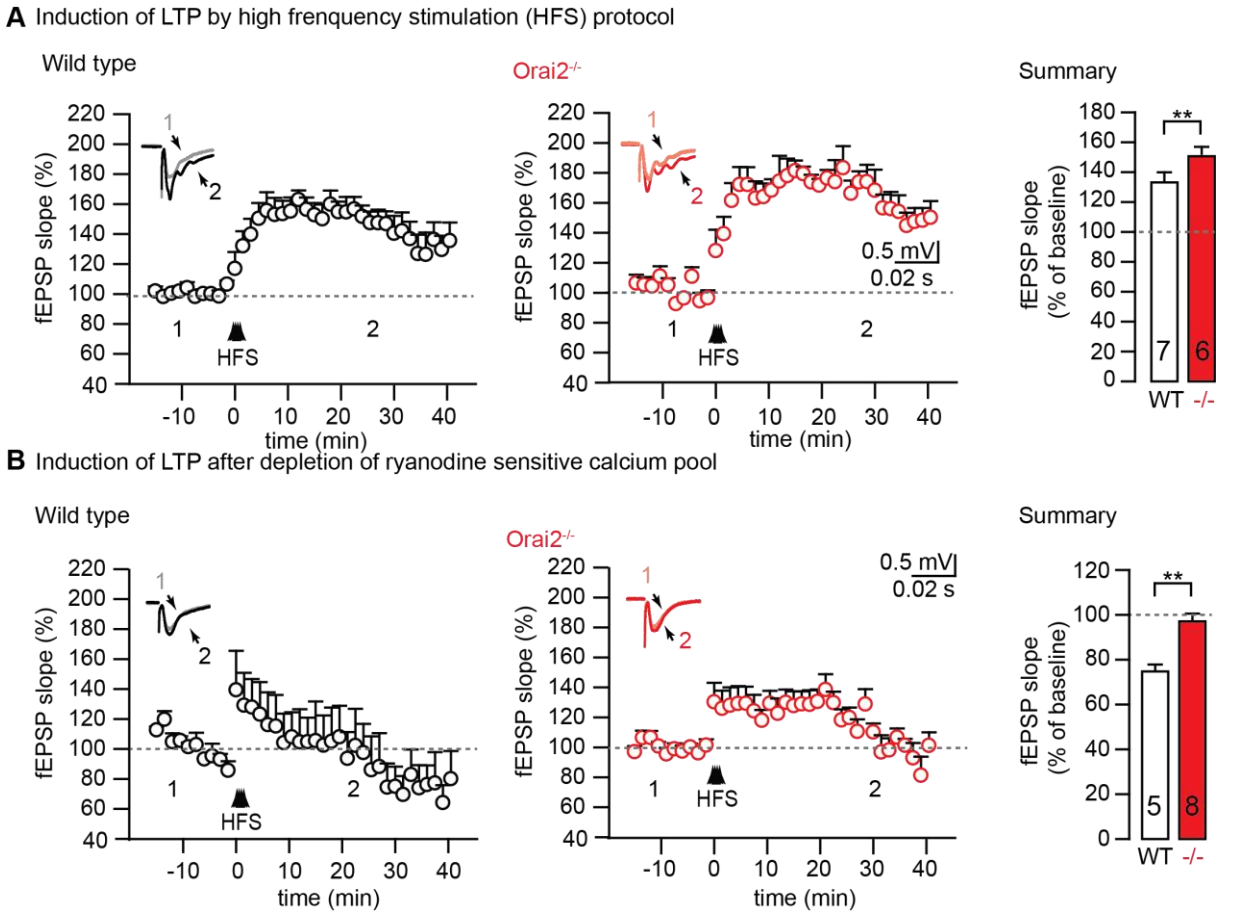

Figure 3.16- Role of IP3- and Ry-sensitive stores on LTP in CA1 pyramidal neurons

(A) *Left:* LTP induced by high-frequency stimulation (HFS) of the Schaffer collateral pathway (4 bursts of 100 pulses at 100 Hz with 20 s interval) in slices from WT (*black*) and Orai2$^{-/-}$ (*red*) mice. The scatter graph shows the average change of the fEPSP slope (mean ± S.E.M) over time in WT (n=7) and Orai2$^{-/-}$ (n=6) mice. The inset shows an example of averaged traces during baseline recording (a) and after HFS (b) in WT (*left*: *gray* for baseline and *black* for the time after HFS) and Orai2$^{-/-}$ (*right*: *pink* for baseline and *red* for the time after HFS). *Right*: The bar graph represents the mean of the fEPSP slope in the final ten minutes of recoding in WT (*white*) and Orai2$^{-/-}$ (*red*) mice **(B)** *Left:* Scatter graph represents the change of mean ± S.E.M fEPSP slopes over the course of the experiment in the presence of ryanodine (0.01 mM) in WT (*black*, n=5) and Orai2$^{-/-}$ (*red*, n=8). The inset shows the respective responses before HFS in WT (a, *gray*) and Orai2$^{-/-}$ (a, *pink*) and after HFS in WT (b, *black*) and Orai2$^{-/-}$(b, *red*). *Right*: The bar graph shows the mean fEPSP slopes in the final ten minutes of recoding in WT (*white*) and Orai2$^{-/-}$ (*red*) mice. (*** p<0.001, Mann-Whitney-U-Test).

Furthermore, I addressed the role of Orai2 in the induction of mGluR1/5-dependent LTD (Ayala et al., 2009; Kim and Linden, 2007; Luscher and Huber, 2010; Wisniewski and Car, 2002). The experimental setup was the same as for the LTP experiments described above. LTD was induced chemically by bath application of DHPG (0.1 mM) for 10 min in WT and Orai2$^{-/-}$ mice (Huber et al., 2000). After bath-application of DHPG, both WT and Orai2$^{-/-}$ cells showed LTD (Figure 3.17 A, left). The average of the fEPSP slope after chemical LTD induction in WT is smaller than in Orai2$^{-/-}$ (WT: 26.94 ± 1.23, Orai2$^{-/-}$: 31.28 ± 1.07; $p<0.05$) (**Figure 3.17 A, right**).

In a third series of experiments directed at elucidating the role of Orai2 and IP_3-sensitive stores for synaptic plasticity, I tested the suppression of LTP. This term describes the phenomenon that mGluR1/5-dependent LTD precludes the later induction of LTP with HFS (Fujii et al., 2000). Suppression of LTP is impaired in mice lacking the IP_3R1 (Fujii et al., 2000). In order to test whether Orai2 and the IP_3-sensitive calcium stores are involved in the suppression of LTP, LTD was first chemically induced by bath-application of DHPG (0.1 mM, 10 min). After LTD was stably induced analogously to the experiments in **Fig. 3.17 A**, I applied HFS (4 x 100 pulses @ 100 Hz with a 20 s burst interval) to induce LTP. In WT mice, the induction of LTP was inhibited by prior LTD (22.12 ± 0.9%) induction. However, in Orai2$^{-/-}$ cells the suppression of LTP was less pronounced (**Figure 17 B, left**) and the slopes of fEPSP increased to 61.71 ± 3.03% after LTP induction ($p<0.001$). Thus, Orai2 and the IP_3-sensitive calcium store are important for LTP suppression.

Hence, Ry-sensitive stores appear to be crucial for LTP induction, while IP_3-sensitive stores appear to be critical for LTP suppression.

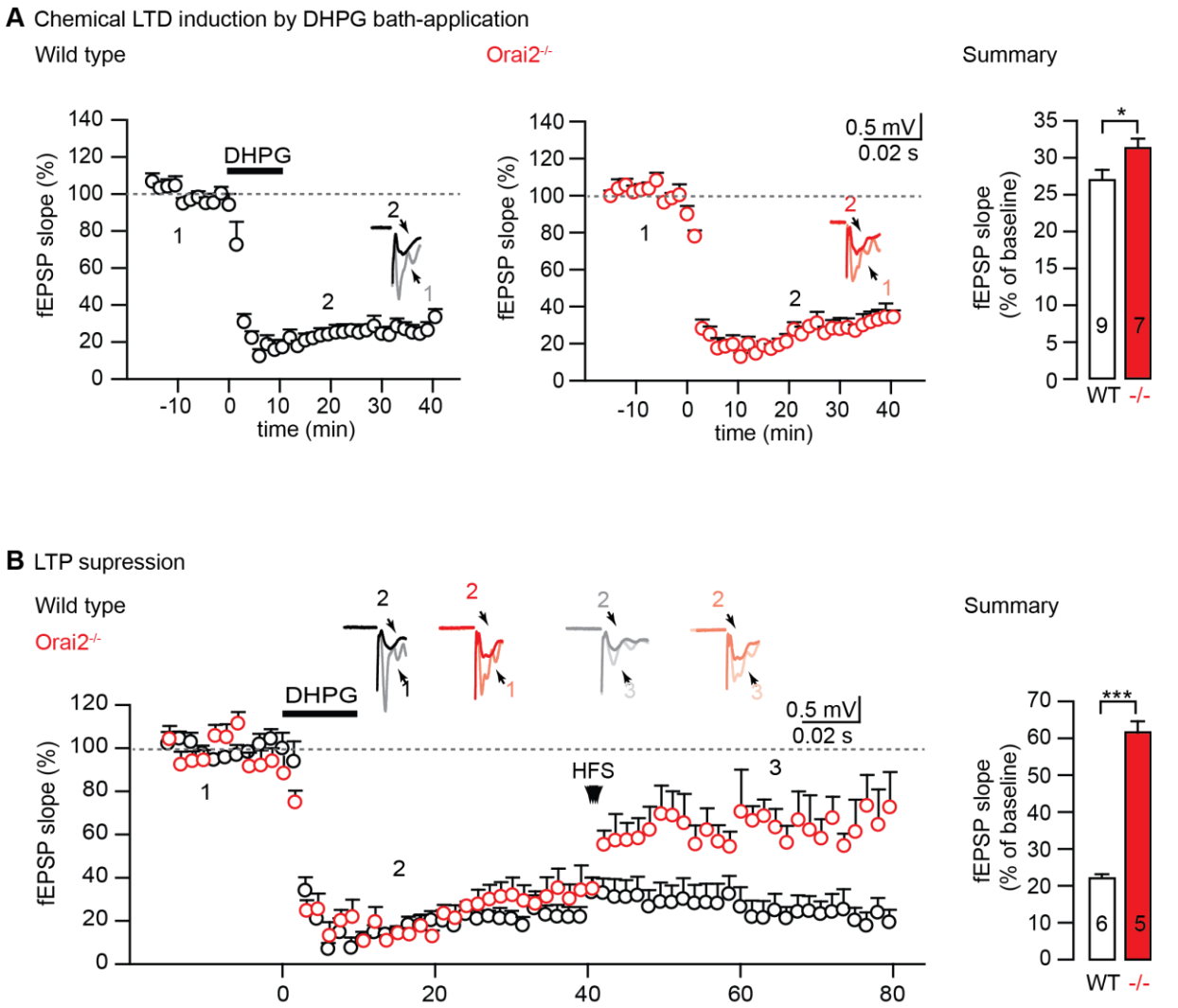

Figure 3.17- Chemically induced LTD by DHPG bath application in WT and Orai2$^{-/-}$ mice.

(A) *Left*: Scatter graph represents the averaged fEPSP slope (mean ± S.E.M) normalized to the baseline in WT (*black*, n=9) and Orai2$^{-/-}$ (*red*, n=7). LTD was induced by bath application of DHPG (*filled gray bar*; 0.1 mM) for 10 minutes. The inset shows traces in WT (*left*) and Orai2$^{-/-}$ (*right*) before (a) and after (b) DHPG application. *Right*: Bar graph shows the mean fEPSP slope in the final ten minutes of recoding in WT (*white*) and Orai2$^{-/-}$ (*red*).

(B) *Left*: Scatter graph shows time course of fEPSP recordings during a LTP suppression experiments in WT and Orai2$^{-/-}$ mice. The inset shows representative traces of baseline (# 1), LTD-induced (# 2) and LTP-induced (# 3) in WT (*black*; n=6) and Orai2-/- (*red*; n=5) mice. *Right*: Bar graph shows the mean fEPSP slope in the final ten minutes of recoding in WT (*white*; n=6) and Orai2-/- (*red*; n=5) mice. (*** p<0.001; * p<0.05, Mann-Whitney-U-Test).

4. Discussion

In this study the properties of ER-associated calcium signaling in CA1 pyramidal neurons with a special emphasis on the role of the calcium-permeable ion channel Orai2 were investigated. In acute hippocampal slices from WT and Orai2-deficient mice at various postnatal ages calcium release from ER calcium stores was evoked by group I mGluR agonist (DHPG) application, IP_3 uncaging, bAPs in the presence of DHPG and by caffeine application. It was found that group I mGluR-dependent IP_3R-mediated calcium release in CA1 pyramidal neurons older than P16 critically depends on Orai2, in contrast to younger postnatal ages, consistent with the upregulation of *Orai2* expression in development that was also analyzed with a quantitative PCR approach. In contrast to the IP_3R-dependent calcium signaling, the RyR-dependent calcium release from ER stores is to a small part dependent of Orai1 and 3 but independent of Orai2 at late postnatal age (>P16). The replenishment of Ry-sensitive stores is strongly dependent on the activity of VGCCs. IP_3- and Ry-sensitive calcium stores are largely independent and mutually exclusive and share only ca. 20% of the total ER calcium pool. Thus, in addition to the Ry-sensitive ER calcium store that was characterized earlier (Garaschuk et al., 1997), there is a novel type of ER calcium store in CA1 pyramidal neurons, namely a Ry-insensitive but IP_3-sensitive Orai2-dependent store. Based on the analysis of three types of synaptic plasticity of SC synapses in CA1 pyramidal neurons of WT and Orai2$^{-/-}$ mice, it was found that both calcium stores play opposite roles for LTP at SC synapses of CA1 pyramidal neurons: Ry-sensitive stores are required for LTP induction, and IP_3-sensitive stores for LTP suppression.

4.1 Role of Orai2 in neuronal calcium homeostasis

Throughout the animal kingdom, in practically all tissues cells utilize the same mechanism of ER Ca^{2+} store replenishment by store-operated Ca^{2+} entry (SOCE). The *stromal interaction molecule 1* (STIM1) together with the Ca^{2+} release-activated Ca^{2+} (CRAC) channel subunit Orai1 were first identified as the main components of the responsible pathway (Feske et al., 2006; Roos et al., 2005; Vig et al., 2006). The molecular interaction between STIM1 and Orai1 and their activation mechanisms have been studied extensively in non-excitable cells (Prakriya and Lewis, 2015). Although the homologs of STIM1 and Orai1, STIM2 (Liou et al., 2005; Williams et al., 2001) and Orai2/3 (Feske et al., 2006; Mercer et al., 2006; Vig et al., 2006), respectively, were discovered at the same time, much less is known about their cellular functions.

This study for the first time demonstrates the crucial importance of Orai2 for calcium homeostasis in the native cellular environment of a central mammalian neuron in intact brain tissue. Sparse data that point to a role of Orai2 in SOCE that is similar or complementary to Orai1 were mostly obtained in non-excitable cell lines. It was reported that co-expression of Orai1 and Orai2 with STIM increases the CRAC current (I_{crac}) that is needed for calcium store refilling (Hoth and Penner, 1992) in HEK293 cells (DeHaven et al., 2007; Lis et al., 2007; Mercer et al., 2006) and that silencing of *Orai2* attenuated SOCE in leukemia-relevant HL60 cells (Diez-Bello et al., 2017). Interestingly, in this cell line, the silencing of Orai2 reduces SOCE stronger than the knockdown of Orai1. This is different in human lung mast cells, in which only a minor reduction in SOCE was observed without functional Orai2 (Ashmole et al., 2013). However, both publications

support the view of Orai2 as being homologous to Orai1. In contrast, in chondrocyte cells (Inayama et al., 2015) and dissociated T-cells (Vaeth et al., 2017) silencing or deletion of *Orai2*, respectively, increases SOCE. It was suggested that Orai2 forms heteromeric channels with Orai1 and attenuates CRAC channel function (Vaeth et al., 2017). Thus, in non-excitable cells, the actions of Orai2 appear to be very diverse, depending on the cell type.

The only study about the role of Orai2 in neurons that is available so far showed that Orai2 is required for neuronal SOCE (Zhang et al., 2016). This is consistent with the data presented here. Zhang et al. claimed that Orai2 in hippocampal neurons forms a channel complex with the member of the subfamily of *classical transient receptor potential channels* TRPC6. However, there are several reasons why it is very unlikely that this is the case in CA1 pyramidal neurons. First, Zhang et al.'s experiments were done in primary cultures of mixed hippocampal neurons. The hippocampal region that provides the largest number of cells to such a culture is the dentate gyrus. Yet, in contrast to the CA1 region, the dentate gyrus also has a very high expression of TRPC6 (Lein et al., 2007). Second, the experimental evidence for an involvement of TRPC6 in neuronal SOCE that they provide is the activation of SOCE by hyperforin, which is supposedly a TRPC6-specific agonist (Leuner et al., 2007; Zhang et al., 2016). More recently, however, it was demonstrated that hyperforin, rather than activating TRPC6, is a protonophore (Sell et al., 2014). In my own experiments on dentate gyrus granule cells in hippocampal slices, I found that the derivative of hyperforin, Hyp9, induced inward currents in whole-cell patch-clamped granule cells in the absence of TRPC6 in TRPC6-deficient knockout mice (data not shown). For these reasons, the idea of an Orai2-

channel that contains also TRPC6 subunits is to be dismissed for CA1 pyramidal neurons.

In view of its high expression in many areas of the brain, including the hippocampus (Lein et al., 2007), the question was put forward whether Orai2 is “the neuronal Orai1” (Hoth and Niemeyer, 2013). In mushroom spines of cultured hippocampal neurons, it was shown for the first time that indeed Orai2 and not Orai1 is decisive for the replenishment of neuronal calcium stores (Zhang et al., 2016). The release of calcium ions in their study was evoked by DHPG and thus was IP_3R-mediated. The data presented in this thesis add a novel and surprising aspect to the answer whether Orai2 is the equivalent of Orai1 in neurons. Orai2, on the one hand, is crucial for the refilling of IP_3-sensitive ER calcium stores in CA1 pyramidal neurons after P16-17 - unlike Orai1/3 that are important very early in development (**Figure 3.3**). On the other hand, Orai2 has no apparent role for the calcium homeostasis of Ry-sensitive stores. This seems to be different in cerebellar Purkinje cells where both IP_3R- and RyR-mediated calcium responses are largely reduced in the absence of Orai2 in Orai2$^{-/-}$ mice (Dijke, Hartmann & Konnerth, personal communication). However, in this cell type also the IP_3Rs and RyRs share a common calcium pool (Khodakhah and Armstrong, 1997). It remains to be elucidated whether the exclusive regulation of IP_3-sensitive calcium stores by Orai2 is a feature that is common in neurons and is masked only by different degrees of overlap between the two types of calcium stores.

4.2 The role of Orai2 in development

The postnatal developmental time line in the mouse hippocampus can be divided into three periods: E16-P1 is the stage when massive neuronal proliferation takes place, P1

to P7 is the peak for cell differentiation and the beginning of synapse formation, and P7 to P30 is the main period for synapse formation and maturation (Mody et al., 2001). The mRNA expression profile from P16 mouse hippocampus showed increased expression levels of brain-derived neurotrophic factor (BDNF), synaptophysin and synaptic vesicle-associated protein (VAMP2) and thus indicated the maturation of synapses at this period. Place field formation in CA1 (Wills and Cacucci, 2014; Wills et al., 2014) starts at P17 in rats. At this stage, rats also begin to explore their environments (Wills and Cacucci, 2014; Wills et al., 2014). Moreover, at this postnatal age rats are able to find a hidden platform in the Morris water maze test (Wills et al., 2014) which indicates that at this stage the mechanisms required for hippocampus-dependent spatial learning are functional. It has been demonstrated numerous times that intact mGluR1/5-dependent synaptic signaling is crucial for this hippocampal function (Balschun et al., 1999a; Mukherjee and Manahan-Vaughan, 2013; Popkirov and Manahan-Vaughan, 2011). Moreover, it was demonstrated in mice that genes associated with IP_3R-related pathways are also upregulated at P16 (Mody et al., 2001). This includes genes encoding protein kinase C (PKC), phospholipase Cβ1 (PLCβ1), diacylglycerol (DAG) kinase, SERCA, calcineurin and the immunophilin FK506 binding protein (FKBP12). This suggests that IP_3R-associated signaling could be critical for this period of hippocampal development (Mody et al., 2001). In addition, another expression study based on protein analysis performed in rats revealed that the presence of IP_3R1 protein during post-natal development in CA1 increases from P10 to P20 and remains stable after P20 (Dent et al., 1996). As my own experiments demonstrated, Orai2 is directly involved in IP_3R-mediated calcium signaling (**Figure 3.5**) and the increase in Orai2 expression from P11 to P22 that is demonstrated in this thesis (**Figure 3.2**) also parallels the developmental

expression profile of IP_3R1 and other proteins associated with it. The observation that Orai2 is required for the stability of mushroom spines in hippocampal neurons (Zhang et al., 2016) supports the assumption that the upregulation of Orai2 in development is relevant for synaptogenesis. The fact that 12% of CA1 pyramidal neurons remain responsive to DHPG and IP_3 in the absence of Orai2 at P18-20 probably reflects the gradual character of this developmental transition that possibly proceeds at different rates in individual neurons.

4.3 Separate calcium pools in ER calcium stores in CA1 pyramidal neurons

There is a long-standing debate in cellular neurophysiology whether IP_3- and Ry-sensitive ER calcium stores are identical, partly overlapping or completely separate entities (Golovina and Blaustein, 1997; Mattson et al., 2000; Verkhratsky, 2002, 2005).

The existence of separate intracellular calcium stores was demonstrated so far mainly in non-neuronal cell types. High-resolution microscopic imaging of the calcium dynamics in intracellular calcium stores in mouse cortical astrocytes revealed that there are several calcium compartments. The calcium stores in astrocytes could be divided into CPA- and caffeine-sensitive stores (Golovina and Blaustein, 1997). In vascular smooth muscle cells, thapsigargin- and caffeine-sensitive stores were identified (Tribe et al., 1994). Moreover, in HEK293 cells it was demonstrated that there might be more than one IP_3-sensitive calcium pool. Calcium release in response to carbachol was $IP_3R1/3$-mediated

and IP_3R2-dependent release was found to be responsible for the cAMP-mediated potentiation of carbachol-triggered calcium release from stores (Konieczny et al., 2017; Tovey and Taylor, 2013). The $IP_3R1/3$- and IP_3R2-endowed stores were refilled and depleted independently (Konieczny et al., 2017).

In cerebellar Purkinje cells, in contrast, emptying Ry-sensitive calcium stores strongly reduced calcium release evoked by IP_3 uncaging indicating that in this cell type both stores largely overlap (Khodakhah and Armstrong, 1997). In line with this, the deletion of the *Stim1* gene and hence the elimination of the mechanism of Orai-mediated calcium homeostasis almost equally abolished IP_3R- and RyR-mediated calcium responses (Hartmann et al., 2014). In CA1 pyramidal neurons, synaptically evoked IP_3R-mediated calcium release is blocked in the presence of ryanodine that blocks RyRs in the open state but not with Ruthenium Red that prevents the opening of RyRs. It was concluded that Ry- and IP_3-sensitive stores communicate although RyRs themselves do not contribute to the synaptic calcium release (Nakamura et al., 1999). Similarly, in their experiments the presence of caffeine inhibited the potentiating effect of a group I mGluR-agonist (tACPD) on calcium transients evoked by bAPs. This result seems to contradict observations described here. However, caffeine has known side effects that could distort observations on calcium signals in its prolonged presence. It is known that it interacts with fluorescent calcium indicators (Muschol et al., 1999) and in some preparations it inhibits IP_3Rs (Parker and Ivorra, 1991). The exclusive effect of the genetic deletion of *Orai2* on the IP_3-sensitive calcium store as it is demonstrated here is a convincing way to prove the independence of both stores. Quite the opposite was found with similar methods in rat sensory neurons. There, the depletion of IP_3-sensitive stores prevented calcium release through RyRs and vice versa, indicating that IP_3Rs

and RyRs in this cell type are located on the same calcium store and command the same calcium pool (Solovyova and Verkhratsky, 2003). Obviously, there is some variety with regard to the degree of overlapping of both calcium pools depending on the cell type. It remains to be elucidated how this affects the different functions of these cells.

This thesis presents data that clearly point to the fact that IP_3Rs and RyRs in CA1 pyramidal neurons release calcium from largely separate calcium pools. This raises the question whether both types of stores are morphologically connected or whether there are separate IP_3- and Ry-sensitive membrane compartments. When Purkinje cells were injected with the lipophilic dye DiI, it diffused in continuous bilayers and the labeling spread through the soma, into the dendrites and axons. Therefore, it was concluded that there is a continuous compartment of ER in cerebellar Purkinje cells (Terasaki et al., 1994). Also regarding other types of neurons, the vesicular-tubular continuity of the ER in neurons is the current dogma, although it is not supported by many observations.

With the assumption of a continuous ER network in CA1 pyramidal neurons, the observed separate regulation of IP_3- and Ry-sensitive calcium stores can possibly be attributed to functional compartmentalization. The question that researchers in the field are investigating for a long time are inhomogeneities in the properties of the ER calcium store with regard to the intraluminal calcium concentration, receptor distribution and contact regions with organelles and membranes, especially the plasma membrane.

Clusters of either IP3Rs or RyRs were identified in NGF-differentiated PC12 cells and cultured hippocampal neurons (Koizumi et al., 1999), in sensory neurons (Thayer et al., 1988), cerebellar granule cells (Simpson et al., 1996), and in myenteric neuron (Turner

et al., 2001). On a functional level, the consequence of an uneven distribution of IP_3Rs was demonstrated in CA1 pyramidal neurons. There, it was observed that calcium release signals do not appear in the same way throughout the entire cell. Instead, large calcium waves based on IP_3R-dependent release from stores were found predominantly on the thick apical dendritic shaft. The synaptically activated waves originated at branch points of oblique dendrites from the primary dendrite (Nakamura et al., 1999) This is in line with the distribution of IP_3Rs in CA1 pyramidal neurons. It was found that they are inhomogeneously distributed along the ER. They are located in clusters that are often situated on dendritic branch points. These clusters seem to underlie “hot spots”, where IP_3R-dependent calcium release is evoked, in contrast to “cold spots”, where this signal is not observed (Fitzpatrick et al., 2009).

Based on spot photo-release experiments in neuroblastoma cells, the diffusion coefficient for IP_3 in the cytosol was determined recently (280 $\mu m^2 s^{-1}$), and it was used to predict that the range of action for IP_3 is approximately 5 μm (Dickinson et al., 2016). This means that in neurons with dendrites spreading hundreds of μm, IP_3 must be regarded rather as a local than as a global messenger. This property of IP_3 likely contributes to synapse- or branch-specificity in neuronal signaling and thus to “contrast enhancement” in information processing.

Inhomogeneities in the ER calcium store have been found also with regard to the intraluminal calcium concentration. In non-excitable (HeLa) cells using ER calcium imaging and the kinetic analyses of local calcium concentration changes during store refilling, calcium sub-compartments containing higher and lower calcium concentrations in the lumen of the ER were identified (Montero et al., 1997).

In pancreatic acinar cells, in contrast, there appears to be a continuous calcium pool in the ER. This conclusion was made based on experiments involving ER calcium imaging with photobleaching and diffusion analysis during the depletion and refilling of IP_3-sensitive calcium stores. In this cell type, calcium diffuses relatively freely inside the lumen of the ER (Park et al., 2000). In acinar cells, calcium entry occurs at the base of the cell, whereas the calcium-dependent secretion takes place at the apical pole. The “problem” in this cell type is solved by tunneling of calcium ions inside the lumen of the ER (Mogami et al., 1997; Petersen and Tepikin, 2008; Toescu et al., 1994). A similar mechanism was suggested to exist in a specific type of neurons, namely rod photoreceptors. During prolonged depolarization (e.g. in the dark), a calcium gradient develops within the ER from the soma to the terminal that promotes diffusion of calcium to the terminal and thus maintains RyR-dependent synaptic release (Chen et al., 2015). Whether calcium gradients exist in the lumen of the ER of CA1 pyramidal neurons needs to be investigated.

Locally restricted calcium signaling associated with the ER can occur at sites where the ER protrudes into extensions of cells like it is the case for neuronal spines, including spines of CA1 pyramidal neurons. This is especially important for the comparison of IP_3- and Ry-sensitive stores, since spines in this cell type contain predominantly RyRs but not IP_3 receptors (Sharp et al., 1993).

Calcium binding proteins were also found to be non-homogeneously distributed in the ER. The ER calcium binding protein calsequestrin e.g. was located in macromolar complexes that contain RyRs (Terentyev et al., 2007). Thus, the combination of calcium

release, uptake, storage and replenishment is conferred by the localized expression of specific proteins.

Cutting-edge novel technology in microscopy possibly provides the tools for the reconciliation of the observed division between different types of ER calcium stores on a functional level and the assumption of a morphological continuity. Advanced ultrathin section electron microscopy applied to cortical neurons revealed that stacked ER sheets form a continuous membrane system in which the sheets are connected by helicoids (Terasaki et al., 2013). With the use of five different super-resolution microscopy techniques, the “sheets” were later identified in COS7 cells as dense tubular matrices. Furthermore, it was found that the structure of the ER is very dynamic. There are oscillations of ER tubules and junctions, with matrices rapidly interconverting from tight to loose arrays (Nixon-Abell et al., 2016). One can speculate that these dynamic tiny structures could represent diverse functional compartments because at the ends of the tubules the membrane curvature is very large (as it is in the case of helicoids), and this possibly creates a diffusion barrier for movement into and out of them both for calcium ions in the lumen as well as for diffusion of proteins (like the IP_3Rs and RyRs) in the membrane.

4.4 Different refilling mechanisms of IP_3- and Ry-sensitive ER calcium stores in CA1 pyramidal neurons

In this thesis, convincing evidence is provided for a difference in calcium store replenishment mechanisms for IP_3- and Ry-sensitive stores in CA1 pyramidal neurons. Whereas IP_3-sensitive stores depend on Orai1/3 at a young postnatal age <P16 and on

Orai2 at more mature postnatal stages, the Ry-sensitive stores appear to be independent of Orais and being regulated by VGCCs instead.

The replenishment of ER calcium stores by STIM/Orai complexes following IP_3R-mediated calcium release has been investigated in many different cell types. Because of the requirement for direct molecular interaction between STIM proteins in the ER and Orai channels in the plasma membrane (PM) the activation of Orai channels occurs at ER-PM contact sites, or ER-PM junctions. There, Orai subunits are organized in large supramolecular complexes that include IP_3Rs and SERCA, ensuring highly localized and specific calcium reuptake (Fernandez-Busnadiego et al., 2015; Orci et al., 2009; Poteser et al., 2016). This was also observed with the use of total internal reflection fluorescence microscopy (TIRFM) in HEK293 cells. Upon calcium release, STIM1 proteins that were located closely to the IP_3Rs accumulated at ER-PM junctions and there bound to Orai1 channels (Thillaiappan et al., 2017).

However, it was also demonstrated that, unlike in CA1 pyramidal neurons, IP_3-sensitive calcium stores can be refilled by the activity of VGCCs. In amygdala neurons and smooth muscle cells the L-type VGCC antagonist nifedipine blocked the mGluR1/5- and carbachol-evoked calcium release (Power and Sah, 2005; Wu et al., 2002) indicative for an involvement of L-type VGCCs calcium IP_3-sensitive store refilling. In cerebellar Purkinje cells, empty IP_3-sensitive stores can be refilled by depolarizing pulses and VGCC-mediated calcium influx (Hartmann et al., 2014). However, as mentioned before, the IP_3-sensitive stores in this cell type is practically identical with the Ry-sensitive store (Hartmann et al., 2014; Khodakhah and Armstrong, 1997) which may explain this difference to CA1 pyramidal neurons.

In striatal spiny neurons, in contrast, the activation of the PLCβ1-IP_3R pathway reduces the calcium currents mediated by L-type VGCCs (Hernandez-Lopez et al., 2000). In addition, co-expression of STIM1 and the L-type VGCC, $Ca_V1.2$, reduced the number of $Ca_V1.2$ molecules in the plasma membrane after calcium store depletion and decreased the calcium influx through $Ca_V1.2$ in primary cultures of cortical and hippocampal neurons (Park et al., 2010). It was demonstrated that activated STIM1 is responsible for this inhibitory effect on $Ca_v1.2$. The type of interaction between VGCCs and IP_3-sensitive stores thus seems to be cell type-specific.

There is still an open question which particular types of VGCC replenish Ry-sensitive stores in CA1 pyramidal neurons. In a previous study in CA1 pyramidal neurons, it was suggested that the refilling of the Ry-sensitive store can occur at resting membrane potential and might involve capacitive calcium entry channels that are sensitive to nickel and D600 but not sensitive to the L-type VGCC inhibitor nifedipine (Garaschuk et al., 1997). In line with this, in rat sensory neurons the refilling of Ry-sensitive stores was not inhibited in the presence of L-, P/Q- and N-type VGCC blockers (Usachev and Thayer, 1999). These data raise the possibility that the replenishment of the Ry-sensitive store might be mediated by T-type VGCCs which are activated at resting membrane potential. This hypothesis is supported by findings in dopamine neurons in midbrain slices from neonatal rats in which RyR-mediated calcium release was abolished by a T-type VGCC blocker (Cui et al., 2004). However, in my own experiments, 0.1 mM Nickel that specifically block T-type VGCCs did not prevent the spontaneous refilling of Ry-sensitive calcium stores in CA1 pyramidal neurons (data not shown). One other VGCC that is still left out is the type 3 L-type VGCC ($Ca_V1.3$). $Ca_V1.3$ is highly expressed in the hippocampus of the rat and has been shown to interact with RyR2 (Kim et al., 2007).

However, there is so far no pharmacological inhibitor, which specifically targets $Ca_V1.3$. It is not sensitive to dihydropyridine, the commonly used L-type VGCC blocker (Lipscombe et al., 2004; Xu and Lipscombe, 2001). Without a transgenic animal model, it is currently not possible to test whether $Ca_V1.3$ is involved in the refilling of Ry-sensitive calcium stores and the question about the exact mechanism remains unanswered.

4.5 Role of Orai2, IP_3- and Ry-sensitive stores in synaptic plasticity

The finding that LTP at SC synapses of CA1 pyramidal neurons does not require Orai2 and thus is independent of IP_3-sensitive stores (**Figure 3.17 A**) is consistent with previous findings that LTP which is induced through strong tetanization (4 bursts with 10 second inter-burst interval in 100 Hz for 1 second) and theta-bursts (400ms at 100 Hz) is not affected in the absence of mGluR1/5 in CA1 pyramidal neurons of rats and mice (Balschun et al., 1999a; Xu et al., 2014). When a similar tetanization protocol was used, LTP was also intact in the absence of IP_3R1 in CA1 (Fujii et al., 2000). These findings suggest that the entire mGluR1/5-IP_3R pathway is not involved in LTP induced with strong tetanization in CA1 pyramidal neurons. In addition, with a different LTP induction protocol (synaptic stimulation at 5 Hz for 16s combined with somatic 2 nA current injection for 2ms after 5ms synaptic stimulation) in CA1 pyramidal neurons, LTP was not inhibited when IP_3R1 was blocked by an antibody or when the *IP_3R1* gene was deleted in a knockout mouse.

However, based on the findings regarding the tetanization-induced LTP it cannot be concluded that hippocampal LTP is generally independent of Orai2 and the IP_3-sensitive store. In a conditional CA1 pyramidal neurons-specific mGluR5 knockout, the low-

frequency induced priming of synapses for subsequent theta burst potentiation was impaired, and mutant mice exhibited a deficit in temporal information processing in a foot-shock behavior test (Xu et al., 2014). Previous work has shown that depending on the stimulation protocol different calcium sources are recruited for the induction of LTP (Futatsugi et al., 1999; Konieczny et al., 2017; Raymond and Redman, 2006). LTP induced by four theta-bursts relies on the activation of IP_3R-dependent calcium release (Futatsugi et al., 1999; Konieczny et al., 2017; Raymond and Redman, 2006). In addition, there is a short tetanization-induced LTP which is not blocked by the NMDAR antagonist AP-5 but depends on L-type VGCCs and mGluR1/5 (Futatsugi et al., 1999).

Whether and how Orai2 and the IP_3-sensitive calcium store contribute to this is an open question. It would be worthwhile to start out with a thorough behavioral analysis of Orai2-/- mice and after the detection of possible specific memory deficits determine the underlying impairment in synaptic plasticity.

A single theta-burst induces LTP at SC synapses of CA1 pyramidal neurons through the RyR-dependent activation of calcium release, and with eight theta bursts LTP is induced by the activation of L-type VGCCs. In contrast, the IP_3-sensitive store experiments presented here show that the Ry-sensitive calcium store is critical for LTP induction by strong tetanization (**Figure 3.17 B**). This finding confirms a previous study which showed that RyR-mediated calcium release is involved in strong tetanization-induced LTP in mouse hippocampal slices (Lu and Hawkins, 2002).

Experiments included in my thesis demonstrate that in Orai2$^{-/-}$ mice, although the DHPG-evoked calcium response at a late postnatal stage (>P16) (**Figure 3.5**) is abolished, there is no requirement for Orai2 for the induction of chemical LTD by bath

application of an mGluR1/5 agonist (**Figure 3.18 A**). Pharmacological evidence indicates that this type of LTD depends on mGluR5 but not mGluR1 (Fitzjohn et al., 1999; Schnabel et al., 1999). However, it is not dependent on cytosolic calcium as was demonstrated with the use of the calcium chelator BAPTA and the SERCA antagonists CPA and thapsigargin (Fitzjohn et al., 2001; Schnabel et al., 1999). The fact that the mGluR5-dependent LTD is independent of Orai2, as I demonstrated here, shows that it does not require a regular intraluminal calcium concentration on IP_3-sensitive calcium stores either. The factor that is responsible for the induction of this type of LTD thus must be located upstream of IP_3-signaling stores in the signaling cascade initiated by mGluR5 activation.

In a third series of experiments that addressed the relevance of Orai2 for synaptic plasticity, an impairment in LTP suppression following the calcium independent chemical LTD was found (**Figure 3.18 B**) in Orai2$^{-/-}$ mice. This again is in line with findings obtained in IP_3R1 knock-out mice. In the absence of IP_3, in these mice neurons in hippocampal slices exhibited a higher excitability compared to the control group and this impaired the inhibition of LTP in CA1 (Fujii et al., 2000; Nishiyama et al., 2000). This finding although confirmatory at a first glance is interesting because it implies that a mGluR5-dependent signaling cascade other than the PLC-IP_3R-dependent pathway is activated by the chemical LTD and, under normal conditions, targets Orai2-channels and / or the IP_3-sensitive calcium store in order to prevent LTP induction. Candidate signaling molecules are Homer (Kammermeier and Worley, 2007), β-arrestin and Src (Gerber et al., 2007) that are activated by mGluR1/5 but independent of PKC.

Besides LTP and LTD, SOCE channels are also involved in the maintenance and plasticity in spine structure and in synaptogenesis. Knock-down of Orai1 or 2 by RNAi reduced the number of mushroom spines and increased the number of immature filopodia in hippocampal CA1 (Korkotian et al., 2017; Zhang et al., 2016). Since RyRs are highly expressed in CA1 pyramidal spine but Ry-sensitive stores are independent of Orais this seems to be an intriguing result for which there is currently no satisfying explanation. Moreover, it has been shown that STIM1 promotes dendritic spines growth and increases the ER content in spine (Dittmer et al., 2017b). All in all, these results point out the importance of the role of ER calcium homeostasis in maintaining neuronal synaptic plasticity in LTP, LTD, synaptogenesis and maintenance of synaptic structure.

5. Conclusion

My work shows a developmental switch in Orai expression from Orai1/3 at postnatal ages <P16 to Orai2 at later postnatal ages. Consistent with that, mGluR1/5-IP_3R-mediated calcium signaling becomes strongly dependent on Orai2 at postnatal ages >P17. Moreover, RyR-mediated calcium release remains unaltered in the absence of Orai2. These observations identify two largely non-overlapping ER calcium stores in CA1 pyramidal neurons – the IP_3-sensitive and the Ry-sensitive calcium store. They can be depleted almost independently of one another with a small overlap of the respective calcium pools of 15-20%. Both stores refill spontaneously but through different mechanisms: The IP_3-sensitive store critically depends on Orai2, whereas the Ry-sensitive store is refilled by calcium influx through a yet unidentified VGCC (**Fig. 5.1**). Both types of stores seem to have complementary roles for synaptic plasticity at SC synapses of hippocampal pyramidal neurons: Ry-sensitive stores are required for induction of LTP, IP_3-sensitive stores are important for the suppression of LTP. The ER calcium store that is sensitive to IP_3 but insensitive to Ry in CA1 pyramidal cells is a novel type of ER calcium store in this cell type and has not been characterized before. It was also not shown before in other cell types that Orai2 replenishes specifically only this type of ER calcium store. The independence of Ry-sensitive sto res from Orai channels is the third novel and significant finding from this work that adds significantly to our knowledge about ER-associated calcium signaling in central mammalian neurons.

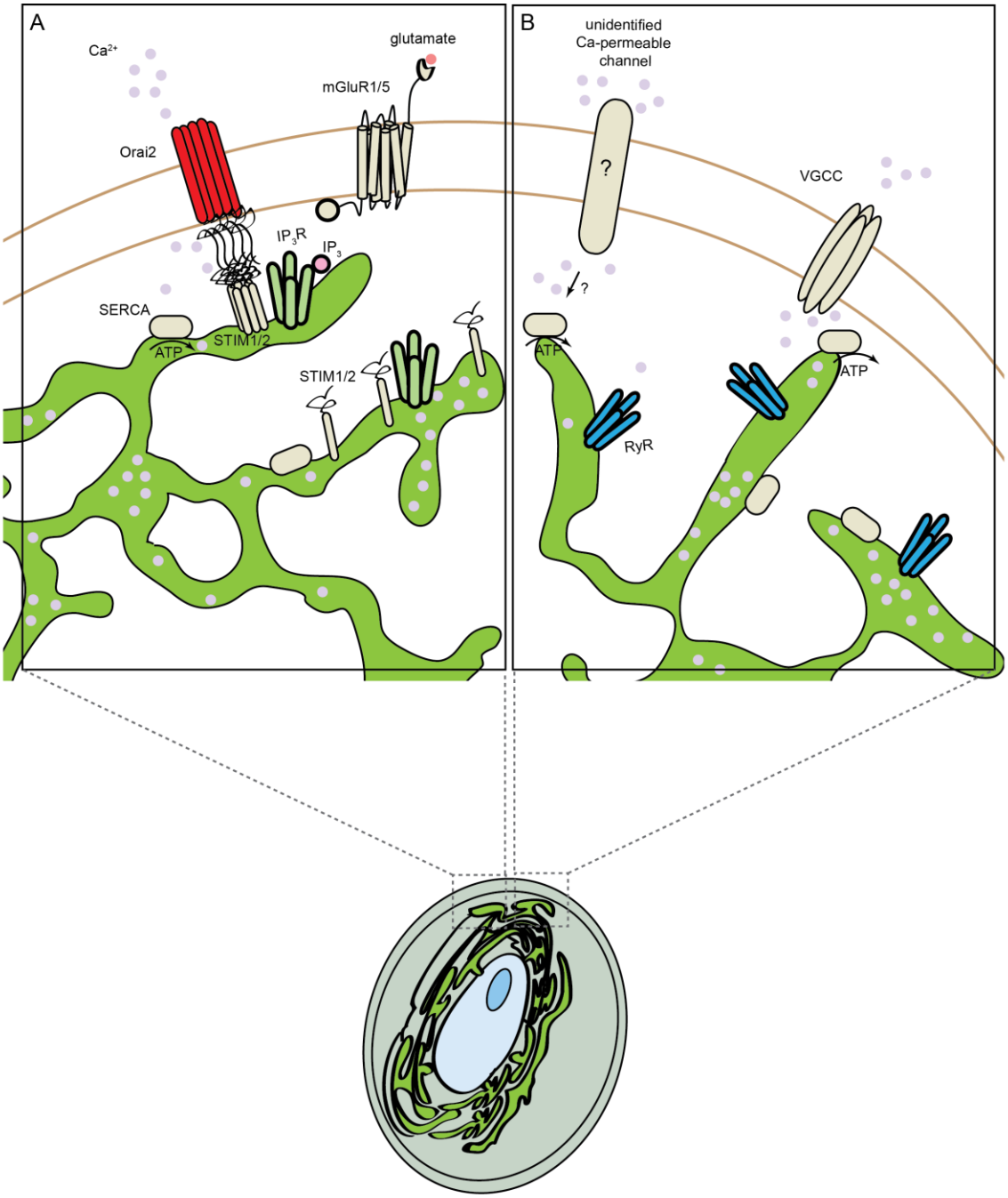

Figure 5.1 Schematic representation of the t wo stores model and the role of Orai2 in hippocampal CA1 pyramidal neuron

(A) The cartoon figure shows the activation and refilling mechanism in the IP_3-sensitive store and (B) in the Ry-sensitive store in a CA1 pyramidal neuron. Please see text for more details.

6. Publications

Chen, HJ, Hartmann J, Konnerth A

Orai2 determines calcium signaling in a novel intracellular store of hippocampal pyramidal cells (in preparation)

7. References

Amaral, D.G., and Witter, M.P. (1989). The three-dimensional organization of the hippocampal formation: a review of anatomical data. Neuroscience *31*, 571-591.

Andersen, P., Bliss, T.V., Lomo, T., Olsen, L.I., and Skrede, K.K. (1969). Lamellar organization of hippocampal excitatory pathways. Acta Physiol Scand *76*, 4A-5A.

Ashmole, I., Duffy, S.M., Leyland, M.L., and Bradding, P. (2013). The contribution of Orai(CRACM)1 and Orai(CRACM)2 channels in store-operated Ca2+ entry and mediator release in human lung mast cells. PLoS One *8*, e74895.

Ayala, J.E., Chen, Y., Banko, J.L., Sheffler, D.J., Williams, R., Telk, A.N., Watson, N.L., Xiang, Z., Zhang, Y., Jones, P.J.*, et al.* (2009). mGluR5 positive allosteric modulators facilitate both hippocampal LTP and LTD and enhance spatial learning. Neuropsychopharmacology *34*, 2057-2071.

Balschun, D., Manahan-Vaughan, D., Wagner, T., Behnisch, T., Reymann, K.G., and Wetzel, W. (1999a). A specific role for group I mGluRs in hippocampal LTP and hippocampus-dependent spatial learning. Learn Mem *6*, 138-152.

Balschun, D., Wolfer, D.P., Bertocchini, F., Barone, V., Conti, A., Zuschratter, W., Missiaen, L., Lipp, H.P., Frey, J.U., and Sorrentino, V. (1999b). Deletion of the ryanodine receptor type 3 (RyR3) impairs forms of synaptic plasticity and spatial learning. EMBO J *18*, 5264-5273.

Bear, M.F., and Abraham, W.C. (1996). Long-term depression in hippocampus. Annu Rev Neurosci *19*, 437-462.

Berridge, M.J., Bootman, M.D., and Roderick, H.L. (2003). Calcium signalling: dynamics, homeostasis and remodelling. Nat Rev Mol Cell Biol *4*, 517-529.

Berridge, M.J., Lipp, P., and Bootman, M.D. (2000). The versatility and universality of calcium signalling. Nat Rev Mol Cell Biol *1*, 11-21.

Bezprozvanny, I., Watras, J., and Ehrlich, B.E. (1991). Bell-shaped calcium-response curves of Ins(1,4,5)P3- and calcium-gated channels from endoplasmic reticulum of cerebellum. Nature *351*, 751-754.

Bird, C.M., and Burgess, N. (2008). The hippocampus and memory: insights from spatial processing. Nat Rev Neurosci *9*, 182-194.

Borchelt, D.R., Ratovitski, T., van Lare, J., Lee, M.K., Gonzales, V., Jenkins, N.A., Copeland, N.G., Price, D.L., and Sisodia, S.S. (1997). Accelerated amyloid deposition in the brains of transgenic mice coexpressing mutant presenilin 1 and amyloid precursor proteins. Neuron *19*, 939-945.

Buzsaki, G., and Moser, E.I. (2013). Memory, navigation and theta rhythm in the hippocampal-entorhinal system. Nat Neurosci *16*, 130-138.

Caroni, P., Donato, F., and Muller, D. (2012). Structural plasticity upon learning: regulation and functions. Nat Rev Neurosci *13*, 478-490.

Carr, M.F., and Frank, L.M. (2012). A single microcircuit with multiple functions: state dependent information processing in the hippocampus. Curr Opin Neurobiol *22*, 704-708.

Chen, M., Van Hook, M.J., and Thoreson, W.B. (2015). Ca2+ Diffusion through Endoplasmic Reticulum Supports Elevated Intraterminal Ca2+ Levels Needed to Sustain Synaptic Release from Rods in Darkness. J Neurosci *35*, 11364-11373.

Clapham, D.E. (1995). Calcium signaling. Cell *80*, 259-268.

Conn, P.J., and Pin, J.P. (1997). Pharmacology and functions of metabotropic glutamate receptors. Annu Rev Pharmacol Toxicol *37*, 205-237.

Cruts, M., van Duijn, C.M., Backhovens, H., Van den Broeck, M., Wehnert, A., Serneels, S., Sherrington, R., Hutton, M., Hardy, J., St George-Hyslop, P.H.*, et al.* (1998). Estimation of the genetic contribution of presenilin-1 and -2 mutations in a population-based study of presenile Alzheimer disease. Hum Mol Genet *7*, 43-51.

Cui, G., Okamoto, T., and Morikawa, H. (2004). Spontaneous opening of T-type Ca2+ channels contributes to the irregular firing of dopamine neurons in neonatal rats. J Neurosci *24*, 11079-11087.

Cutsuridis, V., Cobb, S., and Graham, B.P. (2010a). Encoding and retrieval in a model of the hippocampal CA1 microcircuit. Hippocampus *20*, 423-446.

Cutsuridis, V., Springer E-books - York University., and SpringerLink (Online service) (2010b). Hippocampal microcircuits a computational modeler's resource book. In Springer series in computational neuroscience v 5 (New York: Springer), pp. xi, 617 p.

DeHaven, W.I., Smyth, J.T., Boyles, R.R., and Putney, J.W., Jr. (2007). Calcium inhibition and calcium potentiation of Orai1, Orai2, and Orai3 calcium release-activated calcium channels. J Biol Chem *282*, 17548-17556.

Dent, M.A., Raisman, G., and Lai, F.A. (1996). Expression of type 1 inositol 1,4,5-trisphosphate receptor during axogenesis and synaptic contact in the central and peripheral nervous system of developing rat. Development *122*, 1029-1039.

Destexhe, A., and Marder, E. (2004). Plasticity in single neuron and circuit computations. Nature *431*, 789-795.

Dickinson, G.D., Ellefsen, K.L., Dawson, S.P., Pearson, J.E., and Parker, I. (2016). Hindered cytoplasmic diffusion of inositol trisphosphate restricts its cellular range of action. Sci Signal *9*, ra108.

Diez-Bello, R., Jardin, I., Salido, G.M., and Rosado, J.A. (2017). Orai1 and Orai2 mediate store-operated calcium entry that regulates HL60 cell migration and FAK phosphorylation. Biochim Biophys Acta *1864*, 1064-1070.

Dittmer, P.J., Wild, A.R., Dell'Acqua, M.L., and Sather, W.A. (2017a). STIM1 Ca2+ Sensor Control of L-type Ca2+-Channel-Dependent Dendritic Spine Structural Plasticity and Nuclear Signaling. Cell Rep *19*, 321-334.

Dittmer, P.J., Wild, A.R., Dell'Acqua, M.L., and Sather, W.A. (2017b). STIM1 Ca(2+) Sensor Control of L-type Ca(2+)-Channel-Dependent Dendritic Spine Structural Plasticity and Nuclear Signaling. Cell Rep *19*, 321-334.

Durand, G.M., Marandi, N., Herberger, S.D., Blum, R., and Konnerth, A. (2006). Quantitative single-cell RT-PCR and Ca2+ imaging in brain slices. Pflugers Arch *451*, 716-726.

Emptage, N.J., Reid, C.A., and Fine, A. (2001). Calcium stores in hippocampal synaptic boutons mediate short-term plasticity, store-operated Ca2+ entry, and spontaneous transmitter release. Neuron *29*, 197-208.

Fernandez-Busnadiego, R., Saheki, Y., and De Camilli, P. (2015). Three-dimensional architecture of extended synaptotagmin-mediated endoplasmic reticulum-plasma membrane contact sites. Proc Natl Acad Sci U S A *112*, E2004-2013.

Ferreira, D.G., Temido-Ferreira, M., Miranda, H.V., Batalha, V.L., Coelho, J.E., Szego, E.M., Marques-Morgado, I., Vaz, S.H., Rhee, J.S., Schmitz, M.*, et al.* (2017). alpha-synuclein interacts with PrP(C) to induce cognitive impairment through mGluR5 and NMDAR2B. Nat Neurosci *20*, 1569-1579.

Feske, S., Gwack, Y., Prakriya, M., Srikanth, S., Puppel, S.H., Tanasa, B., Hogan, P.G., Lewis, R.S., Daly, M., and Rao, A. (2006). A mutation in Orai1 causes immune deficiency by abrogating CRAC channel function. Nature *441*, 179-185.

Finch, E.A., and Augustine, G.J. (1998). Local calcium signalling by inositol-1,4,5-trisphosphate in Purkinje cell dendrites. Nature *396*, 753-756.

Fitzjohn, S.M., Kingston, A.E., Lodge, D., and Collingridge, G.L. (1999). DHPG-induced LTD in area CA1 of juvenile rat hippocampus; characterisation and sensitivity to novel mGlu receptor antagonists. Neuropharmacology *38*, 1577-1583.

Fitzjohn, S.M., Palmer, M.J., May, J.E., Neeson, A., Morris, S.A., and Collingridge, G.L. (2001). A characterisation of long-term depression induced by metabotropic glutamate receptor activation in the rat hippocampus in vitro. J Physiol *537*, 421-430.

Fitzpatrick, J.S., Hagenston, A.M., Hertle, D.N., Gipson, K.E., Bertetto-D'Angelo, L., and Yeckel, M.F. (2009). Inositol-1,4,5-trisphosphate receptor-mediated Ca2+ waves in pyramidal neuron dendrites propagate through hot spots and cold spots. J Physiol *587*, 1439-1459.

Fujii, S., Matsumoto, M., Igarashi, K., Kato, H., and Mikoshiba, K. (2000). Synaptic plasticity in hippocampal CA1 neurons of mice lacking type 1 inositol-1,4,5-trisphosphate receptors. Learn Mem *7*, 312-320.

Furuichi, T., Kohda, K., Miyawaki, A., and Mikoshiba, K. (1994). Intracellular channels. Curr Opin Neurobiol *4*, 294-303.

Futatsugi, A., Kato, K., Ogura, H., Li, S.T., Nagata, E., Kuwajima, G., Tanaka, K., Itohara, S., and Mikoshiba, K. (1999). Facilitation of NMDAR-independent LTP and spatial learning in mutant mice lacking ryanodine receptor type 3. Neuron *24*, 701-713.

Garaschuk, O., Yaari, Y., and Konnerth, A. (1997). Release and sequestration of calcium by ryanodine-sensitive stores in rat hippocampal neurones. J Physiol *502 (Pt 1)*, 13-30.

Gerber, U., Gee, C.E., and Benquet, P. (2007). Metabotropic glutamate receptors: intracellular signaling pathways. Curr Opin Pharmacol *7*, 56-61.

Ghosh, A., and Greenberg, M.E. (1995). Calcium signaling in neurons: molecular mechanisms and cellular consequences. Science *268*, 239-247.

Golovina, V.A., and Blaustein, M.P. (1997). Spatially and functionally distinct Ca2+ stores in sarcoplasmic and endoplasmic reticulum. Science *275*, 1643-1648.

Hartmann, J., Karl, R.M., Alexander, R.P., Adelsberger, H., Brill, M.S., Ruhlmann, C., Ansel, A., Sakimura, K., Baba, Y., Kurosaki, T.*, et al.* (2014). STIM1 controls neuronal Ca(2)(+) signaling, mGluR1-dependent synaptic transmission, and cerebellar motor behavior. Neuron *82*, 635-644.

Hartmann, J., and Konnerth, A. (2015). TRPC3-dependent synaptic transmission in central mammalian neurons. J Mol Med (Berl) *93*, 983-989.

Harvey, J., and Collingridge, G.L. (1992). Thapsigargin blocks the induction of long-term potentiation in rat hippocampal slices. Neurosci Lett *139*, 197-200.

Hayashi, Y., Shi, S.H., Esteban, J.A., Piccini, A., Poncer, J.C., and Malinow, R. (2000). Driving AMPA receptors into synapses by LTP and CaMKII: requirement for GluR1 and PDZ domain interaction. Science *287*, 2262-2267.

Hebb, D.O. (1949). The organization of behavior : a neuropsychological theory (New York: Wiley).

Hernandez-Lopez, S., Tkatch, T., Perez-Garci, E., Galarraga, E., Bargas, J., Hamm, H., and Surmeier, D.J. (2000). D2 dopamine receptors in striatal medium spiny neurons reduce L-type Ca2+ currents and excitability via a novel PLC[beta]1-IP3-calcineurin-signaling cascade. J Neurosci *20*, 8987-8995.

Hoge, J., and Kesner, R.P. (2007). Role of CA3 and CA1 subregions of the dorsal hippocampus on temporal processing of objects. Neurobiol Learn Mem *88*, 225-231.

Holbro, N., Grunditz, A., and Oertner, T.G. (2009). Differential distribution of endoplasmic reticulum controls metabotropic signaling and plasticity at hippocampal synapses. Proc Natl Acad Sci U S A *106*, 15055-15060.

Hollmann, M., and Heinemann, S. (1994). Cloned glutamate receptors. Annu Rev Neurosci *17*, 31-108.

Hoth, M., and Niemeyer, B.A. (2013). The neglected CRAC proteins: Orai2, Orai3, and STIM2. Curr Top Membr *71*, 237-271.

Hoth, M., and Penner, R. (1992). Depletion of intracellular calcium stores activates a calcium current in mast cells. Nature *355*, 353-356.

Huber, K.M., Kayser, M.S., and Bear, M.F. (2000). Role for rapid dendritic protein synthesis in hippocampal mGluR-dependent long-term depression. Science *288*, 1254-1257.

Huggett, J., Dheda, K., Bustin, S., and Zumla, A. (2005). Real-time RT-PCR normalisation; strategies and considerations. Genes Immun *6*, 279-284.

Inayama, M., Suzuki, Y., Yamada, S., Kurita, T., Yamamura, H., Ohya, S., Giles, W.R., and Imaizumi, Y. (2015). Orai1-Orai2 complex is involved in store-operated calcium entry in chondrocyte cell lines. Cell Calcium *57*, 337-347.

Johenning, F.W., Theis, A.K., Pannasch, U., Ruckl, M., Rudiger, S., and Schmitz, D. (2015). Ryanodine Receptor Activation Induces Long-Term Plasticity of Spine Calcium Dynamics. PLoS Biol *13*, e1002181.

Kammermeier, P.J., and Worley, P.F. (2007). Homer 1a uncouples metabotropic glutamate receptor 5 from postsynaptic effectors. Proc Natl Acad Sci U S A *104*, 6055-6060.

Khodakhah, K., and Armstrong, C.M. (1997). Inositol trisphosphate and ryanodine receptors share a common functional Ca2+ pool in cerebellar Purkinje neurons. Biophys J *73*, 3349-3357.

Kim, J.J., and Diamond, D.M. (2002). The stressed hippocampus, synaptic plasticity and lost memories. Nat Rev Neurosci *3*, 453-462.

Kim, S., Yun, H.M., Baik, J.H., Chung, K.C., Nah, S.Y., and Rhim, H. (2007). Functional interaction of neuronal Cav1.3 L-type calcium channel with ryanodine receptor type 2 in the rat hippocampus. J Biol Chem *282*, 32877-32889.

Kim, S.J., and Linden, D.J. (2007). Ubiquitous plasticity and memory storage. Neuron *56*, 582-592.

Koizumi, S., Bootman, M.D., Bobanovic, L.K., Schell, M.J., Berridge, M.J., and Lipp, P. (1999). Characterization of elementary Ca2+ release signals in NGF-differentiated PC12 cells and hippocampal neurons. Neuron *22*, 125-137.

Konieczny, V., Tovey, S.C., Mataragka, S., Prole, D.L., and Taylor, C.W. (2017). Cyclic AMP Recruits a Discrete Intracellular Ca(2+) Store by Unmasking Hypersensitive IP3 Receptors. Cell Rep *18*, 711-722.

Korkotian, E., Oni-Biton, E., and Segal, M. (2017). The role of the store-operated calcium entry channel Orai1 in cultured rat hippocampal synapse formation and plasticity. J Physiol *595*, 125-140.

Kotaleski, J.H., and Blackwell, K.T. (2010). Modelling the molecular mechanisms of synaptic plasticity using systems biology approaches. Nat Rev Neurosci *11*, 239-251.

Kozera, B., and Rapacz, M. (2013). Reference genes in real-time PCR. J Appl Genet *54*, 391-406.

Kraft, R. (2015). STIM and ORAI proteins in the nervous system. Channels (Austin) *9*, 245-252.

Lanner, J.T., Georgiou, D.K., Joshi, A.D., and Hamilton, S.L. (2010). Ryanodine receptors: structure, expression, molecular details, and function in calcium release. Cold Spring Harb Perspect Biol *2*, a003996.

Lee, I., and Kesner, R.P. (2004). Differential contributions of dorsal hippocampal subregions to memory acquisition and retrieval in contextual fear-conditioning. Hippocampus *14*, 301-310.

Lein, E.S., Hawrylycz, M.J., Ao, N., Ayres, M., Bensinger, A., Bernard, A., Boe, A.F., Boguski, M.S., Brockway, K.S., Byrnes, E.J.*, et al.* (2007). Genome-wide atlas of gene expression in the adult mouse brain. Nature *445*, 168-176.

Leuner, K., Kazanski, V., Muller, M., Essin, K., Henke, B., Gollasch, M., Harteneck, C., and Muller, W.E. (2007). Hyperforin--a key constituent of St. John's wort specifically activates TRPC6 channels. FASEB J *21*, 4101-4111.

Lewis, R.S. (2011). Store-operated calcium channels: new perspectives on mechanism and function. Cold Spring Harb Perspect Biol *3*.

Lewis, R.S., and Cahalan, M.D. (1989). Mitogen-induced oscillations of cytosolic Ca2+ and transmembrane Ca2+ current in human leukemic T cells. Cell Regul *1*, 99-112.

Lindholm, D., Wootz, H., and Korhonen, L. (2006). ER stress and neurodegenerative diseases. Cell Death Differ *13*, 385-392.

Liou, J., Kim, M.L., Heo, W.D., Jones, J.T., Myers, J.W., Ferrell, J.E., Jr., and Meyer, T. (2005). STIM is a Ca2+ sensor essential for Ca2+-store-depletion-triggered Ca2+ influx. Curr Biol *15*, 1235-1241.

Lipscombe, D., Helton, T.D., and Xu, W. (2004). L-type calcium channels: the low down. J Neurophysiol *92*, 2633-2641.

Lis, A., Peinelt, C., Beck, A., Parvez, S., Monteilh-Zoller, M., Fleig, A., and Penner, R. (2007). CRACM1, CRACM2, and CRACM3 are store-operated Ca2+ channels with distinct functional properties. Curr Biol *17*, 794-800.

Liu, L., Wong, T.P., Pozza, M.F., Lingenhoehl, K., Wang, Y., Sheng, M., Auberson, Y.P., and Wang, Y.T. (2004). Role of NMDA receptor subtypes in governing the direction of hippocampal synaptic plasticity. Science *304*, 1021-1024.

Lu, Y.F., and Hawkins, R.D. (2002). Ryanodine receptors contribute to cGMP-induced late-phase LTP and CREB phosphorylation in the hippocampus. J Neurophysiol *88*, 1270-1278.

Lu, Y.M., Jia, Z., Janus, C., Henderson, J.T., Gerlai, R., Wojtowicz, J.M., and Roder, J.C. (1997). Mice lacking metabotropic glutamate receptor 5 show impaired learning and reduced CA1 long-term potentiation (LTP) but normal CA3 LTP. J Neurosci *17*, 5196-5205.

Luebke, J.I., Dunlap, K., and Turner, T.J. (1993). Multiple calcium channel types control glutamatergic synaptic transmission in the hippocampus. Neuron *11*, 895-902.

Luik, R.M., Wang, B., Prakriya, M., Wu, M.M., and Lewis, R.S. (2008). Oligomerization of STIM1 couples ER calcium depletion to CRAC channel activation. Nature *454*, 538-542.

Luscher, C., and Huber, K.M. (2010). Group 1 mGluR-dependent synaptic long-term depression: mechanisms and implications for circuitry and disease. Neuron *65*, 445-459.

Luscher, C., Nicoll, R.A., Malenka, R.C., and Muller, D. (2000). Synaptic plasticity and dynamic modulation of the postsynaptic membrane. Nat Neurosci *3*, 545-550.

Majewski, L., and Kuznicki, J. (2015). SOCE in neurons: Signaling or just refilling? Biochim Biophys Acta *1853*, 1940-1952.

Mannaioni, G., Marino, M.J., Valenti, O., Traynelis, S.F., and Conn, P.J. (2001). Metabotropic glutamate receptors 1 and 5 differentially regulate CA1 pyramidal cell function. J Neurosci *21*, 5925-5934.

Mattson, M.P., LaFerla, F.M., Chan, S.L., Leissring, M.A., Shepel, P.N., and Geiger, J.D. (2000). Calcium signaling in the ER: its role in neuronal plasticity and neurodegenerative disorders. Trends Neurosci *23*, 222-229.

Mayford, M., Bach, M.E., Huang, Y.Y., Wang, L., Hawkins, R.D., and Kandel, E.R. (1996). Control of memory formation through regulated expression of a CaMKII transgene. Science *274*, 1678-1683.

McHugh, T.J., Blum, K.I., Tsien, J.Z., Tonegawa, S., and Wilson, M.A. (1996). Impaired hippocampal representation of space in CA1-specific NMDAR1 knockout mice. Cell *87*, 1339-1349.

McNally, B.A., Somasundaram, A., Yamashita, M., and Prakriya, M. (2012). Gated regulation of CRAC channel ion selectivity by STIM1. Nature *482*, 241-245.

Mercer, J.C., Dehaven, W.I., Smyth, J.T., Wedel, B., Boyles, R.R., Bird, G.S., and Putney, J.W., Jr. (2006). Large store-operated calcium selective currents due to co-expression of Orai1 or Orai2 with the intracellular calcium sensor, Stim1. J Biol Chem *281*, 24979-24990.

Miyata, M., Finch, E.A., Khiroug, L., Hashimoto, K., Hayasaka, S., Oda, S.I., Inouye, M., Takagishi, Y., Augustine, G.J., and Kano, M. (2000). Local calcium release in dendritic spines required for long-term synaptic depression. Neuron *28*, 233-244.

Mody, M., Cao, Y., Cui, Z., Tay, K.Y., Shyong, A., Shimizu, E., Pham, K., Schultz, P., Welsh, D., and Tsien, J.Z. (2001). Genome-wide gene expression profiles of the developing mouse hippocampus. Proc Natl Acad Sci U S A *98*, 8862-8867.

Mogami, H., Nakano, K., Tepikin, A.V., and Petersen, O.H. (1997). Ca2+ flow via tunnels in polarized cells: recharging of apical Ca2+ stores by focal Ca2+ entry through basal membrane patch. Cell *88*, 49-55.

Montero, M., Alvarez, J., Scheenen, W.J., Rizzuto, R., Meldolesi, J., and Pozzan, T. (1997). Ca2+ homeostasis in the endoplasmic reticulum: coexistence of high and low [Ca2+] subcompartments in intact HeLa cells. J Cell Biol *139*, 601-611.

Moser, E.I. (2011). The multi-laned hippocampus. Nat Neurosci *14*, 407-408.

Mukherjee, S., and Manahan-Vaughan, D. (2013). Role of metabotropic glutamate receptors in persistent forms of hippocampal plasticity and learning. Neuropharmacology *66*, 65-81.

Murphy, S.N., and Miller, R.J. (1989). Two distinct quisqualate receptors regulate Ca2+ homeostasis in hippocampal neurons in vitro. Mol Pharmacol *35*, 671-680.

Muschol, M., Dasgupta, B.R., and Salzberg, B.M. (1999). Caffeine interaction with fluorescent calcium indicator dyes. Biophys J *77*, 577-586.

Nakamura, T., Barbara, J.G., Nakamura, K., and Ross, W.N. (1999). Synergistic release of Ca2+ from IP3-sensitive stores evoked by synaptic activation of mGluRs paired with backpropagating action potentials. Neuron *24*, 727-737.

Nakamura, T., Nakamura, K., Lasser-Ross, N., Barbara, J.G., Sandler, V.M., and Ross, W.N. (2000). Inositol 1,4,5-trisphosphate (IP3)-mediated Ca2+ release evoked by metabotropic agonists and backpropagating action potentials in hippocampal CA1 pyramidal neurons. J Neurosci *20*, 8365-8376.

Nelson, O., Tu, H., Lei, T., Bentahir, M., de Strooper, B., and Bezprozvanny, I. (2007). Familial Alzheimer disease-linked mutations specifically disrupt Ca2+ leak function of presenilin 1. J Clin Invest *117*, 1230-1239.

Neves, G., Cooke, S.F., and Bliss, T.V. (2008). Synaptic plasticity, memory and the hippocampus: a neural network approach to causality. Nat Rev Neurosci *9*, 65-75.

Neyman, S., and Manahan-Vaughan, D. (2008). Metabotropic glutamate receptor 1 (mGluR1) and 5 (mGluR5) regulate late phases of LTP and LTD in the hippocampal CA1 region in vitro. Eur J Neurosci *27*, 1345-1352.

Ng, A.N., Krogh, M., and Toresson, H. (2011). Dendritic EGFP-STIM1 activation after type I metabotropic glutamate and muscarinic acetylcholine receptor stimulation in hippocampal neuron. J Neurosci Res *89*, 1235-1244.

Nishiyama, M., Hong, K., Mikoshiba, K., Poo, M.M., and Kato, K. (2000). Calcium stores regulate the polarity and input specificity of synaptic modification. Nature *408*, 584-588.

Niswender, C.M., and Conn, P.J. (2010). Metabotropic glutamate receptors: physiology, pharmacology, and disease. Annu Rev Pharmacol Toxicol *50*, 295-322.

Nixon-Abell, J., Obara, C.J., Weigel, A.V., Li, D., Legant, W.R., Xu, C.S., Pasolli, H.A., Harvey, K., Hess, H.F., Betzig, E.*, et al.* (2016). Increased spatiotemporal resolution reveals highly dynamic dense tubular matrices in the peripheral ER. Science *354*.

Oliet, S.H., Malenka, R.C., and Nicoll, R.A. (1997). Two distinct forms of long-term depression coexist in CA1 hippocampal pyramidal cells. Neuron *18*, 969-982.

Orci, L., Ravazzola, M., Le Coadic, M., Shen, W.W., Demaurex, N., and Cosson, P. (2009). From the Cover: STIM1-induced precortical and cortical subdomains of the endoplasmic reticulum. Proc Natl Acad Sci U S A *106*, 19358-19362.

Park, C.Y., Hoover, P.J., Mullins, F.M., Bachhawat, P., Covington, E.D., Raunser, S., Walz, T., Garcia, K.C., Dolmetsch, R.E., and Lewis, R.S. (2009). STIM1 clusters and activates CRAC channels via direct binding of a cytosolic domain to Orai1. Cell *136*, 876-890.

Park, C.Y., Shcheglovitov, A., and Dolmetsch, R. (2010). The CRAC channel activator STIM1 binds and inhibits L-type voltage-gated calcium channels. Science *330*, 101-105.

Park, M.K., Petersen, O.H., and Tepikin, A.V. (2000). The endoplasmic reticulum as one continuous Ca(2+) pool: visualization of rapid Ca(2+) movements and equilibration. EMBO J *19*, 5729-5739.

Parker, I., and Ivorra, I. (1991). Caffeine inhibits inositol trisphosphate-mediated liberation of intracellular calcium in Xenopus oocytes. J Physiol *433*, 229-240.

Peinelt, C., Vig, M., Koomoa, D.L., Beck, A., Nadler, M.J., Koblan-Huberson, M., Lis, A., Fleig, A., Penner, R., and Kinet, J.P. (2006). Amplification of CRAC current by STIM1 and CRACM1 (Orai1). Nat Cell Biol *8*, 771-773.

Penna, A., Demuro, A., Yeromin, A.V., Zhang, S.L., Safrina, O., Parker, I., and Cahalan, M.D. (2008). The CRAC channel consists of a tetramer formed by Stim-induced dimerization of Orai dimers. Nature *456*, 116-120.

Petersen, O.H., and Tepikin, A.V. (2008). Polarized calcium signaling in exocrine gland cells. Annu Rev Physiol *70*, 273-299.

Pin, J.P., and Duvoisin, R. (1995). The metabotropic glutamate receptors: structure and functions. Neuropharmacology *34*, 1-26.

Popkirov, S.G., and Manahan-Vaughan, D. (2011). Involvement of the metabotropic glutamate receptor mGluR5 in NMDA receptor-dependent, learning-facilitated long-term depression in CA1 synapses. Cereb Cortex *21*, 501-509.

Poteser, M., Leitinger, G., Pritz, E., Platzer, D., Frischauf, I., Romanin, C., and Groschner, K. (2016). Live-cell imaging of ER-PM contact architecture by a novel TIRFM approach reveals extension of junctions in response to store-operated Ca(2+)-entry. Sci Rep *6*, 35656.

Power, J.M., and Sah, P. (2005). Intracellular calcium store filling by an L-type calcium current in the basolateral amygdala at subthreshold membrane potentials. J Physiol *562*, 439-453.

Prakriya, M., Feske, S., Gwack, Y., Srikanth, S., Rao, A., and Hogan, P.G. (2006). Orai1 is an essential pore subunit of the CRAC channel. Nature *443*, 230-233.

Prakriya, M., and Lewis, R.S. (2015). Store-Operated Calcium Channels. Physiol Rev *95*, 1383-1436.

Purgert, C.A., Izumi, Y., Jong, Y.J., Kumar, V., Zorumski, C.F., and O'Malley, K.L. (2014). Intracellular mGluR5 can mediate synaptic plasticity in the hippocampus. J Neurosci *34*, 4589-4598.

Putney, J.W., Jr. (1986). A model for receptor-regulated calcium entry. Cell Calcium *7*, 1-12.

Raymond, C.R. (2007). LTP forms 1, 2 and 3: different mechanisms for the "long" in long-term potentiation. Trends Neurosci *30*, 167-175.

Raymond, C.R., and Redman, S.J. (2006). Spatial segregation of neuronal calcium signals encodes different forms of LTP in rat hippocampus. J Physiol *570*, 97-111.

Reyes-Harde, M., Empson, R., Potter, B.V., Galione, A., and Stanton, P.K. (1999). Evidence of a role for cyclic ADP-ribose in long-term synaptic depression in hippocampus. Proc Natl Acad Sci U S A *96*, 4061-4066.

Reyes, M., and Stanton, P.K. (1996). Induction of hippocampal long-term depression requires release of Ca2+ from separate presynaptic and postsynaptic intracellular stores. J Neurosci *16*, 5951-5960.

Ribeiro, F.M., Paquet, M., Ferreira, L.T., Cregan, T., Swan, P., Cregan, S.P., and Ferguson, S.S. (2010). Metabotropic glutamate receptor-mediated cell signaling pathways are altered in a mouse model of Huntington's disease. J Neurosci *30*, 316-324.

Roos, J., DiGregorio, P.J., Yeromin, A.V., Ohlsen, K., Lioudyno, M., Zhang, S., Safrina, O., Kozak, J.A., Wagner, S.L., Cahalan, M.D.*, et al.* (2005). STIM1, an essential and conserved component of store-operated Ca2+ channel function. J Cell Biol *169*, 435-445.

Rosado, J.A., Diez, R., Smani, T., and Jardin, I. (2015). STIM and Orai1 Variants in Store-Operated Calcium Entry. Front Pharmacol *6*, 325.

Rose, C.R., and Konnerth, A. (2001). Stores not just for storage. intracellular calcium release and synaptic plasticity. Neuron *31*, 519-522.

Schnabel, R., Kilpatrick, I.C., and Collingridge, G.L. (1999). An investigation into signal transduction mechanisms involved in DHPG-induced LTD in the CA1 region of the hippocampus. Neuropharmacology *38*, 1585-1596.

Scoville, W.B., and Milner, B. (1957). Loss of recent memory after bilateral hippocampal lesions. J Neurol Neurosurg Psychiatry *20*, 11-21.

Selkoe, D.J. (2001). Alzheimer's disease: genes, proteins, and therapy. Physiol Rev *81*, 741-766.

Sell, T.S., Belkacemi, T., Flockerzi, V., and Beck, A. (2014). Protonophore properties of hyperforin are essential for its pharmacological activity. Sci Rep *4*, 7500.

Sharp, A.H., McPherson, P.S., Dawson, T.M., Aoki, C., Campbell, K.P., and Snyder, S.H. (1993). Differential immunohistochemical localization of inositol 1,4,5-trisphosphate- and ryanodine-sensitive Ca2+ release channels in rat brain. J Neurosci *13*, 3051-3063.

Simpson, P.B., Nahorski, S.R., and Challiss, R.A. (1996). Agonist-evoked Ca2+ mobilization from stores expressing inositol 1,4,5-trisphosphate receptors and ryanodine receptors in cerebellar granule neurones. J Neurochem *67*, 364-373.

Sjostrom, P.J., and Nelson, S.B. (2002). Spike timing, calcium signals and synaptic plasticity. Curr Opin Neurobiol *12*, 305-314.

Soboloff, J., Rothberg, B.S., Madesh, M., and Gill, D.L. (2012). STIM proteins: dynamic calcium signal transducers. Nat Rev Mol Cell Biol *13*, 549-565.

Solovyova, N., and Verkhratsky, A. (2003). Neuronal endoplasmic reticulum acts as a single functional Ca2+ store shared by ryanodine and inositol-1,4,5-trisphosphate receptors as revealed by intra-ER [Ca2+] recordings in single rat sensory neurones. Pflugers Arch *446*, 447-454.

Stosiek, C., Garaschuk, O., Holthoff, K., and Konnerth, A. (2003). In vivo two-photon calcium imaging of neuronal networks. Proc Natl Acad Sci U S A *100*, 7319-7324.

Sun, S., Zhang, H., Liu, J., Popugaeva, E., Xu, N.J., Feske, S., White, C.L., 3rd, and Bezprozvanny, I. (2014). Reduced synaptic STIM2 expression and impaired store-operated calcium entry cause destabilization of mature spines in mutant presenilin mice. Neuron *82*, 79-93.

Takechi, H., Eilers, J., and Konnerth, A. (1998). A new class of synaptic response involving calcium release in dendritic spines. Nature *396*, 757-760.

Takemura, H., Hughes, A.R., Thastrup, O., and Putney, J.W., Jr. (1989). Activation of calcium entry by the tumor promoter thapsigargin in parotid acinar cells. Evidence that an intracellular calcium pool and not an inositol phosphate regulates calcium fluxes at the plasma membrane. J Biol Chem *264*, 12266-12271.

Terasaki, M., Shemesh, T., Kasthuri, N., Klemm, R.W., Schalek, R., Hayworth, K.J., Hand, A.R., Yankova, M., Huber, G., Lichtman, J.W*., et al.* (2013). Stacked endoplasmic reticulum sheets are connected by helicoidal membrane motifs. Cell *154*, 285-296.

Terasaki, M., Slater, N.T., Fein, A., Schmidek, A., and Reese, T.S. (1994). Continuous network of endoplasmic reticulum in cerebellar Purkinje neurons. Proc Natl Acad Sci U S A *91*, 7510-7514.

Terentyev, D., Viatchenko-Karpinski, S., Vedamoorthyrao, S., Oduru, S., Gyorke, I., Williams, S.C., and Gyorke, S. (2007). Protein protein interactions between triadin and calsequestrin are involved in modulation of sarcoplasmic reticulum calcium release in cardiac myocytes. J Physiol *583*, 71-80.

Thayer, S.A., Perney, T.M., and Miller, R.J. (1988). Regulation of calcium homeostasis in sensory neurons by bradykinin. J Neurosci *8*, 4089-4097.

Thillaiappan, N.B., Chavda, A.P., Tovey, S.C., Prole, D.L., and Taylor, C.W. (2017). Ca(2+) signals initiate at immobile IP3 receptors adjacent to ER-plasma membrane junctions. Nat Commun *8*, 1505.

Toescu, E.C., Gallacher, D.V., and Petersen, O.H. (1994). Identical regional mechanisms of intracellular free Ca2+ concentration increase during polarized agonist-evoked Ca2+ response in pancreatic acinar cells. Biochem J *304 (Pt 1)*, 313-316.

Tovey, S.C., and Taylor, C.W. (2013). Cyclic AMP directs inositol (1,4,5)-trisphosphate-evoked Ca2+ signalling to different intracellular Ca2+ stores. J Cell Sci *126*, 2305-2313.

Tribe, R.M., Borin, M.L., and Blaustein, M.P. (1994). Functionally and spatially distinct Ca2+ stores are revealed in cultured vascular smooth muscle cells. Proc Natl Acad Sci U S A *91*, 5908-5912.

Tsien, J.Z., Huerta, P.T., and Tonegawa, S. (1996). The essential role of hippocampal CA1 NMDA receptor-dependent synaptic plasticity in spatial memory. Cell *87*, 1327-1338.

Tu, H., Nelson, O., Bezprozvanny, A., Wang, Z., Lee, S.F., Hao, Y.H., Serneels, L., De Strooper, B., Yu, G., and Bezprozvanny, I. (2006). Presenilins form ER Ca2+ leak channels, a function disrupted by familial Alzheimer's disease-linked mutations. Cell *126*, 981-993.

Turner, D.J., Segura, B.J., Cowles, R.A., Zhang, W., and Mulholland, M.W. (2001). Functional overlap of IP(3)- and cADP-ribose-sensitive calcium stores in guinea pig myenteric neurons. Am J Physiol Gastrointest Liver Physiol *281*, G208-215.

Um, J.W., Kaufman, A.C., Kostylev, M., Heiss, J.K., Stagi, M., Takahashi, H., Kerrisk, M.E., Vortmeyer, A., Wisniewski, T., Koleske, A.J.*, et al.* (2013). Metabotropic glutamate receptor 5 is a coreceptor for Alzheimer abeta oligomer bound to cellular prion protein. Neuron *79*, 887-902.

Usachev, Y.M., and Thayer, S.A. (1999). Ca2+ influx in resting rat sensory neurones that regulates and is regulated by ryanodine-sensitive Ca2+ stores. J Physiol *519 Pt 1*, 115-130.

Vaeth, M., Yang, J., Yamashita, M., Zee, I., Eckstein, M., Knosp, C., Kaufmann, U., Karoly Jani, P., Lacruz, R.S., Flockerzi, V.*, et al.* (2017). ORAI2 modulates store-operated calcium entry and T cell-mediated immunity. Nat Commun *8*, 14714.

Varnai, P., Hunyady, L., and Balla, T. (2009). STIM and Orai: the long-awaited constituents of store-operated calcium entry. Trends Pharmacol Sci *30*, 118-128.

Verkhratsky, A. (2002). The endoplasmic reticulum and neuronal calcium signalling. Cell Calcium *32*, 393-404.

Verkhratsky, A. (2005). Physiology and pathophysiology of the calcium store in the endoplasmic reticulum of neurons. Physiol Rev *85*, 201-279.

Vermassen, E., Parys, J.B., and Mauger, J.P. (2004). Subcellular distribution of the inositol 1,4,5-trisphosphate receptors: functional relevance and molecular determinants. Biol Cell *96*, 3-17.

Vig, M., Peinelt, C., Beck, A., Koomoa, D.L., Rabah, D., Koblan-Huberson, M., Kraft, S., Turner, H., Fleig, A., Penner, R.*, et al.* (2006). CRACM1 is a plasma membrane protein essential for store-operated Ca2+ entry. Science *312*, 1220-1223.

Whitlock, J.R., Heynen, A.J., Shuler, M.G., and Bear, M.F. (2006). Learning induces long-term potentiation in the hippocampus. Science *313*, 1093-1097.

Williams, R.T., Manji, S.S., Parker, N.J., Hancock, M.S., Van Stekelenburg, L., Eid, J.P., Senior, P.V., Kazenwadel, J.S., Shandala, T., Saint, R.*, et al.* (2001). Identification and characterization of the STIM (stromal interaction molecule) gene family: coding for a novel class of transmembrane proteins. Biochem J *357*, 673-685.

Wills, T.J., and Cacucci, F. (2014). The development of the hippocampal neural representation of space. Curr Opin Neurobiol *24*, 111-119.

Wills, T.J., Muessig, L., and Cacucci, F. (2014). The development of spatial behaviour and the hippocampal neural representation of space. Philos Trans R Soc Lond B Biol Sci *369*, 20130409.

Wisniewski, K., and Car, H. (2002). (S)-3,5-DHPG: a review. CNS Drug Rev *8*, 101-116.

Wu, C., Sui, G., and Fry, C.H. (2002). The role of the L-type Ca(2+) channel in refilling functional intracellular Ca(2+) stores in guinea-pig detrusor smooth muscle. J Physiol *538*, 357-369.

Xu, J., Antion, M.D., Nomura, T., Kraniotis, S., Zhu, Y., and Contractor, A. (2014). Hippocampal metaplasticity is required for the formation of temporal associative memories. J Neurosci *34*, 16762-16773.

Xu, W., and Lipscombe, D. (2001). Neuronal Ca(V)1.3alpha(1) L-type channels activate at relatively hyperpolarized membrane potentials and are incompletely inhibited by dihydropyridines. J Neurosci *21*, 5944-5951.

Yan, Q.J., Rammal, M., Tranfaglia, M., and Bauchwitz, R.P. (2005). Suppression of two major Fragile X Syndrome mouse model phenotypes by the mGluR5 antagonist MPEP. Neuropharmacology *49*, 1053-1066.

Yeromin, A.V., Zhang, S.L., Jiang, W., Yu, Y., Safrina, O., and Cahalan, M.D. (2006). Molecular identification of the CRAC channel by altered ion selectivity in a mutant of Orai. Nature *443*, 226-229.

Zamponi, G.W., Springer E-books - York University., and SpringerLink (Online service) (2005). Voltage-gated calcium channels. In Molecular biology intelligence unit (Georgetown, Tex.

New York, N.Y.: Landes Bioscience/Eurekah.com ;

Kluwer Academic/Plenum Publishers), pp. 377 p.

Zhang, H., Sun, S., Wu, L., Pchitskaya, E., Zakharova, O., Fon Tacer, K., and Bezprozvanny, I. (2016). Store-Operated Calcium Channel Complex in Postsynaptic Spines: A New Therapeutic Target for Alzheimer's Disease Treatment. J Neurosci *36*, 11837-11850.

Zhang, S.L., Yu, Y., Roos, J., Kozak, J.A., Deerinck, T.J., Ellisman, M.H., Stauderman, K.A., and Cahalan, M.D. (2005). STIM1 is a Ca2+ sensor that activates CRAC channels and migrates from the Ca2+ store to the plasma membrane. Nature *437*, 902-905.

Zhang, W., and Linden, D.J. (2003). The other side of the engram: experience-driven changes in neuronal intrinsic excitability. Nat Rev Neurosci *4*, 885-900.

Zucker, R.S. (1999). Calcium- and activity-dependent synaptic plasticity. Curr Opin Neurobiol *9*, 305-313.

Zucker, R.S., and Regehr, W.G. (2002). Short-term synaptic plasticity. Annu Rev Physiol *64*, 355-405.